

MODELING OF THE FATE AND BEHAVIOR OF OIL SPILLS IN THE SALISH SEA

by

Xiaomei Zhong

Submitted in partial fulfilment of the requirements
for the degree of Master of Applied Science

at

Dalhousie University

Halifax, Nova Scotia

December 2018

© Copyright by Xiaomei Zhong, 2018

TABLE OF CONTENTS

LIST OF TABLES	v
LIST OF FIGURES	vi
ABSTRACT.....	ix
LIST OF ABBREVIATIONS AND SYMBOLS USED	x
ACKNOWLEDGEMENTS	xiii
CHAPTER 1: INTRODUCTION.....	1
1.1 Background	1
1.2 Research Objectives.....	3
1.3 Thesis Organization	4
CHAPTER 2: LITERATURE REVIEW	5
2.1 Background	5
2.2 Oil Weathering Processes.....	5
2.3 The Movement of Spilled Oil	6
2.4 Oil Spill Models.....	8
2.5 Oil Spill Modeling in the Salish Sea	10
CHAPTER 3: A MODELING STUDY ON THE OIL SPILL OF <i>M/V MARATHASSA</i> IN VANCOUVER HARBOUR.....	13
3.1 Abstract.....	13
3.2 Introduction.....	14
3.3 Materials and Methods.....	18
3.3.1 Hydrodynamic Forcing: FVCOM.....	18
3.3.2 Oil Spill Model: OSCAR.....	21
3.3.3 Wind Forcing: HRDPS Model.....	23
3.3.4 Hindcast Study of the <i>M/V Marathassa</i> Oil Spill.....	24
3.3.5 Statistical Analysis on Mass Balance	26
3.4 Results	27
3.4.1 FVCOM Validation	27
3.4.2 Impacts of Studied Factors on Oil Mass Balance and Trajectory.....	31
3.5 Discussion.....	35

3.5.1 FVCOM Validation	35
3.5.2 Hindcast of the <i>M/V Marathassa</i> Oil Spill	35
3.6 Conclusions.....	41
3.7 Supplementary Materials.....	42
3.8 Acknowledgments	43
3.9 Transition Section	43
CHAPTER 4: A STOCHASTIC MODELING STUDY OF THE IMPACT OF OIL SPILL LOCATION ON THE FATE AND TRANSPORT OF OIL SPILLS IN VANCOUVER HARBOUR.....	44
4.1 Abstract.....	44
4.2 Introduction.....	44
4.3 Method and Material.....	46
4.3.1 Studied Area.....	46
4.3.2 OSCAR Model.....	47
4.3.3 Hydrodynamic Forcing	47
4.3.4 Wind Forcing: HRDPS Model.....	47
4.3.5 Model Scenarios.....	49
4.3.6 Tidal Excursion Length.....	50
4.4 Results and Discussion.....	50
4.4.1 Probability of Contamination.....	50
4.4.2 Mass Balances.....	53
4.4.3 Tidal Excursion Length.....	57
4.5 Conclusion	58
4.6 Acknowledgements	59
4.7 Transition Section	59
CHAPTER 5: STOCHASTIC MODELING OF THE FATE AND BEHAVIOURS OF OIL SPILL IN THE SALISH SEA.....	61
5.1 Abstract.....	61
5.2 Introduction.....	61
5.3.1 Studied Area.....	63
5.3.2 OSCAR Model.....	64

5.3.3 Hydrodynamic Forcing	64
5.3.4. Wind Forcing	66
5.3.5. Model Scenarios.....	68
5.4 Results	71
5.4.1. Influence of Oil Discharge Location on Probability of Contamination.....	72
5.4.2. Influence of Oil Discharge Volume on Probability of Contamination.....	75
5.4.3. Influence of Discharged Oil Type on Probability of Contamination.....	79
5.5 Discussion.....	83
5.6 Conclusion	85
5.7 Acknowledgements	86
CHAPTER 6: CONCLUSION.....	87
6.1 Overall Conclusion.....	87
6.2 Future Work.....	87
REFERENCES.....	89
APPENDIX A	97
APPENDIX B	100

LIST OF TABLES

Table 2.1. Examples of 3D oil spill model that use Lagrangian algorithm to calculate transport processes.	12
Table 3.1. The studied factors and their corresponding settings.	25
Table 3.2. Results of statistical analysis between model simulations and observations. .	30
Table 3.3. The <i>p</i> -values for the influence of studied factors on oil mass balances. Significant influence (<i>p</i> -value <0.05) is shown in bold.	32
Table 3.4. Examples of water surface contaminant comparison. The simulated results were compared with observation data.	38
Table 3.5. Examples of shoreline contaminant comparison. The simulated results were compared with observation data.	38
Table 4.1. Average areas (km ²) for more than 5% probability for oil contamination in each group. Oil contamination in the Strait of Georgia was not included.	52
Table 5.1. Basic physical properties of selected oils.	70
Table 5.2. The studied factors and their corresponding settings.	71
Table 5.3. The <i>p</i> -values for the influence of studied factors on contamination areas. Significant influence (<i>p</i> -value < 0.05) is shown in bold.	72
Table S4.1. Areas (km ²) for more than 5% probability for oil contamination. Oil contamination in the Strait of Georgia was not included.	105
Table S5.1. Areas (km ²) for more than 5% probability for oil contamination.	106

LIST OF FIGURES

Figure 3.1. Anchorages' position at the Port of Metro Vancouver (PMV). Modified based on (PMV).	15
Figure 3.2. The <i>M/V Marathassa</i> oil spill situation map (map provided by the City of Vancouver, BC). This map shows the observed spilled oil trajectory on the water surface and the contamination on the shoreline in the English Bay and Vancouver Harbour from 8 to 10 April 2015 (Stormont, 2015). Areas with oil sheen are numbered as 1–10, and contaminated shoreline areas are labeled as A–P.	17
Figure 3.3. Finite-Volume Community Ocean Model's (FVCOM) horizontal grid in the English Bay and Vancouver Harbour. The horizontal grid space is 10 m in Vancouver Harbour and about 2 m around the bridge bases in the Second Narrows.	19
Figure 3.4. Schematic overview of a general oil spill model. Modified based on (Aamo et al., 1997).	22
Figure 3.5. Wind speed and direction from the High-Resolution Deterministic Prediction System (HRDPS) (12 April 2015, 16:00). The area in the red square is the studied area.	23
Figure 3.6. Speed, direction and frequencies of the wind near the oil released site (from 5–12 April 2015).	24
Figure 3.7. Trajectory comparison between Surface Current Tracker 1 (SCT1) drifter data and FVCOM data. The trajectory starts at the star.	27
Figure 3.8. Trajectory comparison between SCT2 drifter data and FVCOM data. The trajectory starts at the star.	28
Figure 3.9. Time series velocities comparison between observed SCT1 drifter data and FVCOM data. U-velocity is on the left, and V-velocity is on the right.	29
Figure 3.10. Time series velocities comparison between observed SCT2 drifter data and FVCOM data. U-velocity is on the left, and V-velocity is on the right.	29
Figure 3.11. The influence of studied factors (a) release start time, (b) wind, (c) discharge duration and (d) recovery action on the mass balance of water surface, shoreline and recovered.	34
Figure 3.12. Example of oil trajectories for the oil spill that started to discharge at 14:00 on 8 April 2015. Spilled oil discharged continuously (22 h) and then tracked with wind and without recovery actions (labeled as Scenario #4 in Table S3.5). Figures from top to bottom are oil distribution at 8:00 on (a) 9 April, (b) 10 April and (c) 11 April 2015.	37
Figure 3.13. Automated Data Inquiry for Oil Spills (ADIOS, version 2.0) model's predictions of evaporated, dispersed and remaining (surface) Intermediate Fuel Oil 380 (IFO-380) oil after three days of simulation.	40

Figure 3.14. OSCAR model’s predictions of evaporated, dispersed, remaining (surface contaminant) and ashore (shoreline contaminant) IFO-380 oil after three days of tracking in Scenario #4 and started at 14:00.....	40
Figure 3.15. OSCAR model’s predictions of evaporated, dispersed, remaining (surface contaminant) and ashore (shoreline contaminant) IFO-380 oil after three days of tracking in Scenario #4 and started at 15:00.....	41
Figure 4.1. Locations of twenty selected anchorages in the English Bay (PMV).	47
Figure 4.2. Speed, direction, and frequencies of the wind near Anchorage #2 (from Feb. 4 th to Mar. 9 th , 2017).	48
Figure 4.3. Wind speed and direction from the HRDPS model (9 p.m. on Feb. 10 th , 2017). The area in the red square is the study area.	48
Figure 4.6. Tidal excursion length (km) in the English Bay and Vancouver Harbour. ...	58
Figure 4.7. Probability of water particles (from the English Bay) that move pass the First Narrow.	58
Figure 5.2. NEMO model Salish Sea currents at 0.5m depth. NEMO model is not able to generate hydrodynamic forcing in the white color areas.	66
Figure 5.3. Finite-Volume Community Ocean Model’s (FVCOM) horizontal grid in the Salish Sea and Burrard Inlet. The horizontal grid space is about 1 km in the Salish Sea, 10 m in the Vancouver Harbor and about 2 m around the bridge bases in the Second Narrows.	67
Figure 5.4. Wind speed and direction from the High-Resolution Deterministic Prediction System (HRDPS) (13 February 2017, 21:00).	67
Figure 5.5. Speed, direction and frequencies of the wind near the oil released site (from 5 February to 7 March 2017).	68
Figure 5.6. The influence of oil discharge locations on the contamination areas in the water column, on water surface and shoreline. TN, SN, FN, A8, SOG, and TP are used to represent Terminal, Second Narrow, First Narrow, Anchorage #8, Strait of Georgia, and Turn Point respectively.	73
Figure 5.7. Probability of oil contamination for 8250 m ³ AWB-W oil release at (1) Strait of Georgia and (2) Turn Point. The oil initially releases at the star.....	74
Figure 5.8. Probability of oil contamination for 8250 m ³ AWB-W oil release at (1) Terminal, (2) Second Narrow, (3) First Narrow, and (4) Anchorage #8. The oil initially releases at the star.....	75
Figure 5.9. The influence of oil discharge volumes on the contamination areas in the water column, on water surface and shoreline.	76
Figure 5.10. Probability of oil contamination for CLB-S oil release at Strait of Georgia with (1) large (16500 m ³), medium (8250 m ³), and small (160 m ³) volume of oil. The oil initially releases at the star. The areas in the black circles was near (a) Gabriola Islands and (b) Sucia Islands.	77

Figure 5.11. Probability of oil contamination for CLB-S oil release at First Narrow with (1) large (16500 m ³), medium (8250 m ³), and small (160 m ³) volume of oil. The oil initially releases at the site marked by a star.	78
Figure 5.12. The influence of discharged oil types on the contamination areas in the water column, on water surface and shoreline.	80
Figure 5.13. Probability of oil contamination for 8250 m ³ of (1) AWB-W, (2) CLB-S, (3) CLB-W, released at Strait of Georgia. The oil initially releases at the star.	81
Figure 5.14. Probability of oil contamination for 8250 m ³ of (1) Synbit and (2) WCS released at Strait of Georgia. The oil initially releases at the star.	82
Figure 5.15. Probability of oil contamination for 8250 m ³ of (1) IFO-380 and (2) MDO released at Strait of Georgia. The oil initially releases at the star.	82
Figure S4.1. The total probability of oil contamination for oil spilled at anchorage #1-4 (from top to bottom). Oil start discharge at the star.	100
Figure S4.2. The total probability of oil contamination for oil spilled at anchorage #5-8 (from top to bottom). Oil start discharge at the star.	101
Figure S4.3. The total probability of oil contamination for oil spilled at anchorage #9-12 (from top to bottom). Oil start discharge at the star.	102
Figure S4.4. The total probability of oil contamination for oil spilled at anchorage #13-15, and #Z (from top to bottom). Oil start discharge at the star.	103
Figure S4.5. The total probability of oil contamination for oil spilled at anchorage #16-18, and #U (from top to bottom). Oil start discharge at the star.	104

ABSTRACT

Growing transportation of diluted bitumen blends and vessel traffic in the Salish Sea, BC coast could increase the risk of marine oil spill. Understanding the fate and behavior of spilled oil are of importance to help with oil spill response. A high-resolution oil spill model, the Oil Spill Contingency and Response (OSCAR) model was used to conduct a hindcast study of the *M/V Marathassa* oil spill in the English Bay (part of the Salish Sea) and the comparison of modeled and observed trajectories showed agreements for 70% of the locations. Following model validation, the influences of oil discharge location, discharge volume, and oil type on the fate and behavior of oil were studied. The stochastic modeling result indicated that these studied factors significantly affect the area and probability of oil contamination.

LIST OF ABBREVIATIONS AND SYMBOLS USED

2D	Two dimensional
3D	Three dimensional
ADCP	Acoustic Doppler Current Profiler
ADIOS	Automated Data Inquiry for Oil Spills
ANOVA	Analysis of Variance
API	American Petroleum Institute
ASA	Applied Science Associate
AWB-W	Access Western Blend-Winter
BC	British Columbia
BTEX	Benzene, Toluene, Ethylbenzene, Xylene
CCG	Canadian Coast Guard
CLB-S	Cold Lake Blend-Summer
CLB-W	Cold Lake Blend-Winter
COZOIL	coastal zone oil spill
DFO	Fisheries and Oceans Canada
ELMs	Eulerian-Lagrangian methods
FVCOM	Finite-Volume Community Ocean Model
GEM	Global Environmental Multiscale
GNOME	General NOAA Operational Modeling Environment
HRDPS	High-Resolution Deterministic Prediction System
IFO-180	Intermediate Fuel Oil-viscosity of 180 cSt @ 15 °C
IFO-380	Intermediate Fuel Oil-viscosity of 380 cSt @ 15 °C
MDO	Marine Diesel Oil
MEOPAR	Marine Environmental Observation Prediction and Response Network
MGO	Marine Gas Oil
MOHID	Modelo Hidrodinâmico
MOSM	Multiphase Oil Spill Model
MOTHY	Modèle Océanique de Transport d'Hydrocarbures
NASP	National Aerial Surveillance Program

NCAG	National Contaminants Advisory Group
NOAA	National Oceanic and Atmospheric Administration
NSERC	Natural Sciences and Engineering Research Council of Canada
OSCAR	Oil Spill Response and Contingency Model
OWM	Oil weathering models
PMV	Port of Metro Vancouver
POM	Princeton Ocean Model
RMSE	Root-Mean-Square-Error
SCAT	Shoreline Cleanup Assessment Technique
SCT	Surface Current Tracker drifters
SINTEF	Stiftelsen for Industriell Og Teknisk Forskning
Synbit	Synthetic bitumen
TMEP	Trans Mountain Expansion Project
UTC	Coordinated Universal Time
WCMRC	Western Canada Marine Response Corporation
WCS	Western Canadian Select

SYMBOL	DESCRIPTION	UNIT
K_x	Horizontal dispersion	m ² /s
K_z	Vertical dispersion	m ² /s
H	Wave height	m
T	Wave period	s
U	Wind speed	m/s
d	Water depth	m
F	Fetch	m
g	Gravitational acceleration	m/s
X_{mod}	Model velocity	m/s
X_{obs}	observed velocity	m/s
\bar{X}_{mod}	average Model velocity	m/s
\bar{X}_{obs}	average observed velocity	m/s
(x_i, y_i)	the position of the particle	-
u	u-velocity at the location of the particle (x_i, y_i)	m/s
v	v-velocity at the location of the particle (x_i, y_i)	m/s

ACKNOWLEDGEMENTS

I would like to thank and express my greatest appreciation to my supervisor, Dr. Haibo Niu, for his professional, scientific and continuous guidance and support throughout my M.A.S.c study. I really appreciate his encouragement, trust and inspiration that greatly motivated me to work hard, act efficiently and accomplish more. I believe I would embed those nice personality and positive attitude to my life and make further progress in the future.

I also appreciate the comments and suggestions from my committee members Dr. Yongsheng Wu and Dr. Lei Liu. Their expertise and patience helped me a lot. I am very grateful to Dr. Pu Li, Shihan Li, and other faculty members and staff as well, for their help and contributions to this research.

At last but not least, I would like to show my appreciation to my families for their continuous encouragements and support that allowed me to pursue my goals at scientific research area.

CHAPTER 1: INTRODUCTION

1.1 Background

Canada has the world largest reserves of oil sands, which is estimated to be equivalent of 165.4 billion barrels of oil in total (Alberta Energy, 2018). It is necessary to note that the majority reserves of oil sand in Canada are located in the province of Alberta. The oil extracted from oil sands, namely bitumen, can be upgraded into various petroleum products (such as gasoline, diesel and aviation fuel) by catalytic hydro-treating processes. About 95% of bitumen produced in Canada is diluted with suitable solvents and then transported to destinations *via* pipelines or by railway (Martínez-Palou et al., 2011). The current capacity of the major pipeline systems in Western Canada is 300,000 barrel/d (CAPP, 2018). However, most of the pipeline systems are already or almost exceed their limited capacity. Therefore, the Trans Mountain Expansion Project (TMEP) was proposed to increase the pipeline transportation capacity of diluted bitumen products from Alberta to British Columbia (BC). TMEP intends to triple the pipeline transportation capacity from Alberta to BC, and this will result in an increase of the oil tanker traffic by seven folds on the BC coast in order to sufficiently distribute the bitumen products worldwide (Zmuda, 2017).

Port of Metro Vancouver (PMV), which locates on the southwest BC coast, is the largest port by tonnage in Canada and the third largest in North America (AAPA, 2016). PMV extending from Robert Banks (parts of Salish Sea) to the Burrard Inlet with 34 anchorages (20 in the English Bay, 8 in the Vancouver Harbour, 4 in the Indian Arm, 1 in Robert Bank, and 1 in Sand Heads). As the largest import and export port in Canada, in 2017, PMV handled 142 million tonnes of cargo, which accounted for about 42% of all cargo through Canada (335 million tonnage) (Government of Canada, 2018; VFPA, 2018). This huge cargo handling resulted in a busy vessel traffic in PMV with approximately 10,000 large cargo vessels traveling through the Salish Sea every year (Washington Nature, n.d.). Oil spills has been of major concern and is regarded as one of the most critical forms of marine pollution in the Salish Sea due to the heavy vessel traffic as mentioned above.

The fate and behavior of spilled oil are of importance for rapid and efficient response to the spill. Numerical modeling is a well-established and cost-effective technique to estimate the oil spill fate and behavior, and it is a crucial component of contingency planning and coastal management. Therefore, several researchers, organizations and consulting companies have evaluated the potential risk of the oil spill in the BC coast, which geographically includes the Burrard Inlet and the Salish Sea (the mouth of Burrard Inlet opens onto the Salish Sea) by using various oil spill models (Genwest System Inc., 2015; Niu, Li, King, & Lee, 2016; Tetra Tech EBA Inc., 2015). Although these studies have provided some information about the fate/transport of oil for the study area, there are still some limitations, especially the resolution and algorithm of the oil spill model. Therefore, a high-resolution/integrated oil spill model is required for the modeling of the oil spill in the Salish Sea. Then, the predictability of the high-resolution/integrated model needs to be validated for the further oil spill modeling study in the Salish Sea.

The predictability of oil spill model can be assessed by comparing the numerical results with the data from real oil spill event (Abascal, Castanedo, Medina, & Liste, 2010; Reed & Gundlach, 1989). For instance, the Coastal Zone Oil Spill Model (COZOIL) has been tested against data from the 1978 *Amoco Cadiz* oil spill event, and it was found that modeled mass balances compared very well with observations in both space and time (Reed & Gundlach, 1989). Also, the OILTRANS model was validated by comparing the modeled data with the aerial observations from the accidental oil release event in the Celtic Sea in 2009. The comparison results indicated that the OILTRANS model is capable of accurately predicting the transport and fate of the oil slick (Berry, Dabrowski, & Lyons, 2012). This method for testing the ability of predictive model on historical data is called “hindcast” study. If the hindcast showed reasonably-accurate fate and behavior of spilled oil, the model would be considered to be validated in terms of its predictability and then it can be further used in the oil spill modeling.

The fate and behavior of spilled oil are highly associated with the initial volume of spilled oil, oil type, and water environment conditions (Fingas, 2015; Lee et al., 2015; Verma, Wate, & Devotta, 2008). The initial oil spill volume can influence the spreading of spilled oil and final contamination area in the marine environment. For example, a

stochastic modeling study was conducted by Tetra Tech EBA Inc. to investigate the impact of spill volume on the fate and behavior of spilled oil in the Salish Sea. The modeling results indicated that the shoreline contamination length was increased with the increasing of the spilled oil volume (Tetra Tech EBA Inc., 2015). Different types of oil have different physicochemical properties that might lead to varied oil fate and behavior after spilling. For instance, Niu et al. (2016) used three types oil to simulate their fate and transport after spilling in the Salish Sea, and it was found that oil contains a more volatile component resulted in a higher proportion of evaporation, as well as a larger area of water column and surface contamination (Niu, Li, King, & Lee, 2016). In addition, the bathymetry and environmental conditions (i.e. temperature, wind) within the studied area can influence currents, waves, tides and freshwater runoff and consequently affect the fate and transport of spilled oil (Hemmera Envirochem Inc., 2015). For example, four locations were selected by Genwest System Inc. to simulate the trajectories of spilled oil in the Burrard Inlet. The simulation results demonstrated that the behavior of spilled oil was influenced by the initial condition of spilled sites that have different currents intensity and their closer proximity to the open sea and shoreline (Genwest System Inc., 2015). Therefore, it is necessary to investigate the influence of the oil spill locations, spilled oil volume, and oil types on the fate and behaviour of oil spill in the Salish Sea.

1.2 Research Objectives

This project aims to use a state-of-art 3D oil spill model (OSCAR) to simulate the fate and behaviour of spilled oil under a wide range of environmental conditions in the Salish Sea. Specific objectives are as follows:

- (1) Using the OSCAR oil spill model forced with high-resolution hydrodynamic data to carry out the hindcast study of the 2015 *M/V Marathassa* oil spill in the English Bay (part of the Salish Sea);
- (2) To study the influence of oil spill locations on the fate and behavior of the spilled oil in the English Bay;

- (3) Using the integrated oil spill model to investigate the influence of the oil spill locations, spilled oil volume, and oil types on the fate and behavior of oil spill in the Salish Sea and the Burrard Inlet.

1.3 Thesis Organization

Chapter 2 presents a literature review on oil spill modeling. Chapter 3 provides a validation of FVCOM model and hindcast study of the *M/V Marathassa* oil spill. Chapter 4 describes the effect of oil release locations on the fate and behavior of the spilled oil in the English Bay and Vancouver Harbour. In Chapter 5, the influence of oil release locations, oil spill volume, and oil types on the fate and behavior of the spilled oil in the Salish Sea and the Burrard Inlet are thoroughly assessed. Chapter 6 provides the overall conclusions of this research and the recommendations for the future work.

CHAPTER 2: LITERATURE REVIEW

2.1 Background

Oil spill modeling is typically referred to the simulation of the fate and behavior of spilled oil by using certain modeling software when taking hydrodynamic and wind forcing into considerations. Once oil is discharged into the water environment, two common transformation processes can occur as follows: 1) the oil weathering process that can significantly change the physicochemical properties of the spilled oil; and 2) the oil movement in the water environment that can increase the contamination area. Both of these two processes are highly associated with the oil spill location, the type of oil, discharge volume etc. (Verma et al., 2008).

2.2 Oil Weathering Processes

The oil weathering processes includes: oil evaporation, emulsification, natural dispersion, dissolution, photo-oxidation, biodegradation, and sedimentation etc. (Fingas, 2011a). Each process starts at different time points after oil is spilled and takes place under different rates. For instance, evaporation starts almost immediately after a spill and acts in a significant short-term, but the water-in-oil emulsification begins relatively slow and accounts for a large proportion oil weathering process (Lee et al., 2015). Moreover, different weathering processes have different effects on the physicochemical properties of the spilled oil in the environment. For example, photo-oxidation and biodegradation are two most important processes that can modify the chemical compositions of the spilled oil (Dutta & Harayama, 2000; Fingas, 2011a). As for the evaporation process, it tends to reduce the volume of the spilled oil and increase the oil density (Fingas, 1995). As parts of the volatile components are evaporated in the initial hours of spill, the remaining heavy components might be combined with sediments in the water column and then submerge/sink, while the rest residual components tend to disperse naturally into the water column (Walker et al., 2016). Emulsification is the process of one liquid dispersing into another one in the form of small droplets, whereby the water-in-oil emulsion formed

(Fingas, 2015). The formation of water-in-oil emulsions usually change the physical properties, such as water content and viscosity, of spilled petroleum products (Fingas, 2011b). However, the detailed emulsification specific process is dependent on the oil types and the environment of spill location (Lee et al., 2015).

Oil weathering processes depend upon currents, wind and waves. For example, the process of emulsification can be increased by the turbulence that created by wind; the oil dissolution was reported to be affected by the wind stress, waves and wave breaking through creating water-side turbulence (Leifer et al., 2012). In addition, wave breaking can break up the oil sheen to small droplets and then these oil droplets were naturally dispersed into the water column (Farmer & Li, 1994).

2.3 The Movement of Spilled Oil

The movement of spilled oil is the process that the spilled oil extends and travels on the water surface and into water column. One of the most important movement processes is spreading that can increase the contamination area (Lee et al., 2015). After an oil discharge, the spilled oil tends to spread into a slick over the water surface due to the force of gravity and the interfacial tension between oil and water (Fingas, 2011a). Over time, the effect of gravity on the oil is diminished, but the effect of interfacial tension continues to spread the oil (Fay, 1969). The spreading rate of spilled oil is determined by environment condition (e.g. topography, water currents, tidal streams and wind speeds), spill type, and oil properties (Dew, Hontela, Rood, & Pyle, 2015; Lee et al., 2015; Lehr, 2001; Wang, Shen, Guo, & Tang, 2008). For example, spilled oil cannot spread out and contact the shoreline immediately in confined waterways (Michel & Rutherford, 2014), but spread rapidly and cover a large areas of the water surface in the open sea (Lee et al., 2015). The spilled oil that contains more low molecular weight (LMW) hydrocarbons (volatile components) could be expected to spread more quickly (Lee et al., 2015). In addition, the spreading area of spilled oil is highly related to the weathering processes. For instance, the spreading area of spilled oil decrease with time due to the evaporation, dissolution, and sinking (Wang et al., 2008). Wind and currents also play the important role to spread the oil out and speed up the process. As spreading progresses, oil slicks elongate in the

direction of the wind and currents, and lead to many shapes depending on the driving forces (Fingas, 2011a).

Another process that increases the contamination area is the advection of oil on the water surface, which is primarily caused by the surface currents and wind. The influence of surface currents and wind on the oil movement varies in different situations. For example, as investigated by Fingas (2011), the movement of spilled oil was almost totally forced by surface currents when oil was discharged in the close land location and the wind speed is less than 10 km/h. By contrast, wind predominated in determining the movement of spilled oil when oil was discharged in the open sea and wind speed was higher than 20 km/h (Fingas, 2011a). However, for most conditions, both wind and surface currents should be considered when determining the spilled oil movement. The velocity of oil movement on the water surface is the vector sum of the wind and surface currents as illustrated in Figure 2.1 (Leifer, Luyendyk, & Broderick, 2006). Typically, the contribution of wind speed to the velocity of oil spill movement is usually around 3 - 3.5% (Jens & Jacob, n.d.). Another factor that induce the oil movement is wave. Although it is widely believed that wave-induced drift effects are relatively small compared to current and wind drift on oil movement, the wave-induced currents, such as Stokes drift, can easily reach the magnitude of the wind and current drift. The wave-induced currents drift can drive oil movement as well (Jens & Jacob, n.d.).

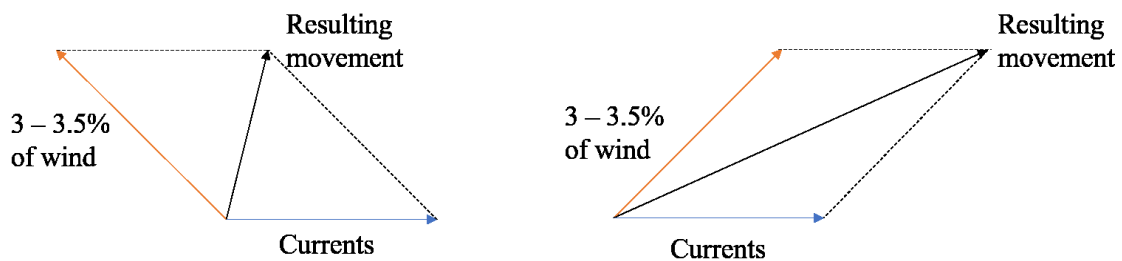


Figure 2.1. The effect of different wind and current directions on the resulting movement of an oil slick. Modified based on (Fingas, 2011a).

2.4 Oil Spill Models

Oil spill modeling are used to assist in planning and emergency decision making for industry and government institutes. Several models have been developed to simulate the fate and behavior of the spilled oil. The oil spill models can be broadly divided into oil weathering models (without oil transport) and trajectory/deterministic models.

Oil weathering models (OWM) mainly simulate how different types of oil weathering (behavior) that undergo physicochemical properties changes, when oil spilled in water environments. The weathering prediction is a useful tool for determining the most effective response and for Environmental Impact Assessment studies in contingency analysis and planning (Prentki et al., 2004). Currently, several oil weathering models have been developed. For instance, the ADIOS (Automated Data Inquiry for Oil Spills) was developed by the National Oceanic and Atmospheric Administration Hazardous Materials Response Division (NOAA/HAZMAT) (Lehr, Jones, Evans, Simecek-Beatty, & Overstreet, 2002; W. J. Lehr, Overstreet, Jones, & Watabayashi, 1992). The major weathering processes calculated by the ADIOS (version 2) model are spreading, evaporation, dispersion, sedimentation, and emulsification (Lehr et al., 2002). This model can also be used to predict the effects of common clean up techniques on released oil, such as chemical dispersion, skimming or burning the oil, and it can explain the environmental processes that might remove oil from the water column, such as sedimentation (Ocean Ecology, 2015). Another commonly used weathering model is the IKU Oil Weathering Model (now known as the SINTEF OWM), which was developed base on small and mesoscale laboratory tests and several full-scale field experiments at SINTEF (*Stiftelsen for industrial of TEknisk Forskning ved NTH* – Foundation for Industrial and Technical Research) (Daling, Aamo, Lewis, & Strøm-Kristiansen, 1997; Reed et al., 2004). The main weathering processes included in the model are evaporation, emulsification, and natural dispersion. Evaporation losses are calculated based on the pseudo-component method. The predictions of oil properties, such as pour point, flash point, and viscosity, are based on laboratory weathering data. The viscosity of the water-in-oil emulsion was calculated according to Mackay's equation (Mackay, Buist, Mascarenhas, & Paterson, 1980; Mackay, Paterson, & Trudel, 1980). Nearly 200 oil types were characterized at SINTEF, and the

database includes fresh oil properties, distillation curves, properties of cuts, and laboratory weathering data (Aamo, Reed, & Daling, 1993).

The fate/transport models can range in capability from the simple trajectory/particle-tracking models (two-dimensional (2D)) to three-dimensional (3D) trajectory and fate models that include simulation of response actions and estimation of biological effects (Reed et al., 1999). In general, a 2D model can only be used to simulate the trajectory of an oil spill on the water surface, whereas a 3D model can be employed to simulate the conditions both on the water surface and in the water column. Currently, the major numerical approaches used in 3D oil spill trajectory models are the Eulerian method, Lagrangian methods, and Eulerian-Lagrangian methods (ELMs). The Eulerian method is used to solve the problem of oil dispersion. This method is relatively simple to calculate dispersion term and easy to obtain high precision. However, the calculation of advection term is relatively difficult (García-Martínez & Flores-Tovar, 1999). The Lagrangian method can describe the trajectory of spilled oil. However, it can not directly illustrate how the oil spills amount impact on the oil dispersion area (Zhang, Zhou, Li, & Wu, 2017). The Euler-Lagrange method is increasingly used and combining the advantages of the Eulerian and Lagrangian method that the Lagrangian method simulates the movement of oil particles on the water surface and the Eulerian method describes the conditions in the water column. It can better to simulate the trajectory and fate of oil spill in the water environment when combines the ELMs with dynamic equations (Oliveira, 1997). Among the 2D oil spill model, most of them are calculated by using the ELMs. For example, the GNOME (General NOAA Operational Modeling Environment) model, which is the well-recognized and leading 2D numeric oil spill trajectory model (NOAA, n.d.); the TELEMAC-2D model that was developed by the National Hydraulics and Environment Laboratory (Laboratoire National d'Hydraulique et Environnement – LNHE) of the Research and Development Directorate of the French Electricity Board (EDF-DRD), in association with other research institutes (Goeury, Hervouet, Benoit, Baudin-Bizien, & Fangeat, 2012). Several models still use the Eulerian method, such as the 2D Multiphase Oil Spill Model (MOSM) (Heydariha & Ghiassi, 2010). As for the 3D oil spill model, according to state-to-the-art review (ASCE, 1996; Reed et al., 1999; Spaulding, 2017), the Lagrangian methods is used

in a large number of 3D oil spill models for the transport processes calculation. The example of 3D Lagrangian model are provided in Table 2.1. By comparison, very few of 3D model use the ELMs to simulate the oil transport processes, such as the Lagrangian/Eulerian oil spill model that developed by Goeury et al. (Goeury, Hervouet, Benoit, Baudin-Bizien, & Fangeat, 2012).

2.5 Oil Spill Modeling in the Salish Sea

As previously mentioned in Section 1.1, the potential risk of oil spill in PMV is expected to increase considerably. Therefore, several numerical modeling efforts have been made to simulate the fate and behaviour of the spilled oil in the Salish Sea and Vancouver Harbour by using various oil spill models. For instance, in 2013, Tetra Tech EBA Inc. used SPILLCALC model to study the oil trajectories, weathering and shore contact of diluted bitumen (dilbit) by both stochastic and deterministic approach in the Salish Sea and Westridge Terminal (locates in Vancouver Harbour) (Stormont, 2015). However, in 2015, Genwest System Inc. argued that there are limitations in the model assumptions in Tetra Tech EBA Inc.'s study (Genwest System Inc., 2015). Therefore, Genwest System Inc. employed GNOME model to simulate the spill trajectories of dilbit in Burrard Inlet to address this issue. Although several oil release volumes and locations in the Salish Sea and Burrard Inlet (consist of the English Bay and Vancouver Harbour) were investigated by Tetra Tech EBA Inc. and Genwest System Inc., there are still some issue that need to be addressed. First, the stochastic model in SPILLCALC was 2D, which only tracked the surface transport of oil and did not provide the probability of water column contamination; and the resolutions of the incorporated hydrodynamic model, H3D, was relatively low (1 km × 1 km horizontal grid space) in the study area. Second, the study used the GNOME model to simulate the trajectory of oil based on rough wind conditions and ocean currents, but the fate/weathering processes was not provided. Niu et al. (2016) employed OSCAR model that was forced by a high-resolution hydrodynamic model-NEMO with a horizontal grid space from 440 m × 440 m to 500 m × 500 m in the Salish Sea to simulate the fate and transport of three types of oil (light crude, dilbit, and heavy crude) in the Salish Sea. The model domain only covers the Salish sea area, therefore it is

not able to simulate the movement of the spilled oil in the Burrard Inlet. To fill this gap, it is worthwhile to develop a high-resolution/integrated oil spill model for the modeling of the oil spill in both Burrard Inlet and Salish Sea.

Table 2.1. Examples of 3D oil spill model that use Lagrangian algorithm to calculate transport processes.

Model	Developer	Reference
MEDSLIK	Oceanography Centre of the University of Cyprus (OC-UCY)	(Lardner et al., 1998, 2006; Zodiatis et al., 2008a)
MEDSLIK-II	Oceanography Centre of the University of Cyprus (OC-UCY)	(De Dominicis, Pinardi, Zodiatis, & Lardner, 2013)
COZOIL	Department of the Interior Minerals Management Service	(Reed, Gundlach, & Kana, 1989)
OSCAR	SINTEF	(Reed, Aamo, & Daling, 1995)
OILMAP	ASA	(Spaulding, Kolluru, Anderson, & Howlett, 1994)
MOTHY	-	(Daniel, 2003)
POSEIDON-OSM	Hellenic Centre for Marine Research (HCMR)	(Annika et al., 2001; Nittis, Perivoliotis, Korres, Tziavos, & Thanos, 2006)
GULFSPILL	-	(Al-Rabeh, Lardner, & Gunay, 2000)
MOHID	MARETEC (Marine and Environmental Technology Research Center)	(Carracedo et al., 2006)
OILTRANS	-	(Berry, Dabrowski, & Lyons, 2012)

CHAPTER 3: A MODELING STUDY ON THE OIL SPILL OF *M/V MARATHASSA* IN VANCOUVER HARBOUR

Copyright permission:

A version of this chapter has been published in J. Mar. Sci. Eng. 2018, 6(3), 106. The copyright has been obtained from Journal of Marine Science and Engineering and co-authors.

Contribution statement:

I was responsible for model simulation setting and running, data analysis and manuscript preparation.

3.1 Abstract

The *M/V Marathassa* oil spill occurred on 8 April 2015 in the English Bay. In the present study, the trajectory and the transport mechanism of the spilled oil have been studied by using the three-dimensional and particle-based Oil Spill Contingency and Response (OSCAR) model forced by the Finite-Volume Community Ocean Model (FVCOM). FVCOM provided the hydrodynamic variables used by the oil spill model of OSCAR. The results showed that the fraction of the oil on the water surface and on the shoreline, as well as the amount of oil recovered were affected by the time of the initial release, the overall duration of the discharge, wind and recovery actions. The hindcast study of the *M/V Marathassa* oil spill showed that the likely starting time for the discharge was between 14:00 and 15:00, on 8 April 2015. The release may have lasted for a relatively long time (assumed to be 22 hours in this study). The results of modeling in this study were found reasonably acceptable allowing for further application in risk assessment studies in the English Bay and Vancouver Harbour. The trajectory of the spill was mainly controlled by the tidal currents, which were strongly sensitive to the local coastline and topography

of First Narrows and that in the central harbour. The model results also suggested that a high-resolution model, which was able to resolve abrupt changes in the coastlines and topography, was necessary to simulate the oil spill in the harbour.

3.2 Introduction

Canada has the world's largest reserves of oil sands, which are deposits of bitumen in sand or porous rock (Hein, Leckie, Larter, & Suter, 2013). The bitumen extracted from oil sands can be upgraded into various petroleum fuels (such as gasoline, diesel and aviation fuel) via proper hydro-treating processes. Due to the increasing bitumen and heavy oil production in Canada, the Trans Mountain Expansion Project (TMEP) was proposed to increase the capacity of bitumen and heavy oil transportation via pipeline from the province of Alberta, which has the majority of oil sands in Canada, to the west coastal province, British Columbia (BC). TMEP intends to triple the pipeline transportation capacity, which will consequently increase the oil tanker traffic by seven times on the BC coast, as well (Zmuda, 2017). The biggest import and export port on the BC coast, Port of Metro Vancouver (PMV), consists of 34 anchorages (20 in the English Bay, 8 in Vancouver Harbour, 4 in the Indian Arm, 1 in Robert Bank, and 1 in Sand Heads), as shown in Figure 3.1. In 2017, PMV handled about 142 million tonnes of cargo, which is 5% more than the previous year (2016) (VFPA, 2018). This busy and growing vessel traffic in PMV increases the potential risk of oil spill. The Canadian Coast Guard (CCG) receives about 600 pollution reports on the BC coast every year, nearly 40 of which occur in the PMV (Butler, 2015). For instance, a small oil spill took place in the English Bay (one of the PMV anchorages) on 8 April 2015, which resulted in at least 2800 liters of oil released from the cargo vessel, *M/V Marathassa* (Butler, 2015).

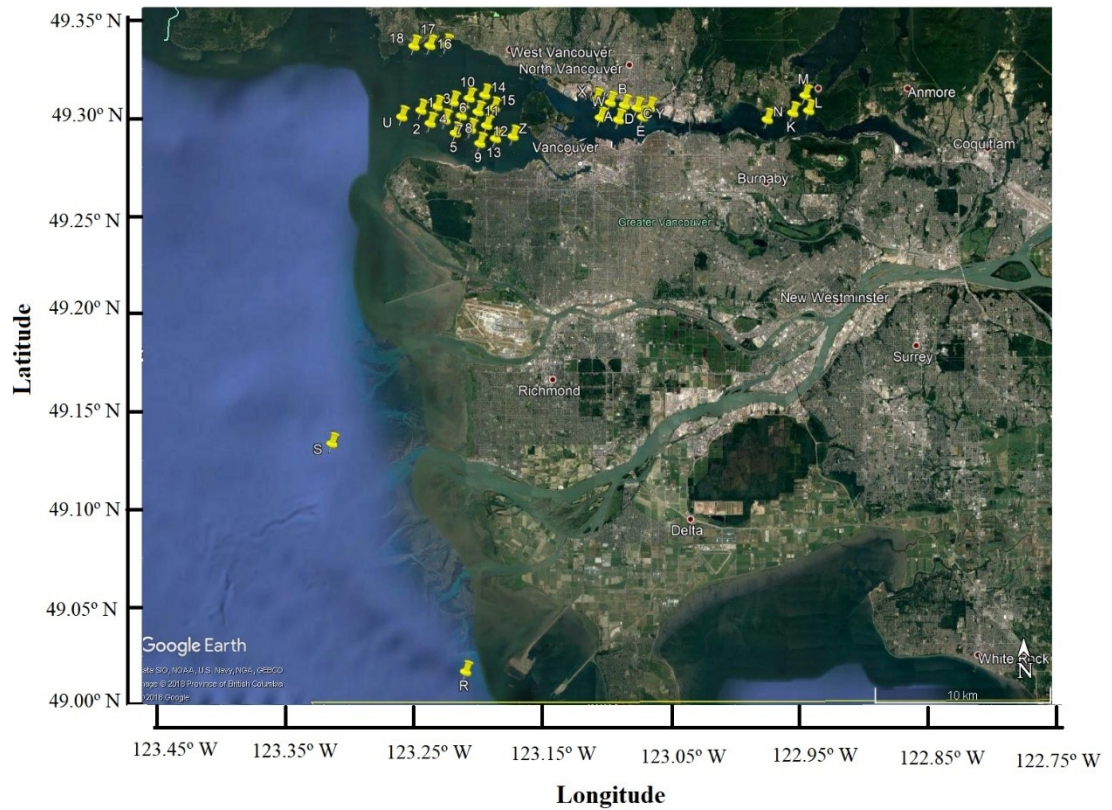


Figure 3.1. Anchorages’ position at the Port of Metro Vancouver (PMV). Modified based on (PMV).

The oil spill was first reported by the public at 16:48 Pacific Time on 8 April 2015 (Gilbert, 2015). It was suspected that IFO-380 (Intermediate Fuel Oil 380) was spilled from the *M/V Marathassa* vessel, which anchored at the location of latitude: 49°17.5167' N, longitude: 123°11.2333' W (Anchorage #12) (Hemmera Envirochem Inc., 2015). During this spill event, several aerial overflights, including the National Aerial Surveillance Program (NASP) flights provided by Transport Canada, were conducted to estimate the pollutant on the water surface and shoreline as shown in Table S3.1. At 12:20 on April 9th, it was estimated that about 2800 liters of spilled oil remained on the water surface (Butler, 2015). This estimate did not include any weathered and previously recovered fuel oil (Butler, 2015). It was estimated that the Western Canada Marine Response Corporation (WCMRC) recovered 1400 L of spilled oil by using three vessels with skimmer equipment (Table S3.2) (Butler, 2015). However, the type and efficiency of the skimmers were not clearly recorded. Later on, the Shoreline Cleanup Assessment Technique (SCAT) teams

surveyed over 85 km of shoreline between 9 April and 23 April 2015 and determined that the most contaminated shoreline was the west side of Stanley Park, North Vancouver, and West Vancouver (Hemmera Envirochem Inc., 2015). On 14 April 2015, the City of Vancouver provided the spilled oil distribution map shown in Figure 3.2, which clearly showed the observed spilled oil on the water surface and the contamination on the shoreline (Stormont, 2015). Unfortunately, the specific cause of this spill was not clear, and the exact volume of spilled oil was unknown.

To understand the fate/trajectory of spilled oil in the marine environment, oil spill models may be used. Examples of this type of model includes: the SPILLCALC by Tetra Tech (Tetra Tech., n.d.), the GNOME (General NOAA Operational Modeling Environment) model by NOAA (National Oceanic and Atmospheric Administration) (NOAA, n.d.), the OSCAR model by SINTEF (Stiftelsen for Industriell of TEknisk Forskning ved NTH – Foundation for Industrial and Technical Research) (SINTEF., n.d.), the OILMAP and SIMAP models by RPS-ASA (Applied Science Associates, Inc.) (RPS-ASA., n.d.-a, n.d.-b), the MOHID water model by MARETEC (Marine and Environmental Technology Research Center) (Fernandes, 2018) and the MIKE Oil Spill model by DHI (Dansk Hydraulisk Institut) (Danish Hydraulic Institute (DHI), n.d.). For application to the TMEP, several organizations and consulting companies have simulated the potential risk of the oil spill in the Burrard Inlet, which geographically includes the English Bay, Vancouver Harbour, as well as in the Salish Sea (the mouth of Burrard Inlet opens onto the Salish Sea) by using various oil spill models. For example, the SPILLCALC model was used to simulate the possible trajectory of spilled diluted bitumen (dilbit) in 2013 (Tetra Tech EBA Inc., 2013); the GNOME model was used to simulate the potential dilbit spill trajectory in 2015 (Genwest System Inc., 2015). However, these previously used models were limited by the following aspects: the stochastic model in SPILLCALC was 2D, which only tracked the surface transport of oil and did not provide the probability of water column contamination, and the study using the GNOME model simulated the trajectory of oil based on rough wind conditions and currents' information, but not the fate/weathering processes.

Oil spill modeling typically incorporates the modeling of hydrodynamic forcing. H3D is a 3D hydrodynamic model that has been used in several studies of the oil spill in the Salish Sea and Burrard Inlet (Stronach & Hospital, 2014; Tetra Tech EBA Inc., 2013, 2015). However, the resolution of this H3D model was relatively low in the study area, with a $1 \text{ km} \times 1 \text{ km}$ horizontal grid space. In order to get a more accurate hydrodynamic forcing for the Salish Sea, the NEMO (Nucleus for European Modeling of the Ocean) model has been applied. The horizontal grid space of the NEMO model was almost uniform from $440 \text{ m} \times 440 \text{ m}$ to $500 \text{ m} \times 500 \text{ m}$ in the Salish Sea (Niu et al., 2016). Unfortunately, this model was unable to simulate currents in the English Bay and Vancouver Harbour. Therefore, a high-resolution hydrodynamic model was needed for the modeling of the oil spill in the English Bay and Vancouver Harbour.

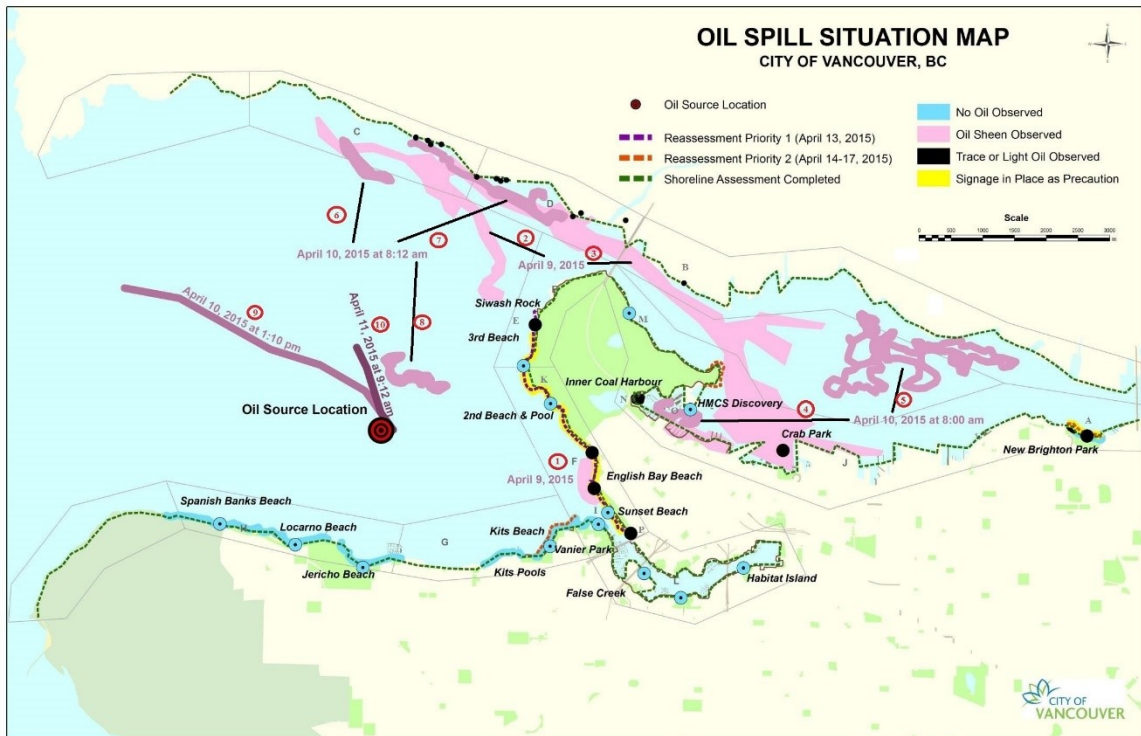


Figure 3.2. The *M/V Marathassa* oil spill situation map (map provided by the City of Vancouver, BC). This map shows the observed spilled oil trajectory on the water surface and the contamination on the shoreline in the English Bay and Vancouver Harbour from 8 to 10 April 2015 (Stormont, 2015). Areas with oil sheen are numbered as 1–10, and contaminated shoreline areas are labeled as A–P.

This study aims to validate a three-dimensional (3D) and high-resolution hydrodynamic model (the Finite-Volume Community Ocean Model (FVCOM)) as the first step. Then, the validated FVCOM output was incorporated into a 3D oil spill model (the Oil Spill Contingency and Response model (OSCAR)) to model the oil spill in the English Bay. Forty numerical simulations were carried out to test this coupled oil spill model based on historical information from the *M/V Marathassa* oil spill. Specifically, the mass balance and trajectory of *M/V Marathassa* spilled oil were simulated by varying different factors, including the oil start of release time, discharge duration, wind forcing and recovery action.

3.3 Materials and Methods

3.3.1 Hydrodynamic Forcing: FVCOM

3.3.1.1 FVCOM Description

The hydrodynamic forcing used for this study was generated using the Finite-Volume Community Ocean Model (FVCOM). It is a 3D, finite-volume and unstructured grid ocean model, which was first developed by Chen et al. (Chen, Liu, & Beardsley, 2003) and further upgraded by joint efforts from researchers at the University of Massachusetts, Dartmouth and Woods Hole Oceanography Institution (Chen, Beardsley, & Cowles, 2006b, 2006a; Chen et al., 2007; Huang et al., 2008). FVCOM allows the use of different resolutions to fit complex coastline and topography by using the triangle mesh system. The model used in the present study was based on the model set up by Wu et al. (Wu, Hannah, O’Flaherty-Sproul, MacAulay, & Shan, Submitted for publication). The model was capable of achieving relatively high resolution in the region of interest (English Bay and Vancouver Harbour in this case), as shown in Figure 3.3. For instance, the horizontal grid spacing is about 10 m in Vancouver Harbour and about 2 m around the bridge bases in the Second Narrows. The vertical grid has twenty-one sigma levels that were stretched gradually, in order to gain higher resolution in the surface and bottom layers. More detailed information of the model can be found in Wu et al. (Wu et al., Submitted for publication).

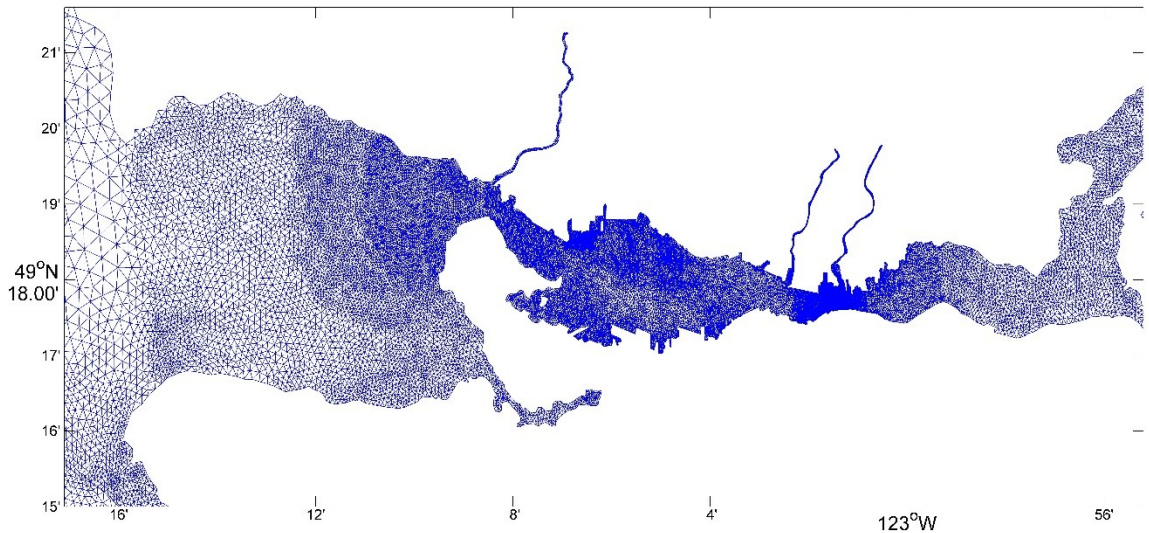


Figure 3.3. Finite-Volume Community Ocean Model’s (FVCOM) horizontal grid in the English Bay and Vancouver Harbour. The horizontal grid space is 10 m in Vancouver Harbour and about 2 m around the bridge bases in the Second Narrows.

3.3.1.2 FVCOM Validation

The overall validation of the model has been done in Wu et al. (Wu et al., Submitted for publication) using tidal gauge water elevations and the ship-mounted Acoustic Doppler Current Profiler (ADCP) current data. Here, we further evaluate the model using surface drifter data, which were obtained from two Surface Current Tracker drifters (SCT). SCT is comprised mainly of wood for the structural support and cellulose sponge for floatation (Page, Hannah, Juhasz, Spear, & Blanken, Submitted for publication). Four aluminum fins are mounted below the sponge to increase the surface area, and a zinc weight is installed at the very bottom of the unit to act as ballast (Page et al., Submitted for publication). There is also a thin aluminum disk installed above the cellulose sponge to facilitate labeling of the SCT with drifter ID and contact information (Page et al., Submitted for publication). SCT is a low-cost, low-impact, easily deployable drifter, tracks the surface currents and reports its location and timestamp (Page et al., Submitted for publication). Two SCT, named SCT1 and SCT2, were released in Vancouver Harbour (SCT1: 49°17.8812' N, 122°57.6414' W; SCT2: 49°17.8788' N, 122°57.6432' W) at 15:11 on 8 November 2015. The drifter’s locations and velocities were recorded every 2–6 minutes. It is notable that a time step of five minutes was applied during simulations.

The modeled trajectory was compared with the observed drifters' trajectory. In addition, the prediction ability of FVCOM was statistically assessed by computing the following measures as shown in Equation (1) - (4) (Spitz & Klinck, 1998; Warner, Geyer, & Lerczak, 2005): The Root-Mean-Square-Error (RMSE):

$$RMSE = \left\{ \frac{1}{N} \sum_{i=1}^N (X_{mod} - X_{obs})^2 \right\}^{\frac{1}{2}} \quad (1)$$

the relative average error (E):

$$E = 100\% \frac{\sum_{i=1}^N (X_{mod} - X_{obs})^2}{\sum_{i=1}^N (|X_{mod} - \bar{X}_{obs}|^2 + |X_{obs} - \bar{X}_{obs}|^2)} \quad (2)$$

the correlation coefficient:

$$R = \frac{\sum_{i=1}^N (X_{mod} - \bar{X}_{mod})(X_{obs} - \bar{X}_{obs})}{[\sum_{i=1}^N (X_{mod} - \bar{X}_{mod})^2 \sum_{i=1}^N (X_{obs} - \bar{X}_{obs})^2]^{\frac{1}{2}}} \quad (3)$$

and the quantitative agreement between model and observations:

$$Skill = 1 - \frac{\sum_{i=1}^N |X_{mod} - X_{obs}|^2}{\sum_{i=1}^N (|X_{mod} - \bar{X}_{obs}| + |X_{obs} - \bar{X}_{obs}|)^2} \quad (4)$$

where X is the variable being compared with a time mean \bar{X} . The subscripts “*mod*” and “*obs*” represent the model results and observations, respectively.

After validating FVCOM, it was run for 10 days (from 5 to –15 April 2015) with a time step of 1 second and saved every 1 hour to generate the hydrodynamic forcing, which did not include the waves, because the study period was reported as “very calm”, the surveillance photo showed no signs of breaking waves (white caps) and the non-breaking wave would also be very low due to low wind. The wave height used in the OSCAR model was computed from winds.

3.3.2 Oil Spill Model: OSCAR

The OSCAR model was used to simulate the mass balance and trajectories of the oil spill, based on the *M/V Marathassa* oil spill's observation data in the English Bay. OSCAR is a 3D particle-based model, which is designed based on SINTEF's experimental field and laboratory data to support oil spill contingency and response decision making. The OSCAR model has broad applications in oil spill modeling and has been validated in many related studies (Aamo, Reed, & Downing, 1997; Abascal et al., 2010; Reed, Aamo, & Downing, 1996; Reed et al., 2000). The general structure of the OSCAR model is similar to most oil spill models as shown in Figure 3.4. The OSCAR model is capable of calculating the oil contamination on the sea surface and shorelines, in the water column and sediment, along with several oil weathering processes. Various oil weathering processes can be simulated by using the OSCAR model, including spreading, drifting, natural dispersion, chemical dispersion, evaporation, stranding, dissolution, adsorption, settling, emulsification and biodegradation of spilled oil. The processes of evaporation, dissolution, and degradation are directly depend on oil composition, while the other processes, such as advection, entrainment, and vertical mixing in the water column are depend on the input components (i.e. tidal, wind and currents) for specific location and time (Reed & Hetland, 2002). To simulate the dispersion, horizontal and vertical advection of entrained and dissolved hydrocarbons in the water column, the random walk procedures were employed. The coefficient for horizontal dispersion (K_x) and vertical diffusion above pycnocline (K_z) can be approximated from data on dye diffusion studies and wave conditions respectively as following (Bowden, 1983; Ichiye, 1967):

$$K_x = 0.0027t^{1.34} \quad (5)$$

$$K_z = 0.028 \frac{H^2}{T} \exp(-2kz) \quad (6)$$

where H is the wave height, T is the wave period, and k is the wave number. In addition, K_z is assumed to be 10^{-4} m²/s for waters below the pycnocline depth.

To calculate the wave height (H) and period (T) in equation (6), the OSCAR model computes the wave condition based on the wind speed (U), water depth (d), fetch (F), and gravitational acceleration (g) as shown in the following equation (US Army Corps of Engineers, 1984):

$$\frac{gH}{U_A^2} = 0.283 \tanh \left[0.530 \left(\frac{gd}{U_A^2} \right)^{3/4} \right] \tanh \left\{ \frac{0.00565 \left(\frac{gF}{U_A^2} \right)^{1/2}}{\tanh \left[0.530 \left(\frac{gd}{U_A^2} \right)^{3/4} \right]} \right\} \quad (7)$$

$$\frac{gT}{U_A} = 7.54 \tanh \left[0.833 \left(\frac{gd}{U_A^2} \right)^{3/8} \right] \tanh \left\{ \frac{0.0379 \left(\frac{gF}{U_A^2} \right)^{1/3}}{\tanh \left[0.833 \left(\frac{gd}{U_A^2} \right)^{3/8} \right]} \right\} \quad (8)$$

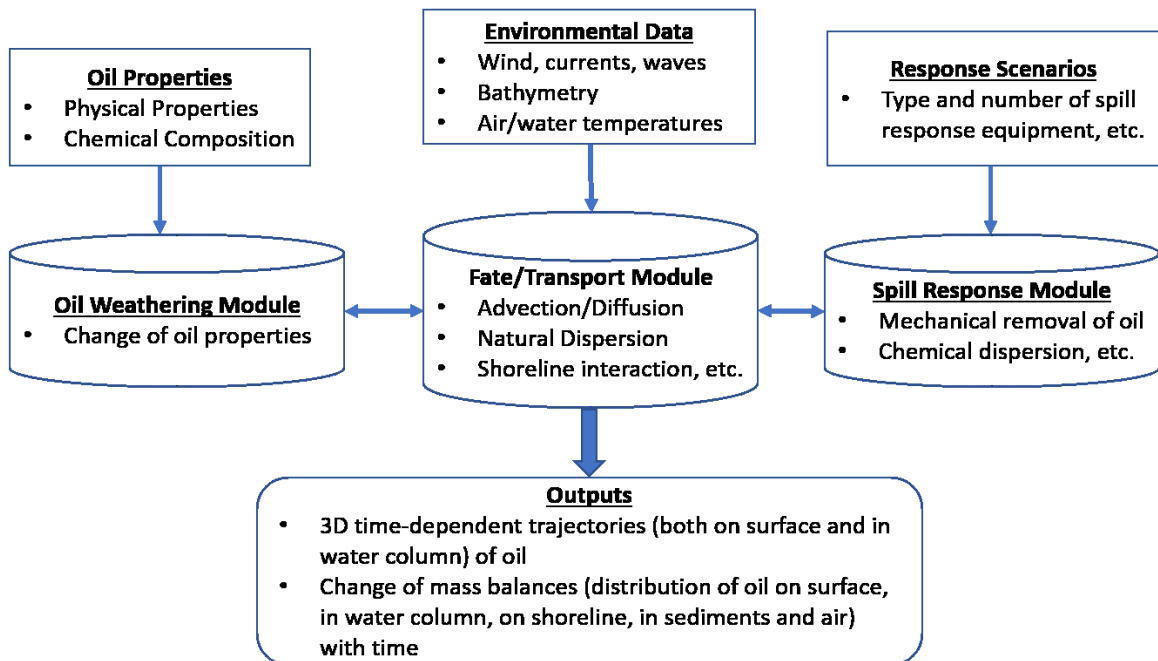


Figure 3.4. Schematic overview of a general oil spill model. Modified based on (Aamo et al., 1997).

3.3.3 Wind Forcing: HRDPS Model

The present study used the wind forcing from the High-Resolution Deterministic Prediction System (HRDPS), which has been employed for weather prediction on the West Coast of Canada (Environment Canada., 2013). HRDPS is a set of the nested and Limited-Area Models (LAM) with forecast grids from the non-hydrostatic version of the Global Environmental Multiscale (GEM) model. This GEM has a 2.5-km horizontal grid spacing. The example of wind speed and direction at 16:00 on 8 April 2015 is shown in Figure 3.5. The dominant wind directions are south, southwest and southeast with speeds below 7 m/s near the release point from 5–12 April 2015, as shown in Figure 3.6.

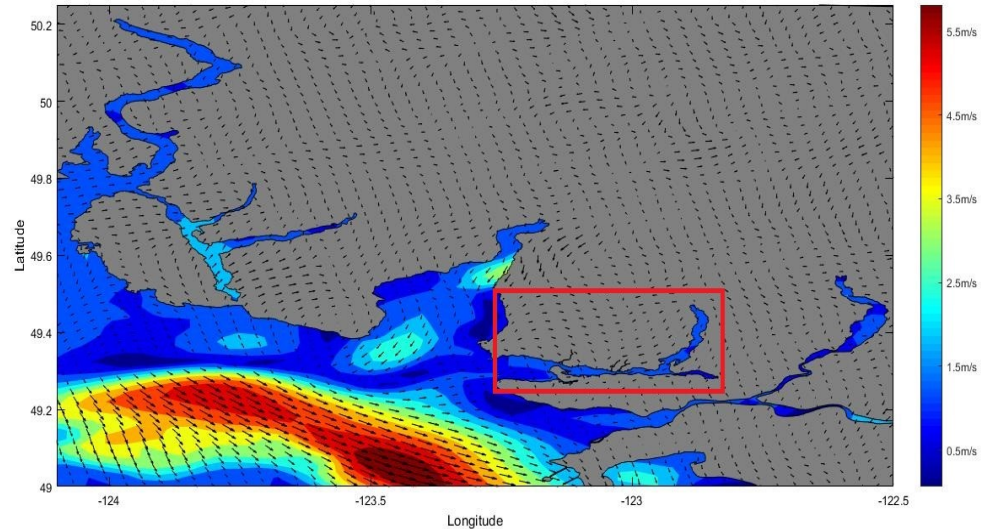


Figure 3.5. Wind speed and direction from the High-Resolution Deterministic Prediction System (HRDPS) (12 April 2015, 16:00). The area in the red square is the studied area.

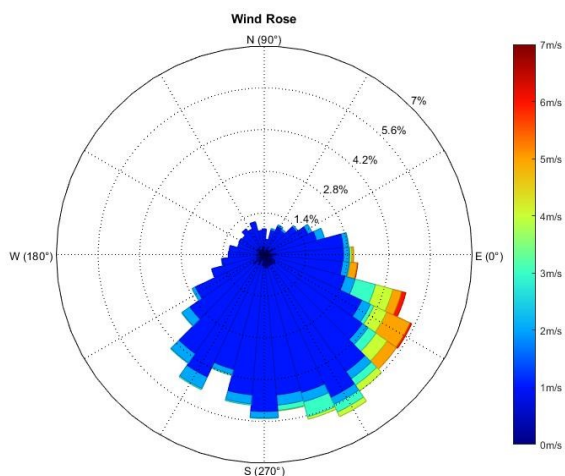


Figure 3.6. Speed, direction and frequencies of the wind near the oil released site (from 5–12 April 2015).

3.3.4 Hindcast Study of the *M/V* Marathassa Oil Spill

3.3.4.1 Identification of Spilled Oil

PMV collected the polluted samples and identified that the spilled oil had an API gravity degree of 13 and a density of 978–979 kg/m³ (979 kg/m³ at 15 °C). The oil chemical compositions were tested as well, and the results showed that the spilled oil contained about 96–99% of bunker fuel. Further testing on oil physiochemical properties illustrated that the spilled oil had comparable physicochemical properties as IFO-380 (Butler, 2015)

IFO-380 is typically classified as a heavy fuel oil with an API gravity of 10–17.1 degrees (density of 950–1000 kg/m³) (Hemmera Envirochem Inc., 2015; Srinivasan, Lu, Sorial, Venosa, & Mullin, 2007). It has a relatively high viscosity (maximum viscosity of 380 cSt at 50 °C (Meng, Wang, & Lee, 2015; SL Ross Environmental Research Ltd., 2004a, 2004b)) and behaves as a semi-solid product at ambient temperature, which leads to a low rate of dispersion and evaporation (Hemmera Envirochem Inc., 2015; Srinivasan et al., 2007). The detailed chemical composition of IFO-380 was adapted from OSCAR’s oil database as shown in Table S3.3.

3.3.4.2 Potentially Influential Factors

As reported, the oil probably began to spill between 11:00 and 16:48 on 8 April 2015, but the exact start time of the release is still unknown. Five possible starting times (12:00, 13:00, 14:00, 15:00 and 16:00) were explored in this study. Although the wind forcing can be obtained via the HRDPS model as illustrated in Section 3.3.3, the wind speed was reported as quite low (<2.6 m/s) during 8–11 April 2015 (Hemmera Envirochem Inc., 2015). It is therefore interesting to study the spilled oil fate and trajectory without taking the influence of the wind into consideration. Because of the lack of information on the duration of oil release and the lack of documentation on the details of recovery actions, the duration of discharge and recovery actions was included in the model study as two additional factors. The discharge duration was assumed as 2 h (a case of a relative instantaneous release) and 22 h (a case of slow release over a long period of time). The case with or without recovery actions was studied to investigate the impact on the fate and trajectory of the spilled oil. It is notable that the assumptions of oil recovery actions were made based on the CCG’s report, as shown in Table S3.4 (Butler, 2015) and the Western Canada Marine Response Corporation’s (WCMARC) website. A summary of the above-mentioned factors that might influence the fate and trajectory of spilled oil is presented in Table 3.1, and detailed setup information for each simulation is shown in Table S3.5.

Table 3.1. The studied factors and their corresponding settings.

Factor	Setting				
	12:00	13:00	14:00	15:00	16:00
Starting-releasing time	12:00	13:00	14:00	15:00	16:00
Wind forcing	With		Without		
Discharge duration	2 h		22 h		
Recovery action	Yes		No		

3.3.4.3 Deterministic Approach

The oil spill modeling can use both deterministic and stochastic approaches. A deterministic approach is used to simulate the fate and behavior of oil from a single model run. This approach is helpful when studying a known historical oil spill event. A stochastic approach, on the other hand, is used to analyze the probability of oil contamination in the

area of concern by overlaying a great number (tens to thousands) of individual deterministic simulations.

In this study, a deterministic approach was employed to study the mass balance and trajectories of the oil spill occurring on 8 April 2015. For each simulation, the oil was assumed to be released at Anchorage #12 (latitude: 49°17.5167' N, longitude: 123°11.2333' W) in the English Bay and then tracked for 3 days. A track duration of 3 days was used, because only a trace amount of spilled oil (5.9 L) remained on the water surface after 3 days, as reported by Transport Canada (Butler, 2015). A time step of 20 min was selected to run the model. Since the hydrodynamic forcing was hourly, the use of a 20-min time step based on interpolation of current data helps to simulate a relatively smooth particle trajectory with less computation requirement compared with smaller steps (such as 1 min). The mass balances and trajectories for each individual simulation were saved every 1 h and represented by using 5000 particles. The chosen number of particles would affect the simulation to some extent. The use of 5000 is based on the preliminary test using 1000, 5000 and 10,000 particles. While the use of 1000 can produce a trajectory similar to that of 10,000, the use of a large number retains more details of the concentration field. Using 5000 can provide better details with less computational demand. This was also discussed in Reed and Hetland (Reed & Hetland, 2002).

3.3.5 Statistical Analysis on Mass Balance

A full factorial design that incorporates the studied factors and their corresponding settings (Table 3.1) was generated by using Minitab software (version 18.1), resulting in $5 \times 2 \times 2 \times 2 = 40$ combinations in total. The mass balance (%) of oil calculated for the water surface, shoreline, water column, atmosphere, biodegradation and recovery were selected as the studied response. Analysis of Variance (ANOVA) was carried out to evaluate the influence statistically of the studied factors on the mass balance. A p -value < 0.05 indicates that a certain factor has a significant influence on the mass balance. The normal distribution and constant variance on the error terms were assured during analysis, as well.

3.4 Results

3.4.1 FVCOM Validation

In order to validate the FVCOM, the simulated trajectory and velocities (U-velocity and V-velocity) from the model were compared with the observational data from the SCT drifters (SCT1 and SCT2). The simulated and observed trajectory are plotted in Figure 3.7 and Figure 3.8 for SCT1 and SCT2, respectively. It can be noticed that both SCT1 and SCT2 moved from east to west (Central Harbour to Second Narrow to Vancouver Harbour), and the modeled trajectory was comparable to the observed trajectories for both SCT1 and SCT2.

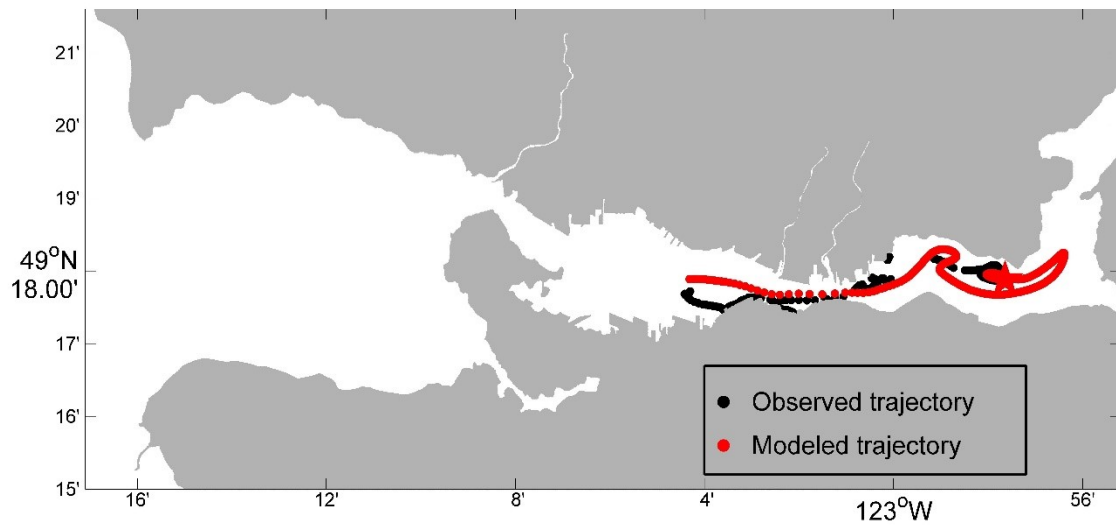


Figure 3.7. Trajectory comparison between Surface Current Tracker 1 (SCT1) drifter data and FVCOM data. The trajectory starts at the star.

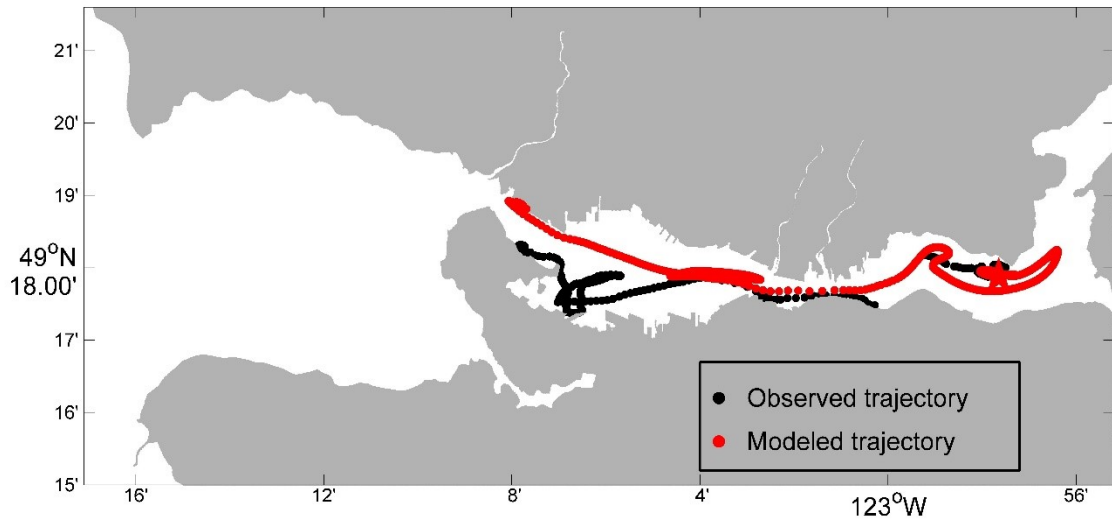


Figure 3.8. Trajectory comparison between SCT2 drifter data and FVCOM data. The trajectory starts at the star.

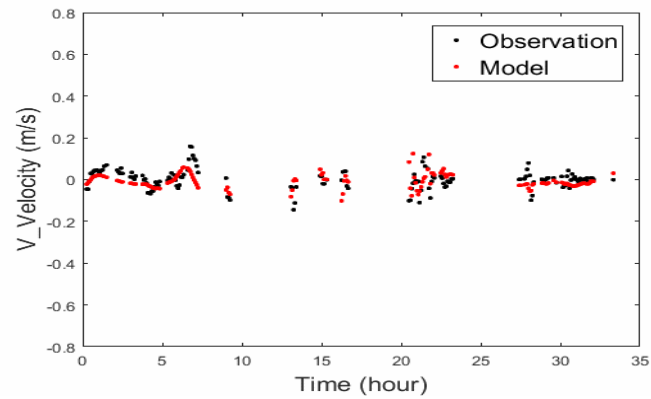
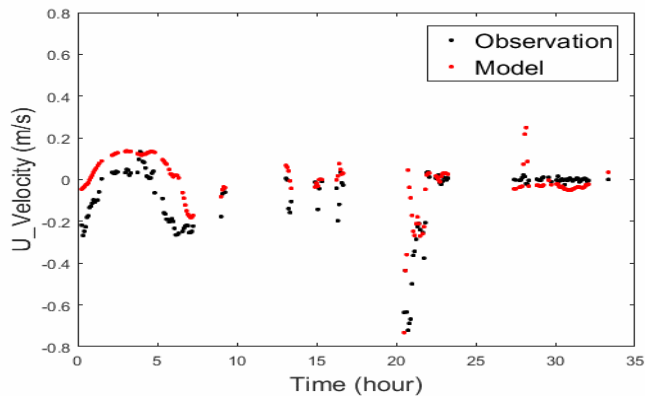


Figure 3.9. Time series velocities comparison between observed SCT1 drifter data and FVCOM data. U-velocity is on the left, and V-velocity is on the right.

29

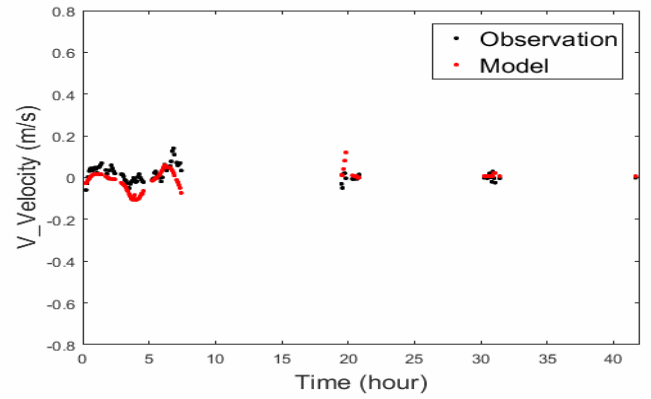
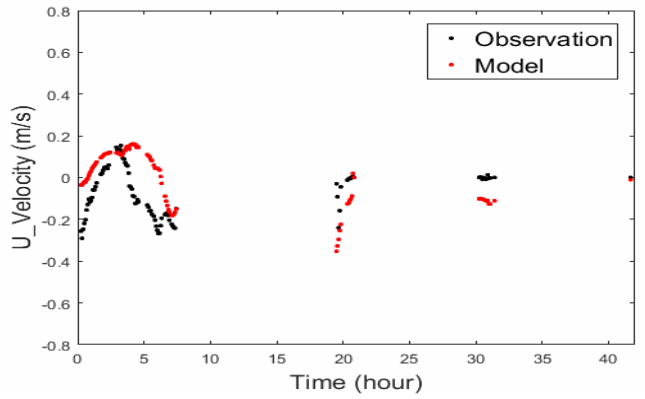


Figure 3.10. Time series velocities comparison between observed SCT2 drifter data and FVCOM data. U-velocity is on the left, and V-velocity is on the right.

To quantify the prediction ability of FVCOM for velocities, statistical analysis, including the RMSE, relative average error (E), correlation coefficient (R) and skill, was carried out as presented in Table 3.2. Both RMSE and E for FVCOM were satisfactorily low (less than 0.16 m/s and 77%, respectively) indicating that only a slight difference existed between modeled and observed velocities. The correlation between the modeled and observed velocities was represented by R values, and their significance levels were indicated by p -values. As shown in Table 3.2, all p -values were lower than 0.05, which again demonstrated the satisfied correlation between modeled and observed velocities. The skill values were all greater than 0.51, which further verified the agreement between modeled and observed velocities.

The time series velocities from simulations and observations for SCT1 and SCT2 are plotted in Figure 3.9 and Figure 3.10, respectively. In general, the simulated velocities matched well with that of observed data, even though some data were not recorded for unknown reasons. Overall, FVCOM was validated by using data from observed drifters, including trajectory and velocities in this study.

Table 3.2. Results of statistical analysis between model simulations and observations.

Statistical Measures	SCT1		SCT2	
	U-Velocity	V-Velocity	U-Velocity	V-Velocity
Root-Mean-Squared-Error ($RMSE$) (m/s)	0.149	0.056	0.158	0.052
Relative average error (E) (%)	48.65	76.38	73.42	68.44
Correlation coefficient (R)	0.618	0.256	0.310	0.383
p -value for R	0.000	0.001	0.003	0.000
Skill	0.719	0.514	0.577	0.551

3.4.2 Impacts of Studied Factors on Oil Mass Balance and Trajectory

After validating FVCOM for hydrodynamic forcing, it was incorporated into the OSCAR model to study the mass balance and trajectory of the oil spilled from the *M/V Marathassa*. Four potential factors mentioned in Section 3.3.4.2 might influence the spilled oil mass balance, including the release start time, oil discharge duration, wind forcing and recovery actions. The raw data on their influence on the mass balance of oil (e.g. water surface, shoreline, water column, sediments, atmosphere, biodegraded and recovered) are presented in Table S3.6. Since the mass balance for the water column, sediments, atmosphere and biodegraded were all less than 3% due to the very weak wind/waves, only the oil components at the water surface, on the shoreline and the oil recovered were statistically analyzed in this study. Analysis of Variance (ANOVA) was carried out, and the *p*-values for the influence of studied factors on the oil mass balance are presented in Table 3.3. The detailed mass balance distributions (after three days of tracking) are provided in Figure 3.11. In addition, the examples of trajectory comparison are shown in Figures S3.1–S3.4.

3.4.2.1 Influence of Release Start Time

From Table 3.3, it can be clearly seen that the oil start of release time had a significant impact on the mass balance of water surface, shoreline and recovered, as their *p*-values were less than 0.05. About 32.7% of spilled oil remained on the water surface and heavy contamination on the shoreline (63%) when the oil started spilling at 12:00, as shown in Figure 3.11a. In comparison with the 12:00 start of release time, the shoreline contamination was reduced (52.8%) along with an increased amount of spilled oil on the water surface (37.9%) when oil spill started from 13:00. If recovery was conducted, 7.46% of the oil was removed when it was released at 13:00. Interestingly, much more spilled oil (36.4%) can be recovered when the start of release time was 14:00, along with 32.9% contamination on the shoreline. The similar contamination on the shoreline was also observed if the oil spill started at 15:00 and/or 16:00, but larger amounts of spilled oil remained on the water surface (54.7% for and 70.5% for 16:00), rather than being recovered. In terms of oil trajectory, overall, the earlier the oil spill occurred, such as 12:00,

the greater the contamination of the water surface and shoreline. However, this difference was not significant when the oil spill started at 14:00 and 15:00 (Figure S3.1).

3.4.2.2 Influence of Wind

The effect of the wind was to increase the amount of oil on the shoreline and decrease the amount of oil on the water surface compared to the no-wind simulation (Table 3.3 and Figure 3.11b). Specifically, the fraction of oil remaining on the surface decreased from 67% to 23%, and the amount of oil on the shore increased from 21% to 56%. This can be seen in the trajectory results (Figure S3.2), which illustrate the heavy contamination on the shoreline of West Vancouver and the western side of Stanley Park. The amount of oil recovered stayed roughly constant at 15–20% and was not influenced by wind forcing in this study.

3.4.2.3 Influence of Discharge Duration

A short discharge duration (2 h) led to more serious shoreline contamination (54.1% vs. 22.2%) than that of long discharge duration (22 h) and resulted in less oil on the water surface (29.6% for 2 h vs. 54.1% for 22 h). Most of the contaminant was still concentrated on the water surface around the release location after 3 days tracking when a long discharge duration was taken into consideration (Figure S3.3). The discharge duration did not play a significant role in the amount of oil recovered.

Table 3.3. The *p*-values for the influence of studied factors on oil mass balances. Significant influence (*p*-value <0.05) is shown in bold.

Source	Water Surface	Shoreline	Recovered
Start-releasing time	0.000	0.001	0.008
Wind	0.000	0.000	0.196
Discharge duration	0.000	0.000	0.760
Recovery action	0.003	0.179	0.000

3.4.2.4 Influence of Recovery Action

Whether the recovery action did not significantly influence the mass balance of the oiled shoreline (Table 3.3), as well as the oil trajectory (Figure S3.4), only about 34.4% of

the spilled oil remained on the water surface, if the recovery action removed 30.2% of the oil, and 33.5% ended up on the shoreline, as shown in Figure 3.11d. When no recovery action was taken (0% of recovered oil), 55.6% of spilled oil remained on the water surface, and 42.8% contaminated the shoreline.

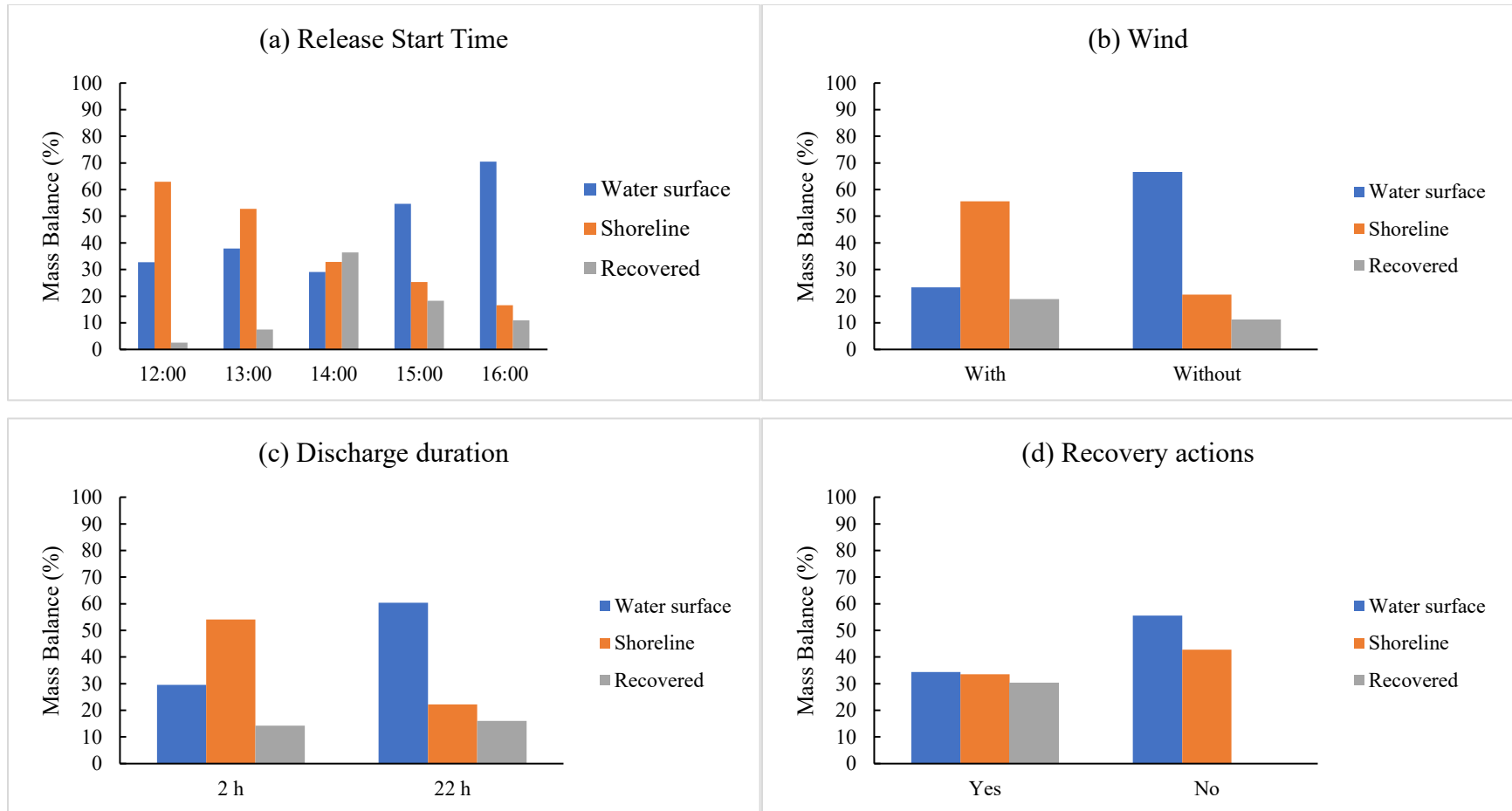


Figure 3.11. The influence of studied factors (a) release start time, (b) wind, (c) discharge duration and (d) recovery action on the mass balance of water surface, shoreline and recovered.

3.5 Discussion

3.5.1 FVCOM Validation

In general, the simulated trajectory and velocities from the FVCOM were comparable with that of SCT drifters in this study. However, it was relatively less capable of predicting SCT2 U-velocity, as shown in Table 3.2. This is likely due to the following three reasons: (1) The SCT drifter used in this study was a shallow water drifter that worked close to the water surface. This type of shallow drifter was therefore susceptible to the surrounding windage, which could potentially cause higher uncertainty on recorded data. This was supported by a similar statement that was proposed by Halverson et al. (Halverson, Gower, & Pawlowicz, 2018) to explain the inconsistency of radial and observed velocities. (2) Relatively more observed data of SCT2 velocity were missed, which resulted in a less thorough comparison of modeled and observed data. (3) The difference between the model and the drifters may also be due to the winds and waves, which are not included in FVCOM.

3.5.2 Hindcast of the *M/V Marathassa* Oil Spill

3.5.2.1 Comparison of Oil Trajectory

The model simulations of oil trajectory were evaluated and compared with the observed oil distributions, as shown previously in Section 3.1 (Table S3.1 and Figure 3.2). The oil distribution map indicated the observed oil trajectory on the water surface and the contamination on the shoreline in the English Bay and Vancouver Harbour from 8–10 April, 2015 (Stormont, 2015). The contaminated water surface area was labeled as 1–10, and the contaminated shoreline area was labeled as A–P. The comparison of the results of modeled and observed for water surface and shoreline contamination are listed in Table S3.7 and Table S3.8, respectively. Four scenarios achieved the highest matches with the observation data. The studied factors' setting in these four scenarios was: (1) oil started to release at 14:00, discharged continuously (22 h), with wind and without recovery actions (labeled as Scenario #4 in Table S3.5); (2) oil started to release at 14:00, discharged

continuously (22 h), with wind and recovery actions (labeled as Scenario #8 in Table S3.5); (3) Scenario #4, which started to discharge at 15:00; (4) Scenario #8, which started to discharge at 15:00.

As described in Section 3.4.2.1 and Section 3.4.2.4, there was almost no difference between the oil trajectories whether or not the recovery action was used, and the difference of trajectories was not significant when oil started to discharge at 14:00 and 15:00. Therefore, as shown in Table 3.4 and Table 3.5, those four scenarios mentioned above have achieved 70% and 62.5% matches in the comparison of surface contamination and shoreline contamination, respectively.

The oil trajectory in Scenario #4 that started at 14:00 is plotted in Figure 3.12. It can be seen that oil was first transported east of the oil release point and then moved to the southwest in the next twelve hours under the forcing of hydrodynamics and wind. Spilled oil was forced and moved into the First Narrow and eventually entered into Vancouver Harbour, which resulted in heavy oil contamination on the water surface and the shoreline around Vancouver Harbour and the First Narrow. There was no oiled shoreline until 19:00 (9 April 2015) when the oil reached English Bay Beach, which confirmed well to the observed information (Butler, 2015; Hemmera Envirochem Inc., 2015). The majority of shoreline contamination was on the west side of Stanley Park, West Vancouver, and North Vancouver, which matched the observation data well (Butler, 2015; Hemmera Envirochem Inc., 2015).

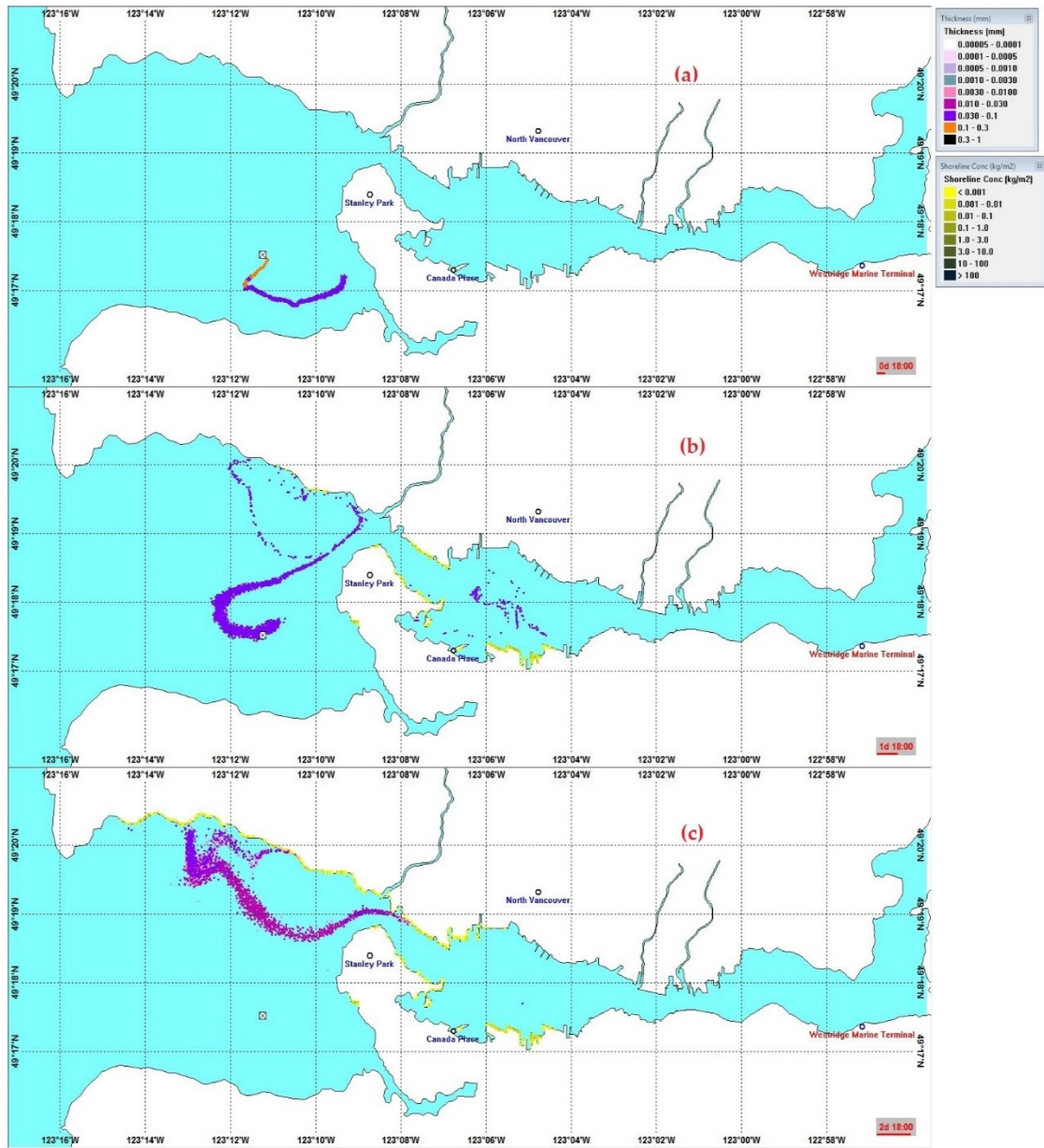


Figure 3.12. Example of oil trajectories for the oil spill that started to discharge at 14:00 on 8 April 2015. Spilled oil discharged continuously (22 h) and then tracked with wind and without recovery actions (labeled as Scenario #4 in Table S3.5). Figures from top to bottom are oil distribution at 8:00 on (a) 9 April, (b) 10 April and (c) 11 April 2015.

Table 3.4. Examples of water surface contaminant comparison. The simulated results were compared with observation data.

Start-Releasing Time	Scenarios #	Labels of Surface Contaminant										Matches (%)
		1	2	3	4	5	6	7	8	9	10	
14:00	4	√	×	√	√	×	√	√	√	√	×	70
	8	√	×	√	√	×	√	√	√	√	×	70
15:00	4	×	√	√	√	√	×	√	√	√	×	70
	8	×	√	√	√	√	×	√	√	√	×	70

Scenario #4 represents oil discharged continuously (22 h), which then moves with the wind and without recovery actions; Scenario #8 represents oil discharged continuously (22 h), which then moves with wind and recovery actions. Detail factors' setting in each scenario is shown in Table S3.5. “×” means the simulated results do not match with the observed data; “√” indicates the simulated results match the observed data.

Table 3.5. Examples of shoreline contaminant comparison. The simulated results were compared with observation data.

Time to Start Spill	Scenarios #	Labels of Shoreline Contaminant																Matches (%)
		A	B	C	D	E	F	G	H	I	J	K	L	M	N	O	P	
14:00	4	×	√	√	√	√	×	√	√	√	√	×	√	×	√	×	×	62.5
	8	×	√	√	√	√	×	√	√	√	√	×	√	×	√	×	×	62.5
15:00	4	×	√	√	√	√	×	√	√	√	√	×	√	×	√	×	×	62.5
	8	×	√	√	√	√	×	√	√	√	√	×	√	×	√	×	×	62.5

Scenario #4 represents oil discharged continuously (22 h), which then moves with the wind and without recovery actions; Scenario #8 represents oil discharged continuously (22 h), which then moves with wind and recovery actions. Detail factors' setting in each scenario is shown in Table S3.5. “×” means the simulated results do not match with the observed data; “√” indicates the simulated results match the observed data.

3.5.2.2. Comparison of Mass Balance

The oil mass balance in the simulations of the above-mentioned four scenarios was compared with that from the 2D, Automated Data Inquiry for Oil Spills (ADIOS, version 2.0) model (in CCG's report) (Hemmera Envirochem Inc., 2015). In CCG's report, the ADIOS2 model was employed to study the mass balance of spilled IFO-380. Three metric tons (about 3067 L) of IFO-380 were assumed to be spilled at 4 Coordinated Universal Time (UTC) on 9 April 2015 (18:00 Pacific time on 8 April 2015) and then tracked for five days. A constant wind speed of 10 knots (about 5.14 m/s) was selected in CCG's modeling (Hemmera Envirochem Inc., 2015).

The modeling results from the ADIOS2 model (Figure 3.13) indicated that approximately 11% and 2% of the oil was expected to evaporate and disperse, respectively after three days post spill. The other 87% of spilled oil was expected to remain on the water surface. This proportion of evaporation and remaining oil was totally different from OSCAR's modeling. In Scenario #4, as shown in Figure 3.14 and Figure 3.15, around 1.4% of spilled oil was predicted to evaporate after three days of tracking. About 24.9% and 43.1% of the spilled oil were expected to contaminate the shoreline in Scenario #4 that started at 14:00 and 15:00, respectively. There are a number of reasons that could contribute to the different mass balance in the ADIOS2 and OSCAR models. The first main reason is that oil was trapped on shorelines as observed by oil spill responders. This process was included in the OSCAR model because it is a 3D fate/transport model that uses geographic and bathymetry data. By contrast, ADIOS2 is a weathering only model, and it has a limitation in accurately representing the significant onshore component. Another main difference is the evaporation, of which the rate is affected by wind, wave, currents and temperature (Hemmera Envirochem Inc., 2015). The wind and currents conditions are very different in this study and CCG's modeling.

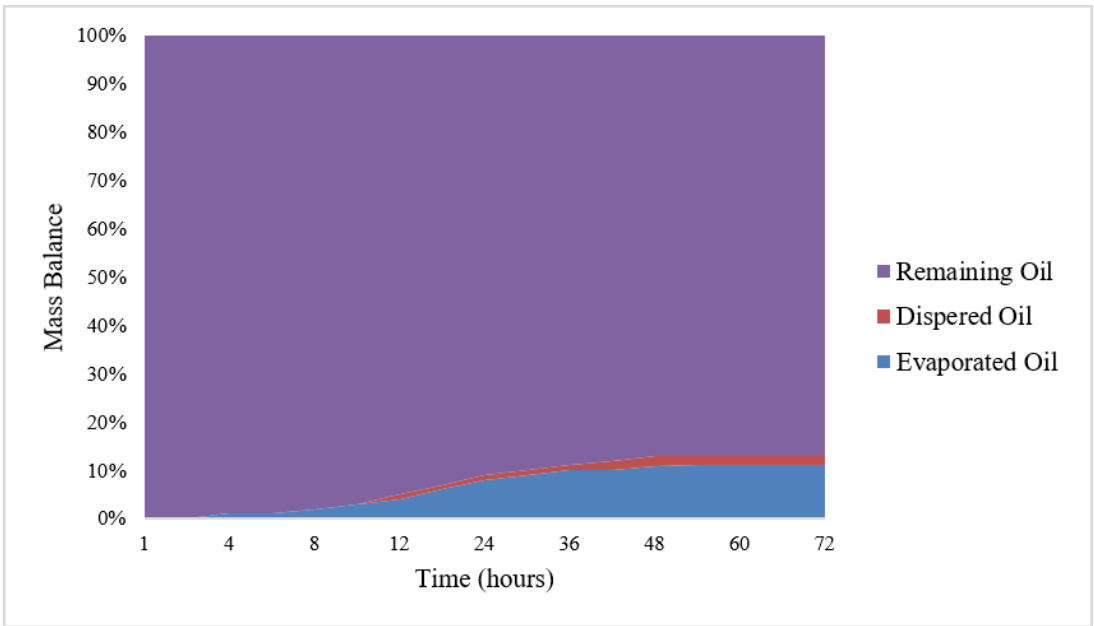


Figure 3.13. Automated Data Inquiry for Oil Spills (ADIOS, version 2.0) model’s predictions of evaporated, dispersed and remaining (surface) Intermediate Fuel Oil 380 (IFO-380) oil after three days of simulation.

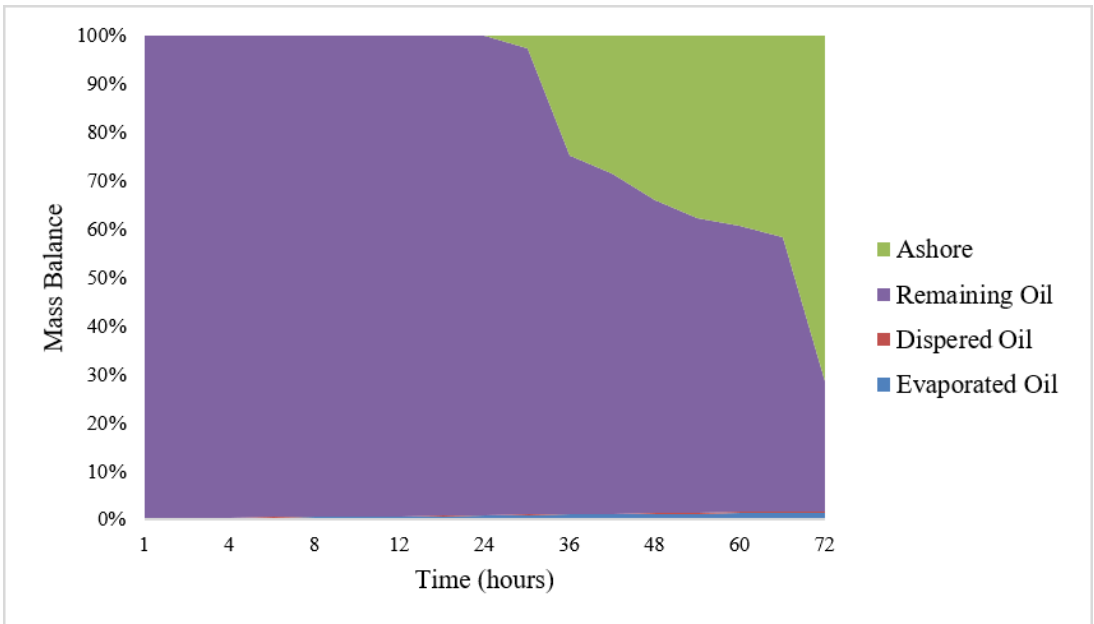


Figure 3.14. OSCAR model’s predictions of evaporated, dispersed, remaining (surface contaminant) and ashore (shoreline contaminant) IFO-380 oil after three days of tracking in Scenario #4 and started at 14:00.

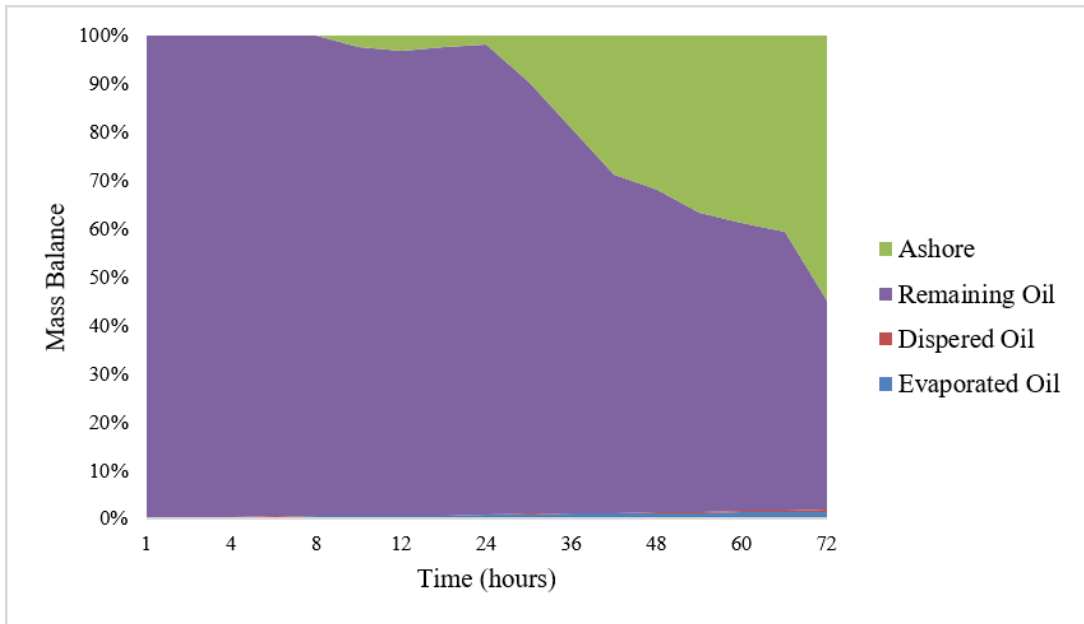


Figure 3.15. OSCAR model’s predictions of evaporated, dispersed, remaining (surface contaminant) and ashore (shoreline contaminant) IFO-380 oil after three days of tracking in Scenario #4 and started at 15:00.

By comparison, a lesser proportion of the spilled oil remained on the water surface in Scenario #8 due to recovery actions. Nearly 61.8% (1730 L) and 65.5% (1834 L) of the spilled oil were recovered when oil was discharged at 14:00 and 15:00, respectively. The modeled recovered oil was more than the actual volume of spilled oil recovered, which was probably due to the lack of information reported by the response vessels.

Overall, among the total number of forty studied scenarios, the results from four scenarios agree well with observations. The results indicate that the *M/V Marathassa* oil spill was most likely started between 14:00 and 15:00 on 8 April 2015. This spill was most likely a continuous slow release for an unknown period (assumed to be 22 h in this study) instead of an instantaneous release.

3.6 Conclusions

The FVCOM implementation for English Bay and Vancouver Harbour was further validated in this study by comparing the simulated trajectory and velocities with that of

observed data from SCT drifters (SCT1 and SCT2). This validated FVCOM was then used to generate the hydrodynamic forcing in English Bay and Vancouver Harbour, which was input in the state-of-art OSCAR model to simulate the *M/V Marathassa* oil spill.

The *M/V Marathassa* oil spill event was numerically simulated to assess the ability of the coupled oil spill model. Forty scenarios were performed using the OSCAR model to study the effects of various input parameters on the fate and transportation of spilled oil. The results were compared with the available data of the *M/V Marathassa* oil spill. The trajectories from four scenarios match well with the observed data. The assumed recovery actions were performed better in the scenario of oil discharged continuously (22 h) with winds at 14:00 than that in the other simulations. The combined results of trajectory and mass balance indicated that the *M/V Marathassa* oil spill probably started between 14:00 and 15:00 (8 April 2015) and kept discharging oil for a relatively long time (assumed to be 22 h in this study). The weathering processes and movement of spilled oil and contamination distribution in the surrounding waters and coastlines were affected by wind and currents.

In general, the oil spill model integrating the OSCAR and FVCOM has effectively simulated the offshore and onshore distributions of the *M/V Marathassa* oil spill. To our best knowledge, this is the first study that modeled the oil spill in the English Bay and Vancouver Harbour by using the OSCAR model.

3.7 Supplementary Materials

The following are available online at <http://www.mdpi.com/2077-1312/6/3/106/s1>: Figure S3.1. Example of oil trajectories for the oil spill with different oil start-releasing time. Figures from top to bottom are oil start release at (a) 12:00, (b) 13:00, (c) 14:00, (d) 15:00 and (e) 16:00; Figure S3.2. Example of oil trajectories for spilled oil forced without wind (top) or with winds (bottom); Figure S3.3. Example of oil trajectories for oil discharge instantly (top) or continuously (bottom); Figure S3.4. Example of oil trajectories for oil spill without (top) or with (bottom) recovery actions; Table S3.1. Aerial overflight surveys for the *M/V Marathassa* oil spill; Table S3.2. Western Canada Marine Response

Corporation's (WCMRC) response to the spill; Table S3.3. The chemical composition of IFO 380 in the OSCAR model; Table S3.4. Assumptions for mechanical response strategies (recovery actions); Table S3.5. Factors' setting in each simulation; Table S3.6. The influence of studied factors on the mass balance of *M/V Marathassa* spilled oil; Table S3.7. Water surface contaminant comparison. The simulated results were compared with observation data; Table S8. Shoreline contaminant comparison. The simulated results were compared with observation data.

3.8 Acknowledgments

The authors acknowledge the Natural Sciences and Engineering Research Council of Canada (NSERC), the Marine Environmental Observation Prediction and Response Network (MEOPAR), the National Contaminants Advisory Group (NCAG) and the Fisheries and Oceans Canada (DFO). SINTEF Marine Environmental Technology is thanked for providing the OSCAR oil spill model.

3.9 Transition Section

Chapter 3 has illustrated hindcast study of *M/V Marathassa* oil spill in the English Bay by using OSCAR model that forced by FVCOM model. In order to further investigate the potential risk of oil spill from other locations in the English Bay, the stochastic modeling of oil spill from the twenty PMV anchorages in the English Bay will be presented in Chapter 4.

CHAPTER 4: A STOCHASTIC MODELING STUDY OF THE IMPACT OF OIL SPILL LOCATION ON THE FATE AND TRANSPORT OF OIL SPILLS IN VANCOUVER HARBOUR

4.1 Abstract

The potential risk of oil spill in Vancouver Harbour, as well as in the English Bay, is expected to increase due to the expected increase of vessel traffic in Port of Metro Vancouver (PMV) as the result of the proposed Trans Mountain Expansion Project (TMEP) in the BC coast. In this chapter, the fate and transport of the oil spills will be modeled using the three-dimensional and particle-based Oil Spill Contingency and Response (OSCAR) model based on stochastically approach. The model will be forced by the hydrodynamic forcing from the Finite-Volume Community Ocean Model (FVCOM). Twenty anchorages in the English Bay were selected to study the impacts of different spill locations on the fate and transport of oil spill in the English Bay and Vancouver Harbour. The tidal excursion length in the English Bay and Vancouver Harbour that calculated based on the hydrodynamic variables from FVCOM model was also studied and compared with the probability of oil contamination. The results indicated that the probability of contamination and the contamination areas in water column, on water surface, and on the shoreline were very sensitive to the oil discharge locations in the English Bay. Moreover, the transport of the spilled oil was mainly controlled by the tidal currents, which were strongly sensitive to the local coastline and bathymetry, and wind in the English Bay and Vancouver Harbour.

4.2 Introduction

Port of Metro Vancouver (PMV) is the largest port by tonnage in Canada and the third largest in North America (AAPA, 2016). PMV locates on the southwest coast of British Columbia (BC), extending from Robert Banks (parts of Salish Sea) to Burrard Inlet with 34 anchorages in total. As the largest import and export port in Canada, in 2017, PMV handled 142 million tonnes of cargo, which accounts for about 42% of all cargo through Canada (335 million tonnage) (Government of Canada, 2018; VFPA, 2018). This huge

amount of cargo handling results in a heavy traffic in the BC coast, especially in Vancouver Harbour. The traffic in BC coast is expected to increase by seven folds due to the proposed Trans Mountain Pipeline Expansion (TMPE) project (Zmuda, 2017). This busy and growing marine traffic in BC coast increases the potential risk of oil spill. Therefore, the local authorities and oil companies have attempted to develop well-structured contingency plans that allow the quick responses to the oil spill if it happens.

The fate and behaviour of the spilled oil in ocean/aquatic environment is an important component of contingency planning, and they can be simulated by the well-established numerical modeling (ASCE, 1996; Reed et al., 1999; Spaulding, 2017). Several numerical modeling efforts have been made to simulate the fate and behaviour of the spilled oil in the Salish Sea and Vancouver Harbour by using various oil spill models (Genwest System Inc., 2015; Niu et al., 2016; Tetra Tech EBA Inc., 2013). However, as shown in Section 2.5, there are still some limitations in these investigations. To fill this gap, in 2018, the OSCAR model incorporated the hydrodynamic forcing from FVCOM model, of which the horizontal grid spacing is about 10 m in Vancouver Harbour and about 2 m around the bridge bases in the Second Narrows, was implemented to simulate the oil spill in the English Bay and Vancouver Harbour (Chapter 3 in this thesis) (Zhong et al., 2018). The prediction ability of this coupled model (OSCAR + FVCOM) was assessed by the hindcast study of *MV Marathassa* oil spill, and about 70% matches between modeled trajectory and observations was achieved. It is worthwhile to mention that although the developed OSCAR+FVCOM model exhibited general satisfactory performance on the oil spill modeling in the English Bay and Vancouver Harbour, only oil spill from one location, the anchorage #12, for *MV Marathassa* oil spill was studied in Chapter 3 (Zhong et al., 2018). However, in English Bay, there are many other anchorages that might encounter oil spills. It is therefore necessary to investigate the impacts of oil release locations on the oil spill fate and transport by using OSCAR+FVCOM model.

The fate and transport of spilled oil is highly associated with the tidal current, especially in tidal-dominated bay (Geyer & Signell, 1992). Tidal excursion length, a net horizontal distance traveled by a water particle from low water slack to high water slack or vice versa (Ji, 2017), is usually used to study the distribution of pollutants in ocean/aquatic

environment (Barrett, 1972; Ji, 2017; Valle-Levinson, 2013). For instance, tidal excursion length was used as a criterion to indicate the potential area that may be influenced by suspended and dissolved materials generated from aquaculture activities (Valle-Levinson, 2013). Currently, there is still a lack of research using tidal excursion length to explain the movement and distribution of oil pollution. Thus, it is worthwhile to utilize the tidal excursion length to investigate the influence of locations on the water particles movement and distribution, which will be helpful to better understand the impact of oil release locations on the fate and transport of the spilled oil.

This study aims to use the OSCAR model that was forced by the hydrodynamic forcing from FVCOM model, to investigate the impacts of oil release locations on the fate and transport of the spilled oil in English Bay. A stochastic approach was employed to study the fate and transport of the oil spill occurring in the twenty anchorages in the English Bay. The tidal excursion length simulated by FVCOM model was also used to assist the above-mentioned investigations in the present work.

4.3 Method and Material

4.3.1 Studied Area

Vancouver Harbour is geographically included by Burrard Inlet, which located in the southeastern of B.C. As shown in Figure 4.1, Vancouver Harbour is separated from the English Bay, which open to Strait of Georgia (part of Salish Sea), at the westward with the First Narrows. In the eastward, the Second Narrows separates the Vancouver Harbour and the Central Harbour.

Oil spill has been of major concern and are regarded as one of the most critical forms of marine pollution in the English Bay and Vancouver Harbour due to the busy vessel traffic. For instance, an oil spill took place in the English Bay (anchorage #12) on 8 April 2015, which resulted in at least 2800 L of oil released from the cargo vessel, *M/V Marathassa* (Butler, 2015). As shown in Figure 4.1, twenty anchorages from PMV are consisted in the English Bay. The locations of these twenty anchorages were selected as

the spill sites to study the impacts of oil spill location on the fate and transport of spilled oil.

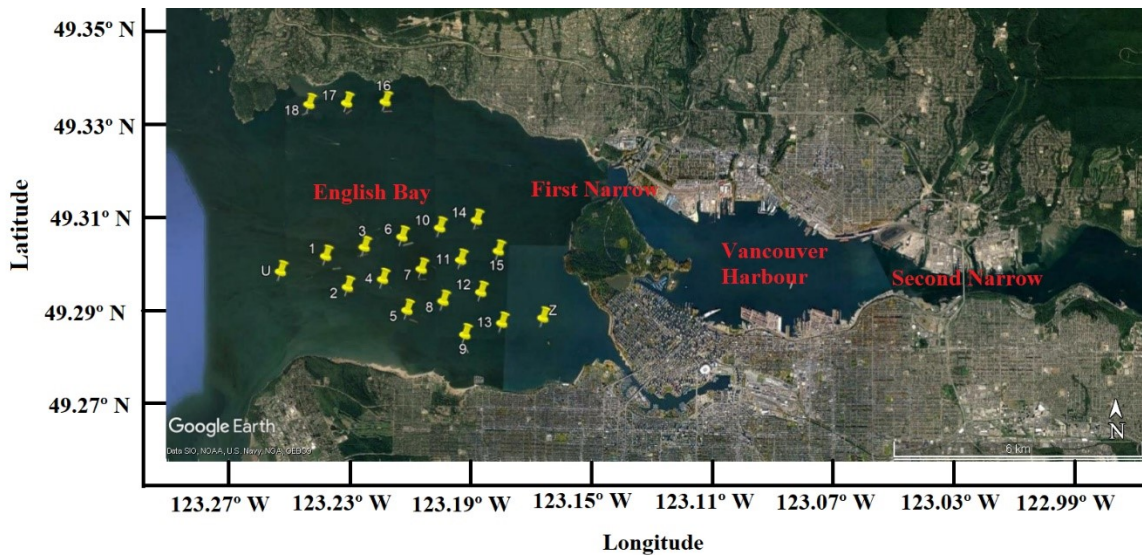


Figure 4.1. Locations of twenty selected anchorages in the English Bay (PMV).

4.3.2 OSCAR Model

Please refer to Section 3.3.2.

4.3.3 Hydrodynamic Forcing

Please refer to Section 3.3.1.1. The period of the available hydrodynamic data was from Feb. 4th to Mar. 9th, 2017.

4.3.4 Wind Forcing: HRDPS Model

The detail description of the HRDPS model was provided in Section 3.3.3. In this section, the period of wind forcing was from Feb. 4th to Mar. 9th, 2017. During the study period, the dominant wind directions were north, northwest, west, and southeast with speeds below 12m/s near the anchorage #2 as shown in Figure 4.2. The example of wind speeds and directions at 9 p.m. on Feb. 10th, 2017 in the west coast of BC were plotted in Figure 4.3.

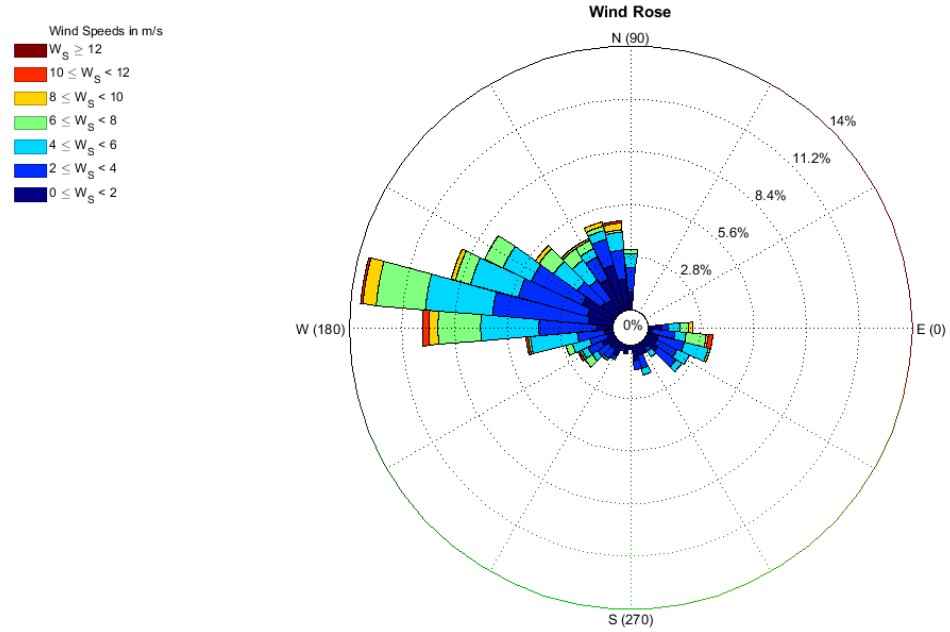


Figure 4.2. Speed, direction, and frequencies of the wind near Anchorage #2 (from Feb. 4th to Mar. 9th, 2017).

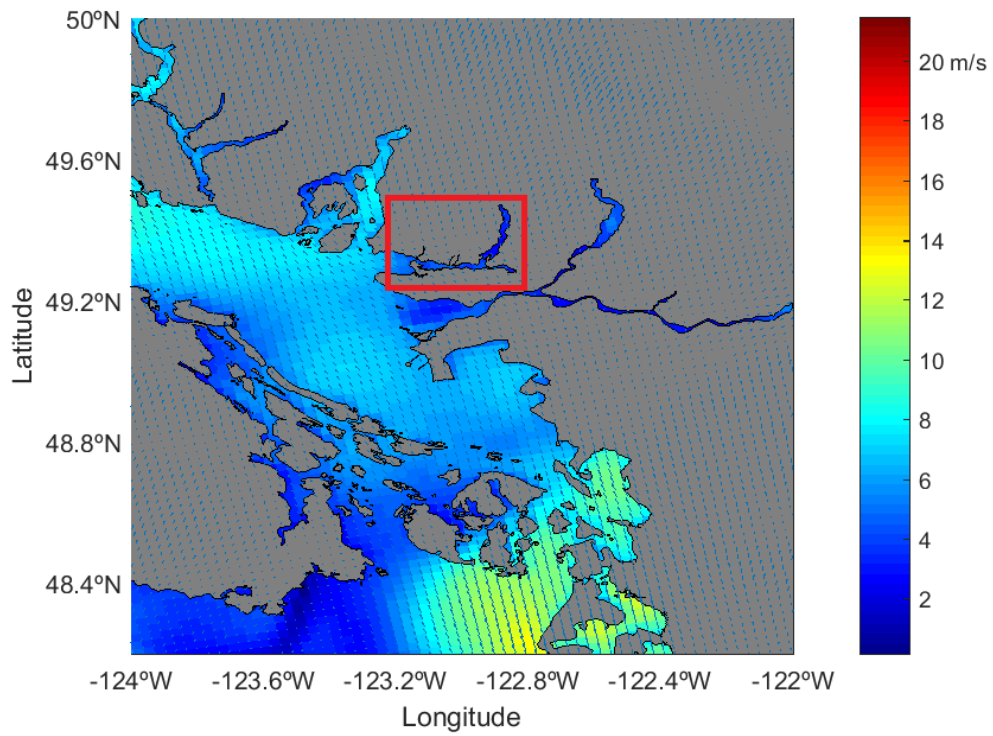


Figure 4.3. Wind speed and direction from the HRDPS model (9 p.m. on Feb. 10th, 2017). The area in the red square is the study area.

4.3.5 Model Scenarios

4.3.5.1 Oil Release

WCMRC and NASP estimated at least 2800 L of IFO-380 was spilled from the suspicious vessel during the *MV Marathassa* oil spill (Butler, 2015). The risk assessment indicated that about 48 km of shoreline, including the west side of Stanley Park, North Vancouver, and West Vancouver, was observed to be contaminated with oil spill from this vessel (anchored at anchorage #12) (Hemmera Envirochem Inc., 2015). The same volume was adopted in this study.

IFO-380 is one of the most commonly used fuel for shipping. Therefore, scenarios for IFO-380 oil spill was considered in this study. The IFO-380 is typically classified as a heavy fuel oil with an API gravity of 10 to 17.1 degree (density of 950-1000 kg/m³) (Srinivasan et al., 2007).

4.3.5.2 Stochastic Modeling Approach

Both deterministic and stochastic approaches can be used in oil spill modeling. A deterministic approach is used to predict a single incident. This approach is helpful to study a known historical oil spill event. For instance, deterministic approach was employed in Chapter 1 to study the *MV Marathassa* oil spill event (Zhong et al., 2018). Stochastic approach, on the other hand, is used to analysis the potential risk of oil spill by overlapping a great number (tens to thousands) of individual deterministic simulations. For example, Niu et al. used stochastic modeling to simulate the fate and transport of oil spill in the Salish Sea (Niu et al., 2016). In this study, a stochastic approach was employed to simulate the fate and transport of an oil spill happening between Feb. 5th, 2017 to Mar. 7th, 2017 (a 30-day period) with available current and wind data. The number of simulations for each selected location, as mentioned in section 4.3.1, was 120. For each individual simulation, the oil was assumed to be released instantaneously (released within 2 hours) and then tracked for 3 days. Maps of the probability of water column, surface, and shoreline contamination were generated according to the mass balance and oil trajectory of each individual simulation.

4.3.6 Tidal Excursion Length

In this study, the stochastic modeling results were compared with the predicted tidal excursion length, which can be calculated based on the trajectories of water particles. The numerical simulation of water particles movement was performed by FVCOM model with a 30-second time step and tracked for seven days. The particle trajectories and instantaneous velocity can be determined numerically by integrating the following equation (Xu & Xue, 2011):

$$\begin{cases} \frac{dx_i}{dt} = u(x_i, y_i, t) \\ \frac{dy_i}{dt} = v(x_i, y_i, t) \end{cases} \quad (1)$$

where the subscript i indicated the i th particle and (x_i, y_i) denoted the position of the particle. (u, v) represents the instantaneous velocity at the location of the particle (x_i, y_i) .

The results of particle trajectories and instantaneous velocities were used to calculate the particle movement distance, which was calculated every five minutes and overlapped to create the map of tidal excursion length. The overall tidal excursion length is the sum of the distribution over a tidal cycle.

Due to topographical factors, once the pollutants (i.e. spilled oil) pass through the First Narrow, Vancouver Harbour has high potential to be contaminated. Therefore, in the present work, the probability of water particles (from the English Bay) that be transported cross the First Narrow was studied as well.

4.4 Results and Discussion

4.4.1 Probability of Contamination

To understand the impacts of oil release locations on the fate and transport of oil spill in the English Bay and Vancouver Harbour, twenty oil release sites were selected in this study (Figure 4.1). They can be generally classified into six groups based on the results of contamination areas. Group A, anchorage #16-17, at the northwestern of the English

Bay, and group B (anchorage #U), C (anchorage #1-4), D (anchorage #5-8), E (anchorage #9-12), F (anchorage #13-15, and #Z) from the western to the eastern of the English Bay. The stochastic approach was used to carry out the oil spill modeling.

The average areas with probability higher than 5% for each studied group were listed in Table 4.1. The detailed areas of contamination for each anchorage were provided in Table S4.1. It is also worthwhile to mention that this study focused on the contamination in the English Bay and Vancouver Harbour, and the contamination on the Salish Sea was not investigated in the present work.

Three types of contamination (surface, water column, and shoreline) were studied as presented in Table 4.1. In terms of surface contamination, it can be clearly observed that the area of contamination was progressively increased from 9.4 km² in group A to 32.3 km² in group F as the oil spill locations moving from westward to eastward of the English Bay. Group A displayed the smallest surface contamination that is mainly because the anchorages in group A were close to coastline, and the spilled oil were more likely to strand onshore rather than floating on water surface. In addition, the spilled oil that was transported into the Salish Sea was considered as “outside” and not calculated in this study. Oil discharged in the locations in the western of the English Bay (close to the Salish Sea), such as group B, C, and D, showed a relatively higher probability of outside contamination as shown in Figure 4.4.

As for the average area of water column contamination, the similar trend to the surface contamination was followed due to the continual exchange of surface and dispersed/dissolved oil in water column (Niu et al., 2016). Generally, the water column contamination area was gradually increase from the anchorages in group A to Group F. The anchorages in group A (1.4 km²) exhibited least contamination due to the high probability of shoreline contamination, followed by group B (13.5 km²) and D (23.4 km²). Similar area of water column contamination was illustrated in group D, E, and F with approximately 28 km². In addition, in group F, the water column contamination area was relatively smaller for oil spill at anchorage # 14-15 (about 21-23 km²) than that of spill at anchorage #13 and #Z (about 30-33 km²) (Table S4.1). This was likely caused by the

relatively larger surface (about 37 km²) and shoreline contamination area (1.7 km²) for oil spill at anchorage #14-15 than that at anchorage #13 and #Z, about 27 km² and 1.4 km² respectively, as shown in Table S4.1.

Table 4.1. Average areas (km²) for more than 5% probability for oil contamination in each group. Oil contamination in the Strait of Georgia was not included.

Group #	Surface	Water Column	Shoreline	Total
A	9.4	1.4	0.6	20.4
B	13.6	13.5	0.3	31.3
C	22.2	23.4	0.5	45.4
D	27.5	28.7	1.0	51.5
E	29.9	28.6	1.3	54.6
F	32.3	27.2	1.6	57.4

In general, the average areas of shoreline contamination were much lower than that of surface and water column contamination for all six groups. The probability of shoreline contamination illustrated a similar pattern as surface contamination, with oil spill in group F covering the largest area (1.6 km²), followed by group E (1.3 km²) and group D (1.0 km²). In terms of the details for each oil release sites, as shown in Table S4.1, the shoreline contamination area was largest for oil spill at anchorage #15 (1.8 km²), followed by anchorage #14 (1.7 km²) and #10 (1.5 km²). The smallest shoreline contamination area was indicated by oil spill at anchorage #U with 0.3 km². Although the overall area of shoreline contamination was low compared with surface and water column, the probability of shoreline contamination still high for some anchorages. For instance, oil spill at anchorages in group A results in a high probability (about 50-60%) of shoreline contamination at the coastline of Sandy Cove (northwest of the English Bay).

After exploring the impact of oil released locations on the contamination areas, the influence of oil released locations on the total probability of contamination was also investigated in this study. The total probability of contamination for the representative location (anchorage #1, 7, 12, 15, 17, and U) from each group were illustrated in Figure 4.4, and the rest total probability figures were provided in Figure S4.1. It is necessary to note that once the spilled oil was transported cross the First Narrow, the waters and

shorelines in Vancouver Harbour are highly possible to be polluted. From Figure 4.4, it can be observed that the probability of the spilled oil moving through the First Narrow was increased when the oil release locations shifted from westward (such as group B and C) to eastward (group F). Moreover, although the anchorage in group A was farther away from the First Narrow as compared to the anchorage in group E and F, the oil released at group A showed a similar probability to be transported through the First Narrow. This is probably due to the influence of current, which will be further discussed in the Section 4.3.3.

Overall, the probability of oil contamination in the English Bay and Vancouver Harbour was influenced by the oil discharge locations in the English Bay. The surface, water column, and shoreline contamination areas, as well as the probability of oil that be transported cross the First Narrow, were increased for the oil spill in the western to the eastern of the English Bay.

4.4.2 Mass Balances

In addition to the investigations on the contamination area and probability, the mass balance of the spilled oil was conducted as well to further evaluate the influence of oil release locations. The mass balance of oil that spilled at anchorage #17, #U, #1, #7, #12, and #15 (from each group) from randomly selected simulation case NO.17 (start at 16:00, February 8th, 2017, and tracked for three days) were plotted in Figure 4.5. Since the mass balance for the sediments, atmosphere and biodegraded were all less than 2% due to the very weak wind/waves, only the oil components at the water surface, in the water column, on the shoreline and the “outside” were analyzed in this study. The term ‘outside’ in the mass balance means the amount of oil moving out from the English Bay to the Salish Sea. From Figure 4.5, it can be observed that this outside percentages were declined for the locations from the western to the eastern of the English Bay. For instance, 99% of oil spilled at anchorage #17 were transported out from the English Bay to the Salish Sea, but only 0.1% of spilled oil were moved out if they were spilled at anchorage #15.

In contrast, the term ‘ashore’, which means the amount of oil stranded onshore, was increased for the locations from the western to eastern of the English Bay with the highest

percentage at the anchorage #15 (98%) and the lowest percentages at anchorage #17 and #1 with 0%. The result of shoreline oil for anchorage #17 in this randomly selected simulation case (NO. 17) was different from the stochastic modeling results as shown in Section 4.4.1, because the oil spill fate and behavior is a complicated issue, which depending on the amount of oil in the water, timing, and location of the spill (Niu et al., 2016). The percentage of oil on water surface and in water column was decreased as the “outside” and the “ashore” increased. As a result, oil spill at anchorage #12 showed the highest proportion of oil on surface (about 12%) and in water column (about 7%) after three days tracking, because the percentage of “outside” and oil on shoreline were relatively lower with approximately 79% in total.

In general, the mass balance of spilled oil is very sensitive to the oil spill locations in the English Bay. A high proportion of “outside” oil could be seen when oil spill at the anchorages in the west part of the English Bay, such as anchorages in group A and B, and was declined as moving to the eastward. For the anchorages in the eastward, such as anchorages in group F, spilled oil illustrated a relatively higher percentage of oil stranded onshore.

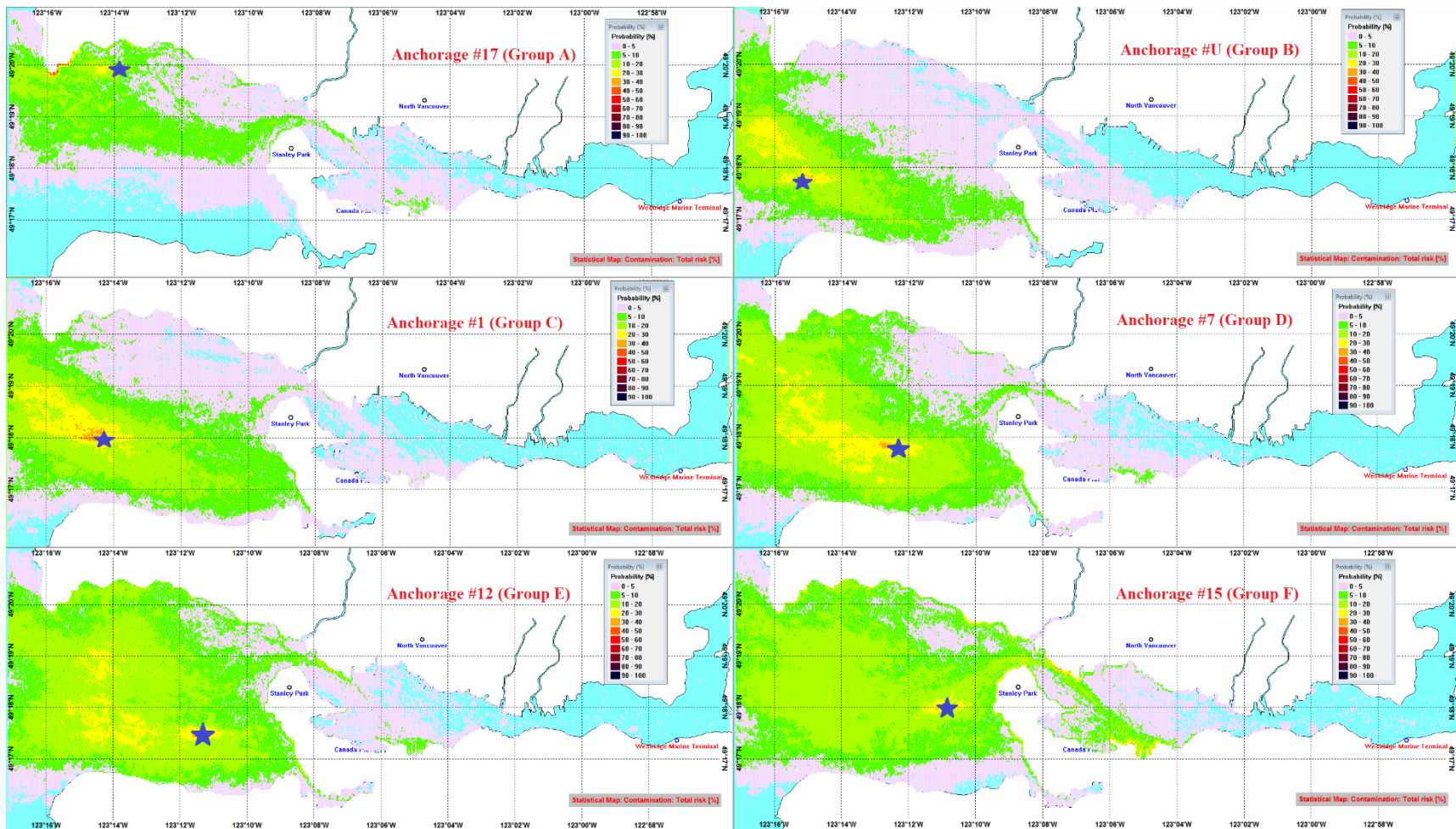


Figure 4.4. The total probability of oil contamination for oil spilled at anchorage #17, #U, #1, #7, #12, and #15. Oil released at the star.

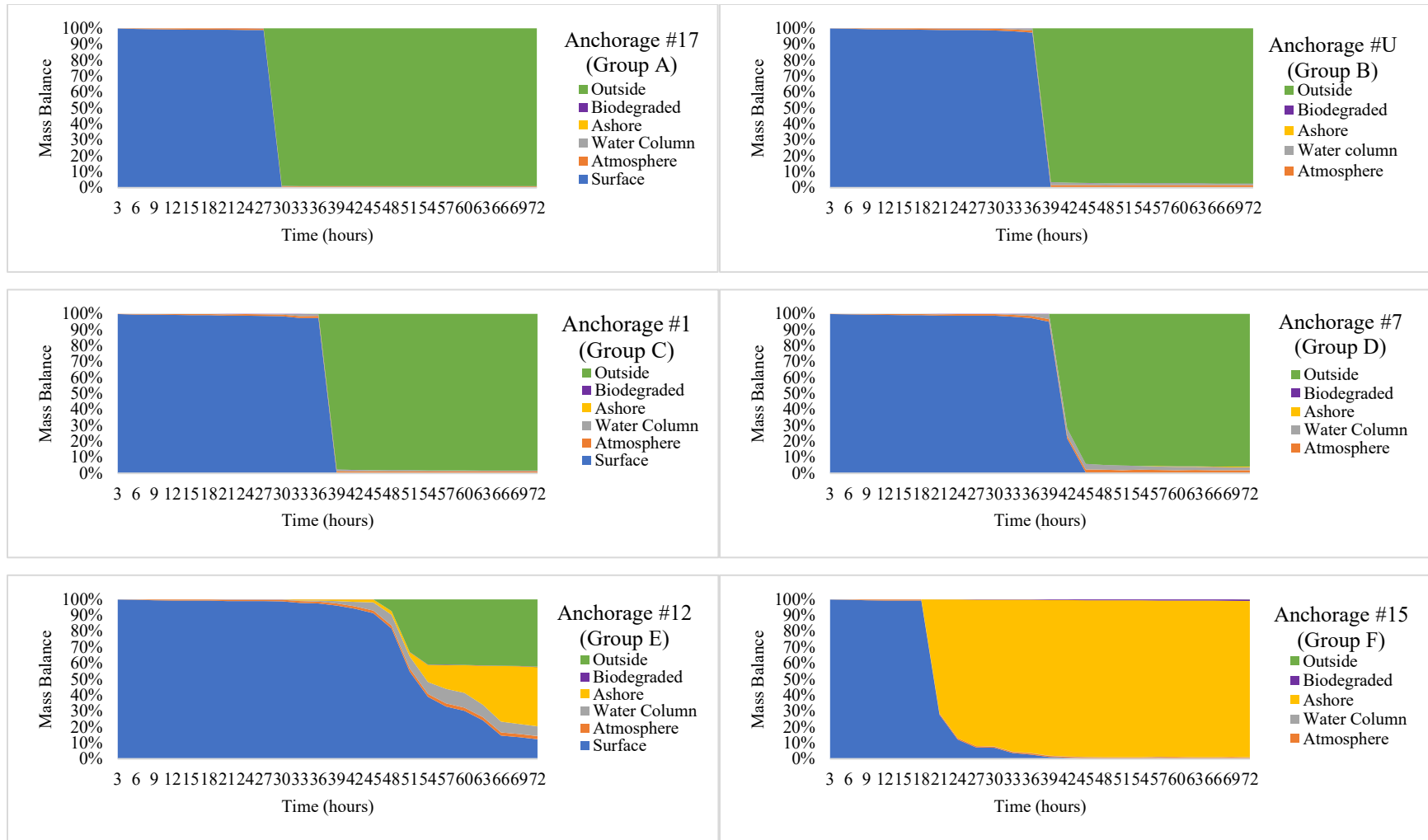


Figure 4.5. Changes in mass balance with time, for selected locations from six groups (#17, #U, #1, #7, #12, and #15, simulation NO. 17).

4.4.3 Tidal Excursion Length

In order to explore the fate and transport of the spilled oil from the tidal current perspective, the tidal excursion length in the English Bay and Vancouver Harbour was estimated as shown in Figure 4.6. In general, for the entire Burrard Inlet (geographically including English Bay and Vancouver Harbour), the longest tidal excursion length was observed in the central harbour and the Second Narrow (about 16 km) and the shortest displacement was in the west and southeast nearshore area of the English Bay (about 1 km). In terms of the English Bay, the tidal excursion length gradually increased from the western to eastern of the English Bay, and this is in agreement with the spilled oil movement and distribution as illustrated in Section 4.4.1 and 4.4.2.

Moreover, as mentioned in section 4.4.1, Vancouver Harbour is highly possible to be contaminated if the spilled oil was transported cross the First Narrow. Thus, the probability of oil and water particles moving cross the First Narrow was studied in the present work. As shown in Figure 4.7, the probability was increased from the western to eastern of the English Bay when approaching the First Narrow. In addition, particles at the nearshore area along the northwest of the English Bay, where group A (anchorage #16-18) locates, showed almost no probability to be transporting to cross the First Narrow. This result is different from the probability of oil spill contamination that spilled oil in group A was possible to be transported cross the First Narrow. This difference of probability was possibly caused by the difference input of wind, which generate the wave and wind-driven currents. In this study, for oil spill modeling, the OSCAR model used wind speed to calculate the waves height, which but it was not included in the tidal excursion calculation. Therefore, the oil spill fate and behavior in the English Bay and Vancouver Harbour was not only affected by tidal current, but also impacted by wind although the wind speed was very low that mean speed was less than 3 m/s (Hemmera Envirochem Inc., 2015). This statement was also demonstrated in Chapter 3 (Zhong et al., 2018) and agreed with the conclusion from Hemmera Envirochem Inc., (2015).

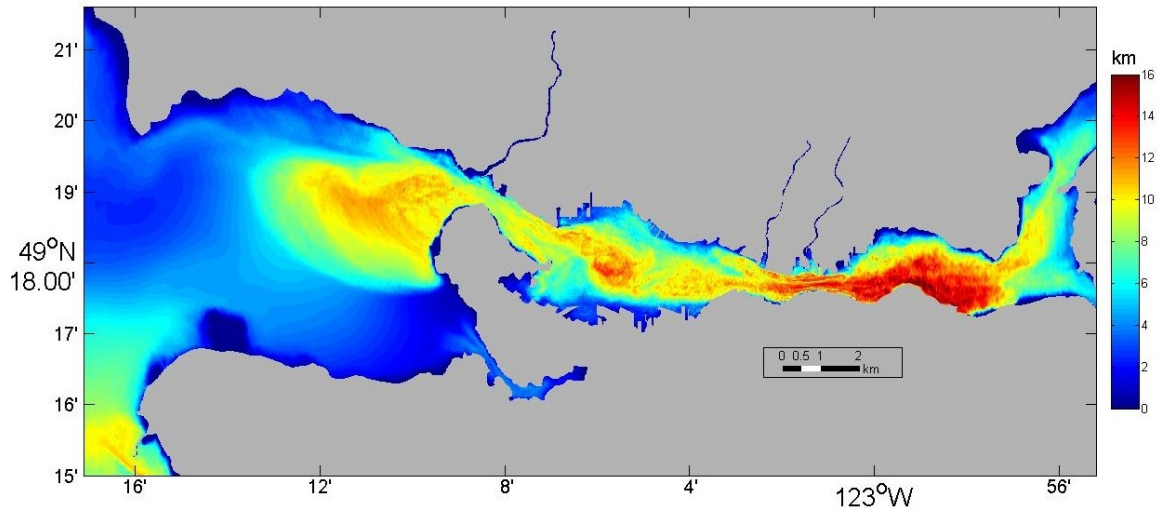


Figure 4.6. Tidal excursion length (km) in the English Bay and Vancouver Harbour.

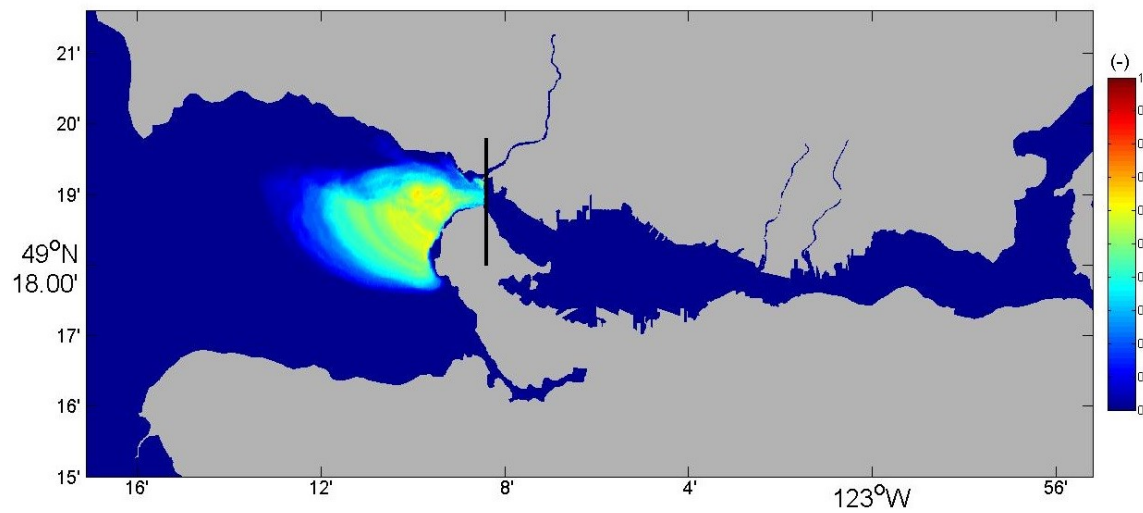


Figure 4.7. Probability of water particles (from the English Bay) that move pass the First Narrows.

4.5 Conclusion

The state-of-the-art OSCAR model was forced by the high resolution atmospheric and oceanographic data to investigate the impacts of oil release locations on the fate and behavior of the spilled oil in English Bay. The probability of oil contamination in Vancouver Harbour and the English Bay from spills originated from twenty anchorages (anchorage #1-18, anchorage #U, and anchorage #Z) were simulated using a stochastic approach. Tidal excursion length in Vancouver Harbour and English Bay was also studied to further explain the stochastic modeling results.

The results indicated that the spills from these twenty oil release locations could lead to a large area being affected which will cause surface, water column, and shoreline contaminations. The surface and shoreline contamination area were gradually increased as oil spill locations change from the west to the east of the English Bay. As the result, water column contamination area was relatively smaller in group E than in group C and D due to the high percentage of oil that stranded onshore in group E. The surface, water column, and shoreline contamination were produced by the oil spill in group A. This was caused by the high “outside” (oil moved to the Salish Sea) proportion of spilled oil and the high percentage of oil stranded on the shoreline of Sandy Cove (northwest of the English Bay). The probability of oil spill contamination distribution matched well with the result of hydrodynamic dispersion, which parametrize by tidal excursion length in this study.

For the probability of discharged oil that could transport cross the First Narrow, the probability was increased as oil spilled in group B to group F (from the west to east of the English Bay). Although the anchorages in group A (anchorages #16-18) is farther away from the First Narrow as compared to the other anchorages, the spilled oil showed the probability to be transported cross the First Narrow. This result disagreed with the probability produced from the tidal excursion study and the main reason is due to the difference input of wind data. Therefore, to study the oil spill fate and behavior in the English Bay, both hydrodynamic and wind need to be used in the modeling setup.

4.6 Acknowledgements

This research was founded by the Natural Sciences and Engineering Research Council of Canada (NSERC), the Marine Environmental Observation. Prediction and Response Network (MEOPAR), and the National Contaminants Advisory Group (NCAG). SINTEF Marine Environmental Technology is thanked for providing the OSCAR oil spill model.

4.7 Transition Section

Chapter 4 demonstrated that oil spill transport and fate in the English Bay was very sensitive to the oil discharge location and the study showed that oil could transported out of the

English Bay and into Salish Sea. To better understand the fate and transport of oil from releases near the west side of English Bay and also from potential locations in the Salish Sea, further modeling work is needed. In addition, the effects of other factors such as oil type and discharge volume on the also need to be studied. Hence, an exploration of the impacts of these factors on fate and behavior of spilled oil in the Salish Sea and Burrard Inlet will be carried out and presented in Chapter 5.

CHAPTER 5: STOCHASTIC MODELING OF THE FATE AND BEHAVIOURS OF OIL SPILL IN THE SALISH SEA

5.1 Abstract

The oil spill risk in the Salish Sea is expected to increase substantially as a result of the proposed pipeline and terminal expansion project. To gain a better understanding on the implications of different oil spill scenarios, a state-of-art three-dimensional (3-D) oil spill model (OSCAR) was employed to simulate the fate and behaviour of the spilled oil in Salish Sea under different conditions. The OSCAR model was forced by the combined currents from a newly developed, high resolution, hydrodynamic and atmospheric model (NEMO) for the Salish Sea and a 3-D finite-volume and unstructured grid ocean model (FVCOM) for the Vancouver Harbour in this study. The effects of three factors, including the oil spill location, spilled oil volume, and the type of spilled oil, were investigated in this study. The stochastic modeling results indicated that the fate and behaviour of spilled oils were very sensitive to the released sites in the Salish Sea. Oil release from the Strait of Georgia (geographically included by the Salish Sea) led to the greatest surface, water column, and shoreline contamination area compared to the other five locations. Released oil volume and oil type were significantly influential for the fate and behaviour of the spilled oil as well. A higher oil spill volume resulted in the larger surface, water column, and shoreline contamination area. The lighter the oil, the larger areas of surface and water column contamination were observed.

5.2 Introduction

The Salish Sea, in particular of the Burrard Inlet that geographically locates within Salish Sea, has very busy vessel traffic. Annually, about 10,000 large cargo vessels and 100 oil tankers travel through/around the Salish Sea (Rossi, 2015; Washington Nature), and they usually carry large amount of petroleum. Oil spill has been of a major concern and is regarded as one of the most critical marine pollutions in the Salish Sea due to the heavy vessel traffic. The vessel traffic in this area is expected to increase substantially, as a result of the proposed pipeline and terminal expansion project. Therefore, it is highly necessary to study the fate and behaviour of potential oil spills in the Salish Sea, which will be helpful for decision makers to develop an appropriate

management plan to minimize the environmental impacts. Many factors might affect the fate and behaviour of oil spills in the marine environment, and the major ones are the initial spill volume, circulation under and around the oil release location, and the physicochemical properties of oil (Verma et al., 2008).

As mentioned above, the majority of vessel traffic in the Salish Sea involve with oil tanker ships and cargo ships. The oil tanker ships are usually used to transport the diluted bitumen that are mainly produced from province of Alberta. The cargo ships are powered by the marine fuel oil. It is therefore necessary to evaluate the potential spill risk of diluted bitumen and marine fuel oil. As compared to the marine fuel oil that have been extensively studied, diluted bitumen presents new challenge for the study on oil spill fate and behaviour. Diluted bitumen is the blends of wide range of diluents with bitumen that extracted from oil sands. The chemical compositions and physical properties of these diluted bitumen products are varied widely as compared with conventional crudes, mainly due to the different dilution rates and parent feedstock varieties (Hart, 2014). Several research have been conducted to investigate the diluted bitumen oil spill in the Salish Sea and Burrard Inlet, along with different initial spill volume and potential oil discharge locations (DNV, 2013; Genwest System Inc., 2015; Tetra Tech EBA Inc., 2013). For instance, two sizes of diluted bitumen spill in six potential discharge sites in the Salish Sea were studied by Tetra Tech EBA Inc. in 2013 with the aims to simulate the trajectories, weathering, and shoreline contact of oil spill (Tetra Tech EBA Inc., 2013). The obtained results illustrated that the length of shoreline contamination was relatively high for the credible worst oil spill case (16500 m³) than that of medium oil spill (8250 m³) (Tetra Tech EBA Inc., 2013). In addition, substantial differences in the fate and behaviour were observed for the oil spilled at different locations in the Salish Sea. The oil spilled at the inshore sites had much less water surface contamination compared to the oil spilled at the continental shelf (Tetra Tech EBA Inc., 2013).

Although the risks of diluted bitumen spills in the Salish Sea have been studied, there is still a lack of investigation on the fate and behaviour of marine fuel oil spill. Therefore, it is worthwhile to study the marine fuel oil spill in the Salish Sea and then compared it with the diluted bitumen spill. Moreover, in the perspective of oil spill model, although several oil spill model and integrated hydrodynamic model have been used to study the oil spill in the Salish Sea (Genwest System Inc., 2015; Niu et al., 2016; Tetra Tech EBA Inc., 2013; Zhong et al., 2018), there is still

some limitations. The stochastic model in SPILLCALC that used by the Tetra Tech EBA Inc. (Tetra Tech EBA Inc., 2013) was 2D, which only tracked the surface transport of oil and did not provide the probability of water column contamination. The GNOME model that employed by Genwest System Inc. (Genwest System Inc., 2015) to simulate the trajectory of oil was based on rough wind conditions and currents' information without the fate/weathering processes. The hydrodynamic model of NEMO showed a high-resolution in the Salish Sea (almost uniform grid spacing of 440 to 500 meters), but was not able to simulate the hydrodynamic variables in the Burrard Inlet (Niu et al., 2016). Although the FVCOM hydrodynamic model that was used in Chapter 1 of this thesis (Zhong et al., 2018), can achieve a high-resolution in the Burrard Inlet (grid spacing of 2 to 10 m), the resolution was relatively low in the Salish Sea (grid spacing of 1 km). Therefore, a integrated high-resolution oil spill model is needed to study the oil spill in the Salish Sea and Burrard Inlet.

The objective of this study is to combine the hydrodynamic variables from FVCOM model (for the Burrard Inlet) and NEMO model (for the Salish Sea) to generate the time series hydrodynamic data in the Salish Sea and the Burrard Inlet. Then, the currents data was incorporated into a 3-D oil spill model (OSCAR) to understand the influence of oil spill locations, spilled oil volume and oil types, on the fate and behaviour of oil spill in the Salish Sea and the Burrard Inlet.

5.3 Method and Materials

5.3.1 Studied Area

The Salish Sea is the intricate network of coastal waterways located between the southwestern portion of the Canadian province of British Columbia and the northwestern portion of the U.S. state of Washington. The Salish Sea (approximately 18000 km²) is comprised of the inland marine waters of Juan de Fuca Strait, Strait of Georgia, and Puget Sound as shown in Figure 5.1. The western boundary of the Salish Sea is the entrance to the Strait of Juan de Fuca, and the southern and northern boundaries reaches the southern end of Puget Sound and the northern end of the Strait of Georgia respectively (Skywater Acres, n.d.). The water of Salish Sea is depth from 410 m at Strait of Georgia (about 6400 km²) to 250 m at Strait of Juan de Fuca (about 4400 km²)

(Western Washington University, 2018) and is heavily used for a wide range of activities, including commercial transportation of crude oil and marine fuel oil.

The Burrard Inlet is a marine inlet that geographically including five main water bodies as shown in Figure 5.1: Outer Harbour (including English Bay and False Creek), Vancouver Harbour, Central Harbour, Port Moody Arm, and Indian Arm. The Outer Harbour and Vancouver Harbour are separated by narrowing of the harbour, known as First Narrow. Moving eastward, Vancouver Harbour is separated from Central Harbour by Second Narrow (a second narrowing of the harbour). Water depth at Burrard Inlet ranges from about 45 m in the Outer Harbour to approximate 10 m in Port Moody Arm (Hemmera Envirochem Inc., 2015).

5.3.2 OSCAR Model

Please refer to Section 3.3.2.

5.3.3 Hydrodynamic Forcing

5.3.3.1. NEMO Model

The hydrodynamic variable used for the Salish Sea in this study was from a 3-D, baroclinic, non-linear, hydrostatic model (UBC, 2015). It is based on the OPA/NEMO model version 3.1 (Madec, 2015) and solves the primitive equations under the Boussinesq approximation using a staggered Arakawa's C-grid discretization in the horizontal. The model grid was rotated 29 degrees counter-clockwise to co-direct the axis of the Juan de Fuca channel with a horizontal axis of the numerical grid. The horizontal grid has an almost uniform grid spacing of 440 to 500 meters. The vertical grid has 40 vertical depths that are stretched gradually to achieve higher resolution in the surface layer. The vertical grid spacing ranges from 1 m in the top 10 meters to 27 m at the bottom. Partial z-levels are utilized to better represent the bathymetry. An example of the currents on Feb. 10th, 2017 (23:00) for forcing the oil spill model is presented in Figure 5.1. The horizontal grid space of NEMO model is relatively higher in the Salish Sea, but this model is unable to simulate the hydrodynamic series at the Burrard Inlet. Therefore, a high-resolution/integrated hydrodynamic model is needed for both Salish Sea and Burrard Inlet in this study.

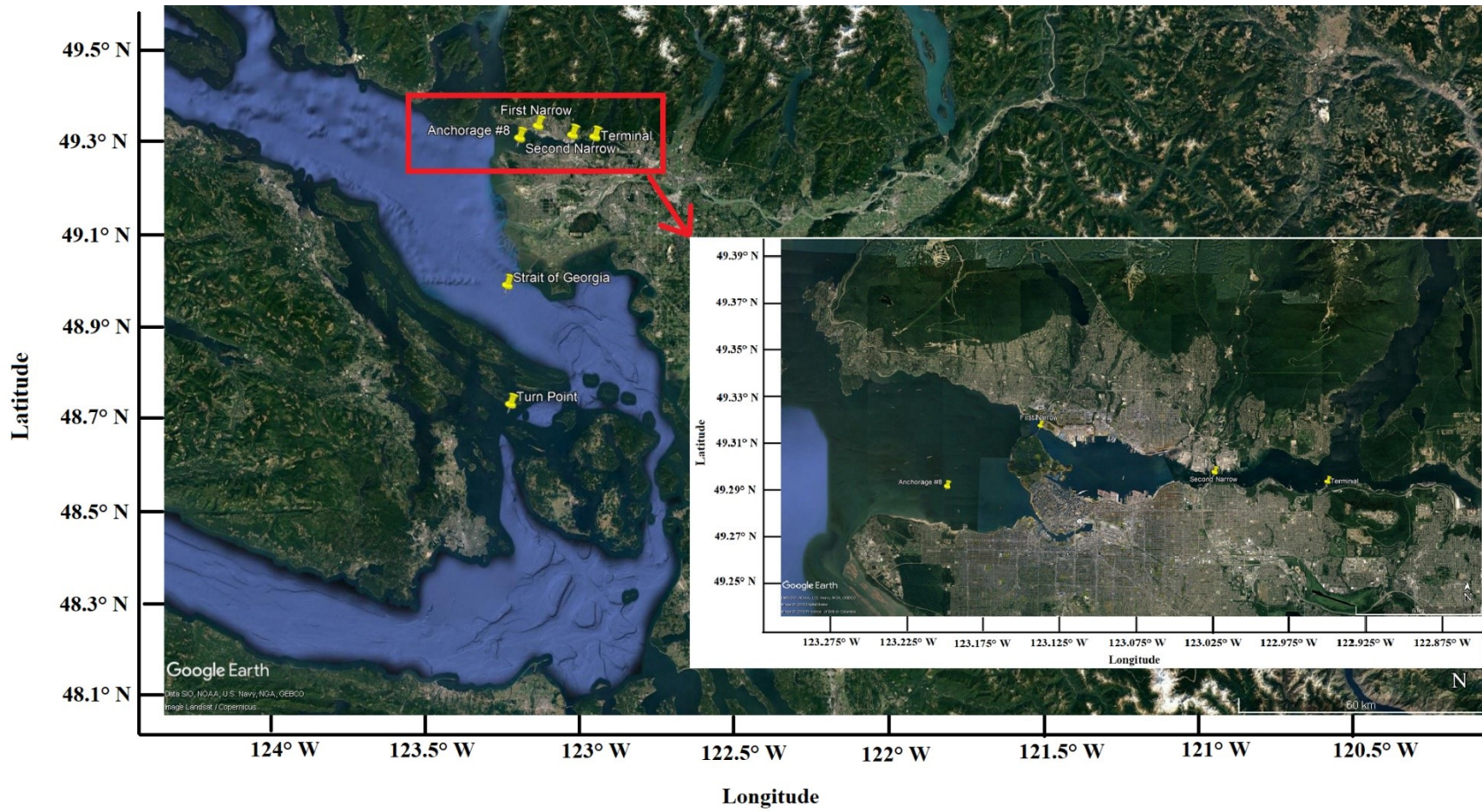


Figure 5.1. Locations for the selected oil discharges.

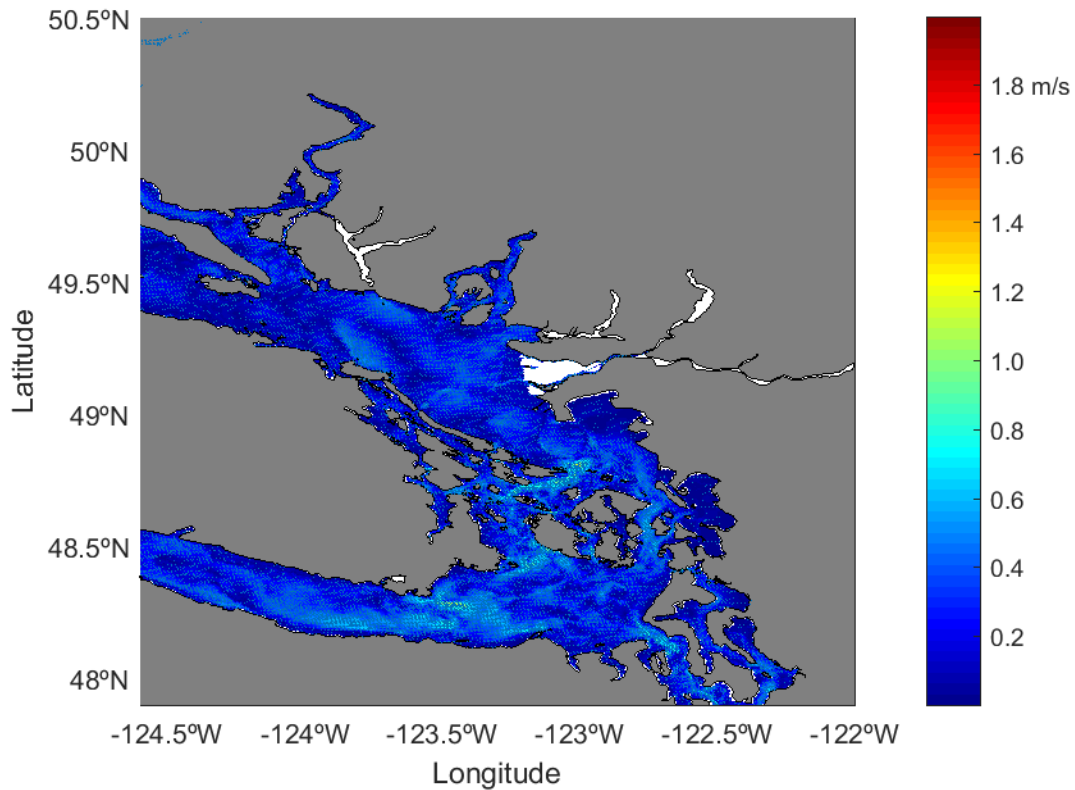


Figure 5.2. NEMO model Salish Sea currents at 0.5m depth. NEMO model is not able to generate hydrodynamic forcing in the white color areas.

5.3.3.2 FVCOM Model

The detail description of FVCOM model was provided in Section 3.3.1.1. Because the model only covers a small area of Salish sea at relatively low horizontal resolution (1 km) as shown in Figure 5.2, this model results will be overlapped with the NEMO model and higher resolution from these two models will be used by OSCAR.

5.3.4. Wind Forcing

The detail description of the HRDPS model was provided in Section 3.3.3. The example of wind speed and direction at 21:00 on 13 February 2017 is shown in Figure 5.3. The dominant wind directions are northwest and southeast with speeds below 12 m/s near one of the release points (Strait of Georgia) from 5 February 2017 to 7 March 2017, as shown in Figure 5.4.

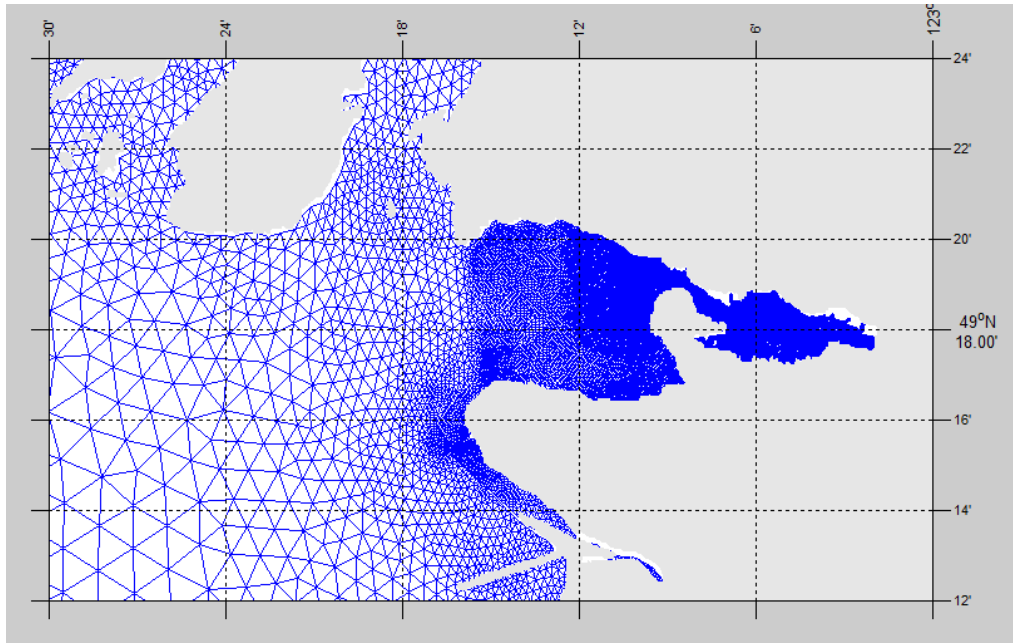


Figure 5.3. Finite-Volume Community Ocean Model's (FVCOM) horizontal grid in the Salish Sea and Burrard Inlet. The horizontal grid space is about 1 km in the Salish Sea, 10 m in the Vancouver Harbor and about 2 m around the bridge bases in the Second Narrows.

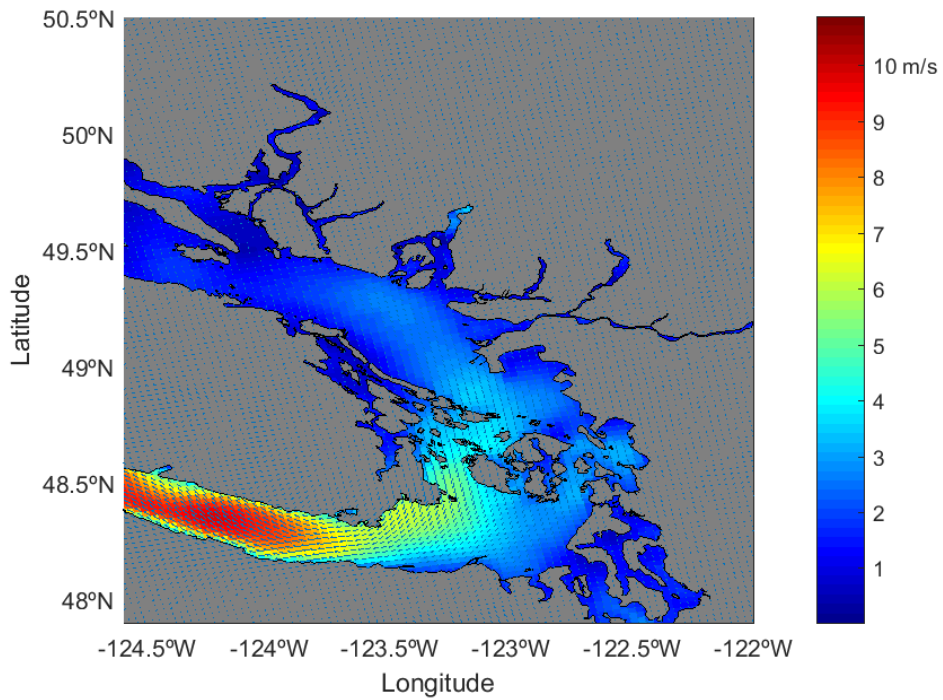


Figure 5.4. Wind speed and direction from the High-Resolution Deterministic Prediction System (HRDPS) (13 February 2017, 21:00).

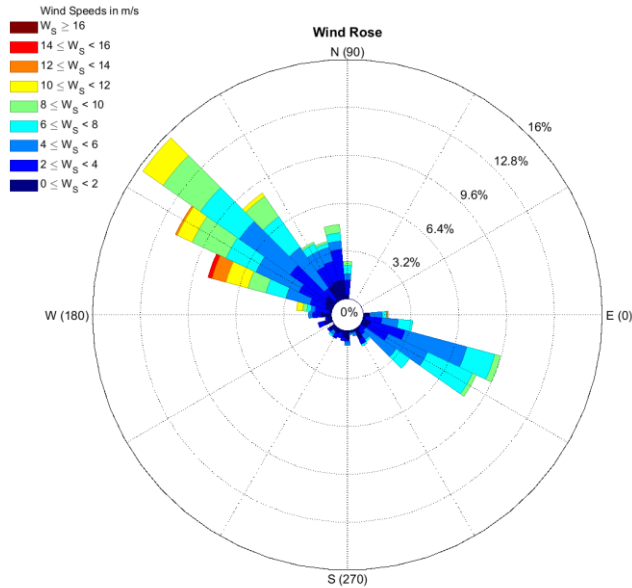


Figure 5.5. Speed, direction and frequencies of the wind near the oil released site (from 5 February to 7 March 2017).

5.3.5. Model Scenarios

5.3.5.1. Oil Discharge Location

There are many possible locations for the oil spill to happen along the shipping lane in the Salish Sea and the Burrard Inlet. The study by Tetra Tech EBA Inc., (2013) investigated spills from four marine sites in the Salish Sea, including Strait of Georgia, Arachne Reef, Strait of Juan de Fuca, and the western entrance of Juan de Fuca Strait (Buoy J) by using stochastic modeling approach. Their study also simulated the oil spill from the Westridge Terminal, which geographically included by the Burrard Inlet. Genwest System Inc. (2015) modeled oil spill trajectories from four oil spill scenarios in Burrard Inlet, which including Westridge Terminal, Second Narrow, First Narrow, and Anchorage #8. Among those possible oil spill locations, two marine sites, Strait of Georgia and Arachne Reef (Turn Point), and four spill locations in the Burrard Inlet (Westridge Terminal, Second Narrow, First Narrow, and Anchorage #8) were selected as the spill site due to the relatively higher level of navigation complexity and its high environmental value (DNV, 2013;

Genwest System Inc., 2015; Niu et al., 2016; Tetra Tech EBA Inc., 2013). The position of selected oil release locations is presented in Figure 5.5.

5.3.5.2. Oil Discharge Volume

Tetra Tech EBA Inc., (2013) reported that the estimated worst spill case and medium spill case to be 16,500 m³ and 8250 m³ for the four marine sites as mentioned in section 5.3.5.1. The same study also simulated the worst spill case of 160 m³ and medium spill case of 10 m³ for the Westridge Terminal (Tetra Tech EBA Inc., 2013). On the other hands, Genwest System Inc. (2015) modeled oil spill scenario in the Burrard Inlet with 8,000 m³ at the Westridge Terminal and 16,000 m³ at the other three spill sites as described in section 5.3.5.1. By combining the scenarios in these two studies, three spill volume of 16500 m³, 8250 m³, and 160 m³ will be used in this study to simulate the worst, medium, and small spill that occurs at Terminal, Second Narrow, First Narrow, Anchorage #8, Strait of Georgia, and Turn Point. The spill sizes for oil spill at Terminal were the same as that for other spill locations to keep the variables consistent.

5.3.5.3. Oil Type

There are four types of the most commonly used marine fuel oil including Marine Diesel Oil (MDO), Marine Gas Oil (MGO), and two grades of Intermediate Fuel Oil (IFO-180 and IFO-380) to supply engine power for the vessels (Friedrich, Heinen, Kamakate, & Kodjak, 2007). MGO is pure distillate, which mainly used in harbour crafts and fishing vessel (Denton, Mazur, Milanes, Randles, & Salocks, 2004). MDO is heavier distillate that may contain some residual components, while IFOs is heavy fuel oil that might contain distillate fuels (Haglind, 2008). In the present work, two types of commonly used marine fuel oil, MDO and IFO-380 will be studied. In addition, five types of diluted bitumen, Access Western Blend-Winter (AWB-W), Cold Lake Blend-Summer (CLB-S), Cold Lake Blend-Winter (CLB-W), Synthetic bitumen (Synbit), and Western Canadian Select (WCS), that could be shipped in the study area will be also studied. Their physicochemical properties have been studied by King et al. (King, Thamer, Wohlgeschaffen, Lee, & Clyburne, 2017). The total number of seven selected oil products in this study are: AWB-W, CLB-S, CLB-W, Synbit, WCS, IFO-380, and MDO. Their physical properties are

presented in Table 5.1. All the diluted bitumen blends have similar viscosity at 15°C, except CLB-S, likely due to the 10% of diluent less than CLB-W (King et al., 2017). MDO, which is a blend of marine gas oil (majority) and heavy fuel oil, has a relatively lower viscosity than that of IFO-380, which contains high proportion of heavy fuel oil (BOMIN, 2015; Friedrich et al., 2007). The chemical compositions of IFO-380 and MDO were taken from OSCAR’s oil database while the compositions of the five types of diluted bitumen blends were based on the data from King et al. (King et al., 2017).

Table 5.1. Basic physical properties of selected oils.

Oil Name	Blends		API Gravity	Viscosity (cSt at 15°C)
	Bitumen/ Residual	Diluent/ Distillate		
Access Western Blend-Winter (AWB-W)	70%	30%	22.3	244
Cold Lake Blend-Winter (CLB-W)	80%	20%	21.5	237
Cold Lake Blend-Summer (CLB-S)	70%	30%	19.3	575
Synthetic bitumen (Synbit)	50%	50%	20.4	205
Western Canadian Select (WCS)	50%	50%	21.9	211
IFO-380	98%	2%	15.1	10000
Marine Diesel Oil (MDO)	Very few	Majority	20.3	287

Adopted from King et al. (King et al., 2017), Friedrich et al. (Friedrich et al., 2007), and OSCAR’s oil database.

5.3.5.4. Stochastic Modeling Approach

Both deterministic and stochastic approaches can be used in oil spill modeling. A deterministic approach is used to predict a single incident. This approach is helpful to study a known historical oil spill event. Stochastic approach, on the other hand, is used to analysis the potential risk of oil spill by overlapping a great number (tens to thousands) of individual deterministic simulations. In this study, a stochastic approach was employed to simulate

the fate and behavior of an oil spill happening between 5 February 2017 to 7 March 2017 (a 30-day period) with available current and wind data. As mentioned above, three factors, including oil release location, oil release volume, and oil type, were studied in this study to investigate their impacts on the fate and behaviour of oil spill. A full factorial design that incorporates the studied factors and their corresponding settings (Table 5.2) was resulting in $6 \times 3 \times 7 = 126$ scenarios in total. The number of simulations for each scenario was 12. For each individual simulation, the oil was assumed to be released instantaneously (2 hours) and then tracked for 7 days. Maps of the probability for water column, surface, and shoreline contaminations were generated according to the mass balance and oil trajectory of each individual simulation.

Table 5.2. The studied factors and their corresponding settings.

Factor	Oil release location	Oil release volume	Oil type
Setting	<ul style="list-style-type: none"> • Terminal • Second Narrow • First Narrow • Anchorage #8 • Strait of Georgia • Turn Point 	<ul style="list-style-type: none"> • Credible worst (Large) • Medium • Small 	<ul style="list-style-type: none"> • Access Western Blend-Winter (AWB-W) • Cold Lake Blend-Winter (CLB-W) • Cold Lake Blend-Summer (CLB-S) • Synthetic bitumen (Synbit) • Western Canadian Select (WCS) • IFO-380 • Marine Diesel Oil (MDO)

5.4 Results

The stochastic modeling approach was applied to run the OSCAR model to study the area and probability of oil contamination in the Salish Sea and Burrard Inlet. It is notable that the combined hydrodynamic data from FVCOM model (for the Burrard Inlet) and NEMO model (for the Salish Sea) along with the wind data were used to force OSCAR model in this study. The raw data with their influences on the area of contamination (e.g. contamination area in the water column, on the surface, and on the shoreline) are presented

in Table S5.1. The contamination areas in the water column, on the surface and shoreline were statistically analyzed by Analysis of Variance (ANOVA) in this study. The obtained *p*-values for the studied factors are presented in Table 5.3, which was detailly discussed in the following sections.

Table 5.3. The *p*-values for the influence of studied factors on contamination areas. Significant influence (*p*-value < 0.05) is shown in bold.

Source	Water column (km ²)	Water surface (km ²)	Shoreline (km ²)	Total (km ²)
Oil spill location	0.000	0.000	0.000	0.000
Volume the spilled oil	0.000	0.000	0.000	0.000
Type of the spilled oil	0.003	0.002	0.019	0.519

5.4.1. Influence of Oil Discharge Location on Probability of Contamination

To investigate the influence of oil discharge locations on the fate and behaviour of the spilled oil, four locations in the Burrard Inlet (Terminal, Second Narrow, First Narrow, and Anchorage #8) and two marine sites in the Salish Sea (Strait of Georgia and Turn Point) were selected in this study. From Table 5.3, it can be clearly seen that the oil discharge location had a significant impact on the contamination areas in the water column, on the water surface and shoreline, as their *p*-values were all less than 0.05. The average contamination areas for each oil discharge location are provided in Figure 5.6.

The largest water column contamination area (3144 km²) was observed when oil spilled at Strait of Georgia, followed by Turn Point (1068 km²), in where the Strait of Georgia and Turn point are the two marine sites. As for the locations in Burrard Inlet, First Narrow and Anchorage #8 had comparable contamination areas (around 860 km²) in water column, while the water column contamination area for Terminal and Second Narrow were much lower (about 53 km²). Thus, the oil spilled in marine sites can lead to larger water column contamination as compared to that of in the Burrard Inlet. The contamination area on surface showed a similar pattern with that in water column, and this is likely due to the

continual exchange of surface and dispersed/dissolved oil in water column. Oil discharged at Strait of Georgia resulted in the highest contamination area with 2544 km², followed by Turn Point (743 km²) and Anchorage #8 (727 km²). The lowest surface contamination area (about 73 km²) was observed for Terminal and Second Narrow.

The area of shoreline contamination was much smaller than that of surface and water column for all six studied locations. As shown in Figure 5.6, the area of shoreline contamination was 97 km² and 53 km² if the oil was spilled at the Strait of Georgia and Turn Point respectively, which were higher than spilling in the Burrard Inlet (< 31 km²).

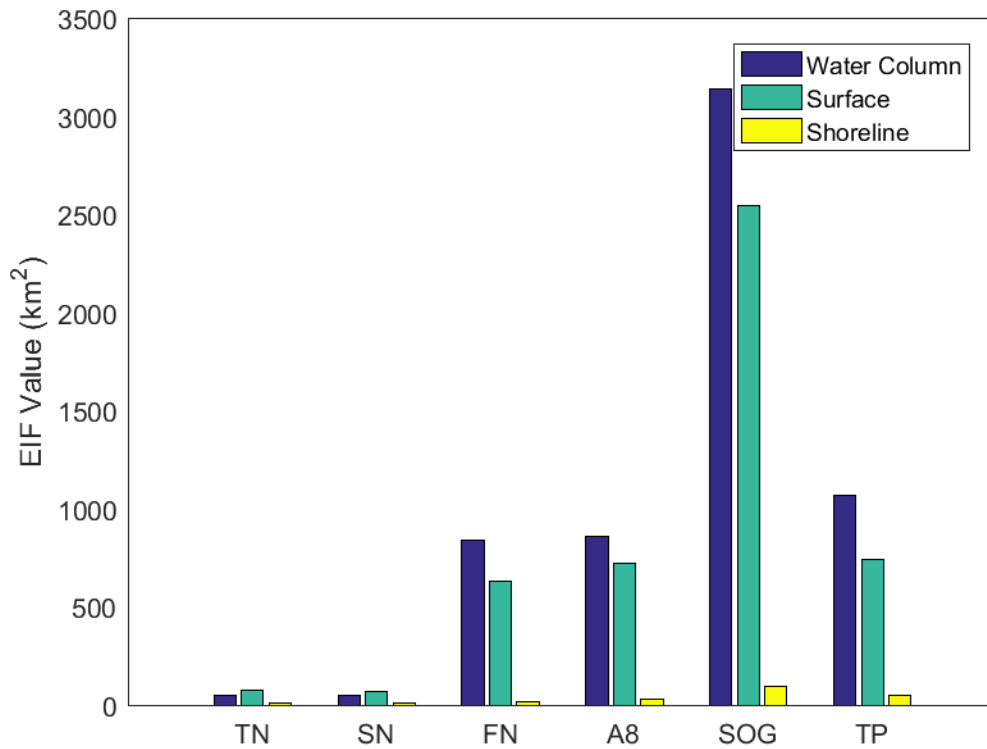


Figure 5.6. The influence of oil discharge locations on the contamination areas in the water column, on water surface and shoreline. TN, SN, FN, A8, SOG, and TP are used to represent Terminal, Second Narrow, First Narrow, Anchorage #8, Strait of Georgia, and Turn Point respectively.

After investigating the impacts of oil discharge locations on the contamination areas, the influence of oil discharge locations on the total probability of contamination was

explored as well. An example (scenarios of 8250 m³ AWB-W oil spill) of probability of contamination map are presented in Figure 5.7-5.8. It was not surprising that the probability of potentially affected area was decreased along with the increase distance from the spill location. In terms of the two marine sites in the Salish Sea, as shown in Figure 5.7, it is obviously that oil released at Strait of Georgia resulted in a relatively high probability of contamination in the Salish Sea, while oil spilled at Turn Point showed a relatively high probability of covering the waters of the Juan de Fuca Strait (the southern of the Salish Sea). In addition, oil spilled from the site Strait of Georgia had a higher probability to contaminate the Burrard Inlet compared to that from the site Turn Point. For the locations in the Burrard Inlet, expect Second Narrow, the spill sites closer the Salish Sea led to higher probability of contamination in waters of the Salish Sea. The oil spill fate and behaviour are complicated issues, which highly depend on the amount of oil in the water, timing, and the type of the spilled oil. Thus, the case that was presented in this study does not provide a direct answer of the question raised, regarding to why the probability of contamination in the Salish Sea's waters for oil spilled at Second Narrow was lower than that at Terminal.

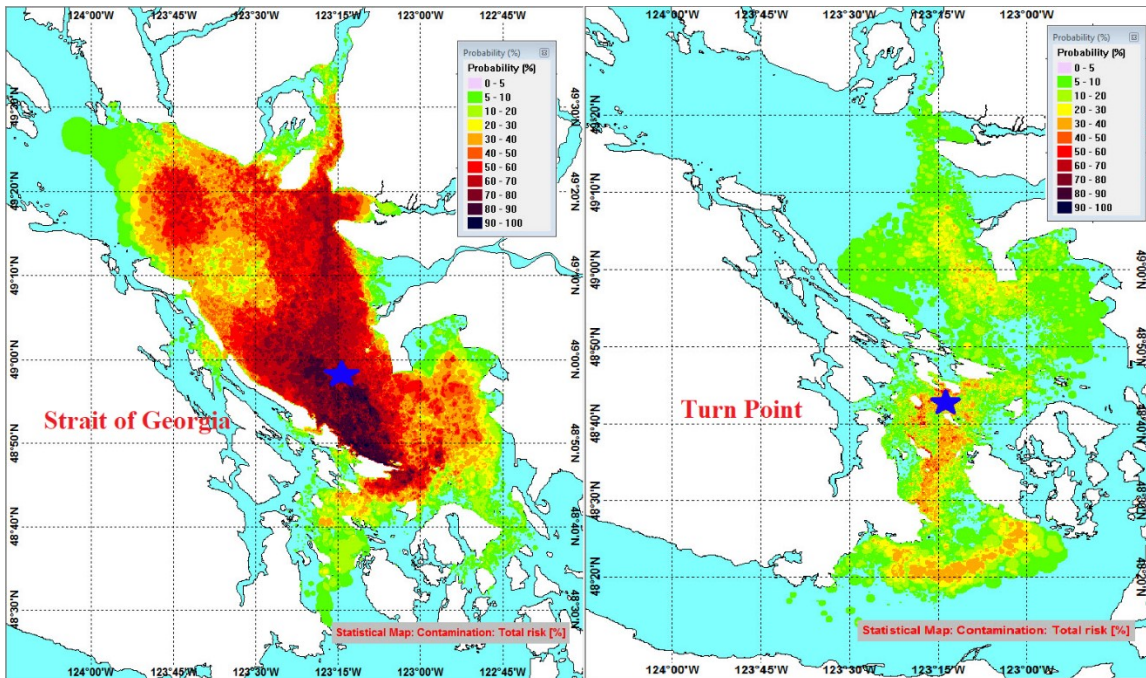


Figure 5.7. Probability of oil contamination for 8250 m³ AWB-W oil release at (1) Strait of Georgia and (2) Turn Point. The oil initially releases at the star.

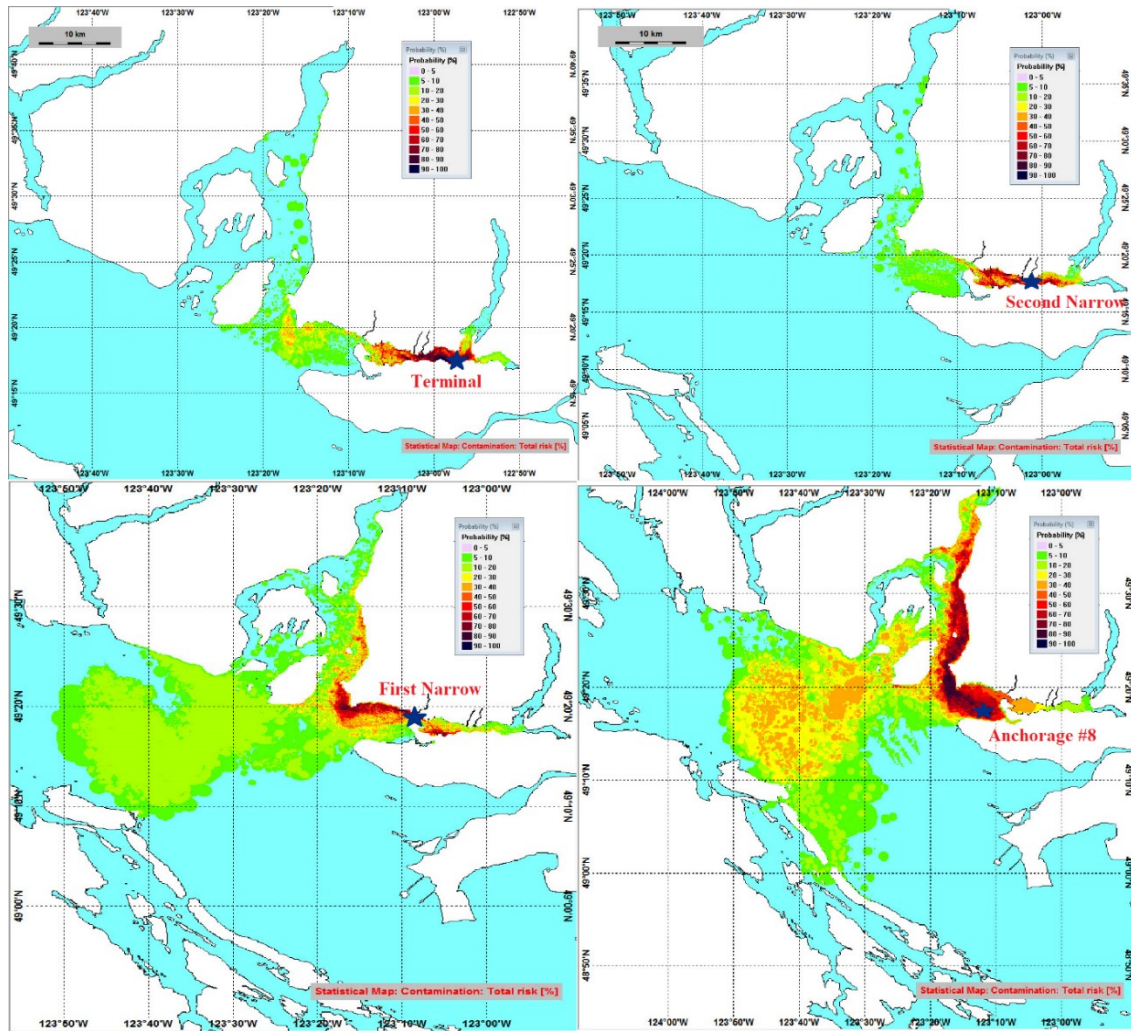


Figure 5.8. Probability of oil contamination for 8250 m³ AWB-W oil release at (1) Terminal, (2) Second Narrow, (3) First Narrow, and (4) Anchorage #8. The oil initially releases at the star.

5.4.2. Influence of Oil Discharge Volume on Probability of Contamination

In this study, three sizes of oil spill volumes were selected to investigate the influence of oil discharge volume on the fate and behavior of oil spill. From Table 5.3, oil discharge volume had a significant impact on the contamination areas in the water column, on the water surface and shoreline, with *p*-values less than 0.05. It was found that the large and medium oil discharge volume had comparable contamination areas in water column, on water surface and shoreline, which were both much higher than that of small oil

discharge volume. Specifically, about 1200 km² water column contamination and 1000 km² water surface contamination can be resulted from large and medium oil discharge volume respectively. However, only approximately 600 km² water column contamination and 400 km² water surface contamination were observed for the small oil discharge volume.

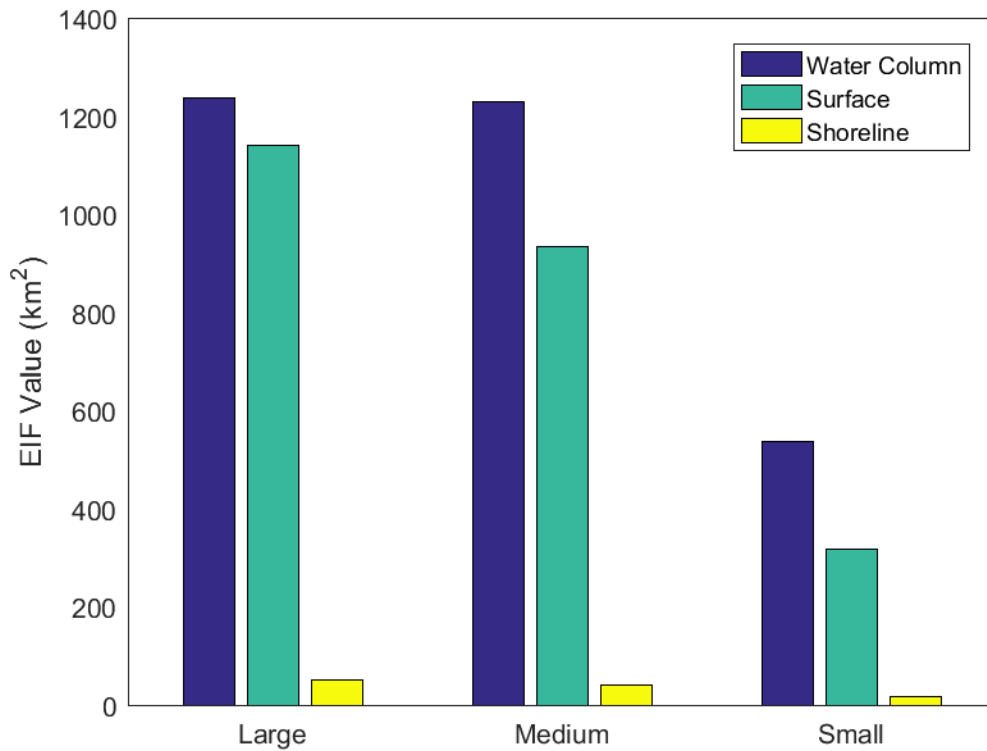


Figure 5.9. The influence of oil discharge volumes on the contamination areas in the water column, on water surface and shoreline.

In order to gain a general understanding of the effect of oil release volume on the total probability of contamination in the Salish Sea and Burrard Inlet, the example probability of contamination map from the scenarios of CLB-S oil release at Strait of Georgia and First Narrows were presented in Figures 5.10-5.11. For oil spill at Strait of Georgia, the large size spill illustrated a higher contamination probability in the Salish Sea than that of small spill size, especially for the waters around the Gabriola Islands and Suci Islands (Figure 5.10). In terms of the spill at First Narrows, as shown in Figure 5.11, the larger the oil spill volume, the higher probability for the spilled oil to move into Salish Seas and cause contaminations consequently.

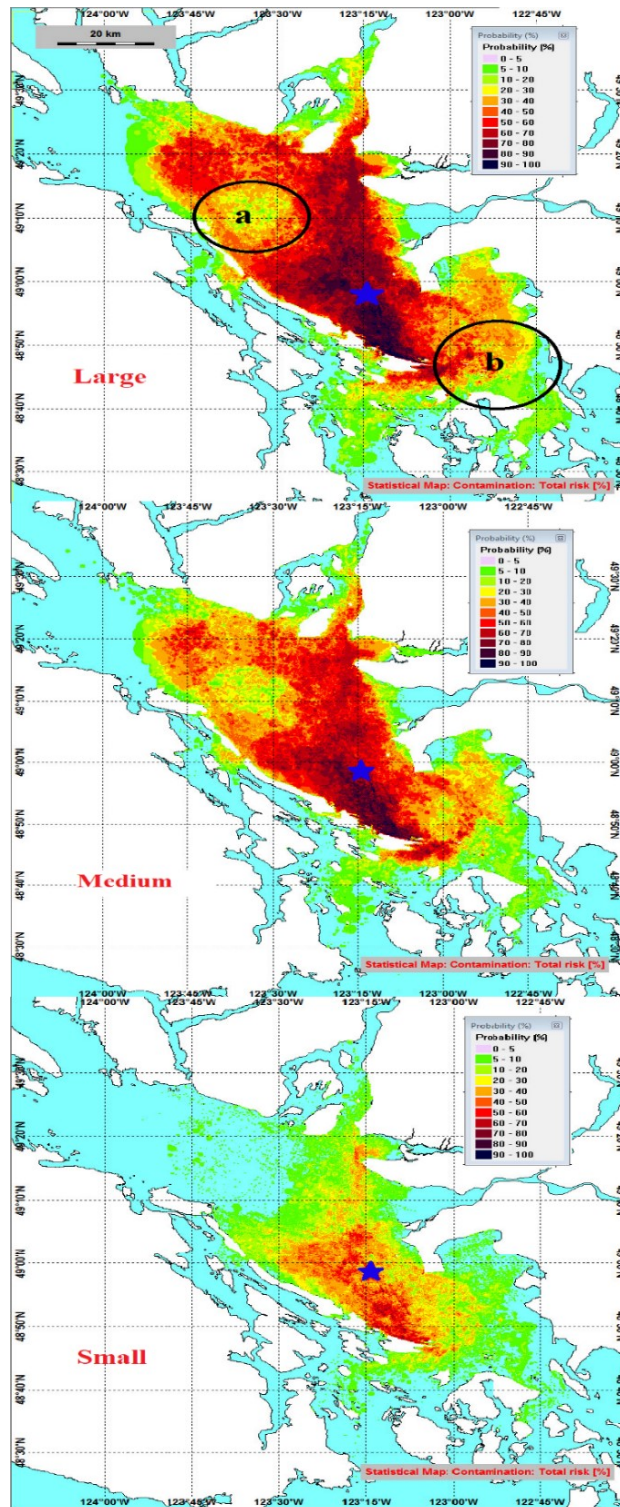


Figure 5.10. Probability of oil contamination for CLB-S oil release at Strait of Georgia with (1) large (16500 m³), medium (8250 m³), and small (160 m³) volume of oil. The oil initially releases at the star. The areas in the black circles was near (a) Gabriola Islands and (b) Suciya Islands.

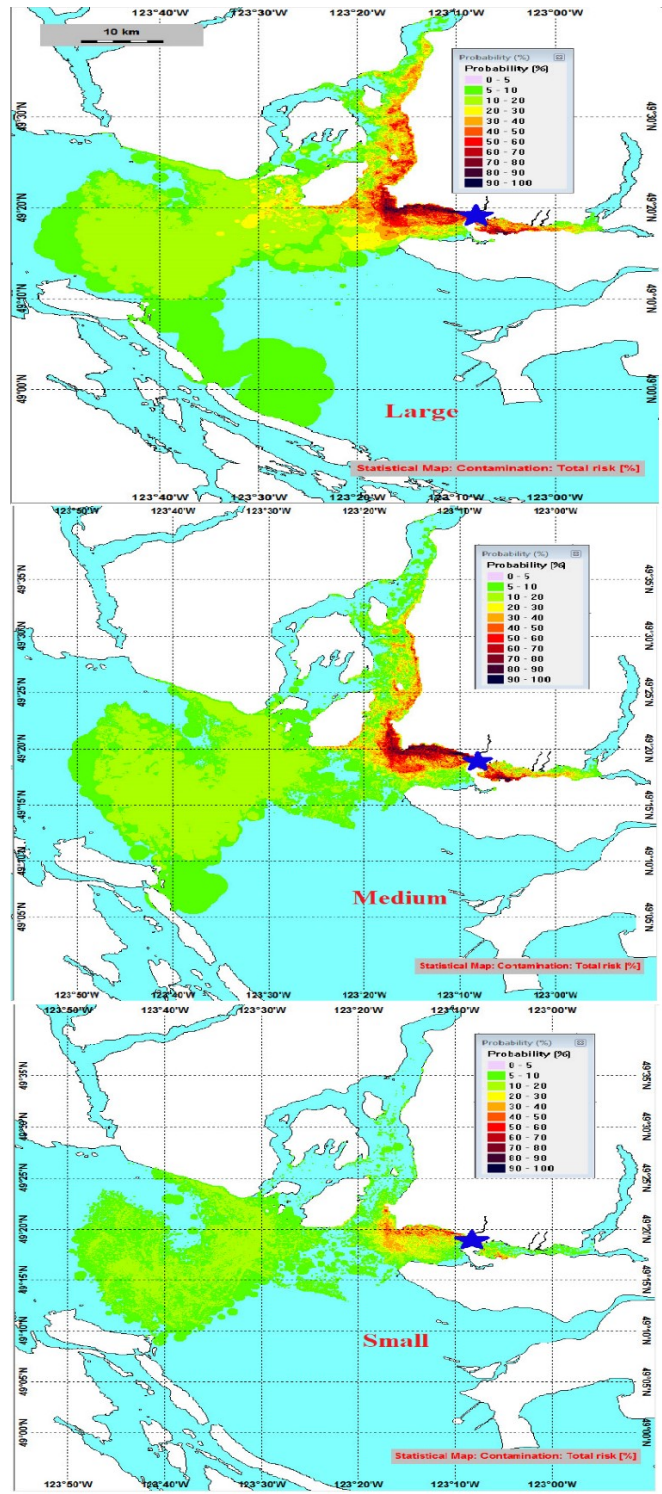


Figure 5.11. Probability of oil contamination for CLB-S oil release at First Narrow with (1) large (16500 m³), medium (8250 m³), and small (160 m³) volume of oil. The oil initially releases at the site marked by a star.

5.4.3. Influence of Discharged Oil Type on Probability of Contamination

Five types of diluted bitumen blends (AWB-W, CLB-S, CLB-W, Synbit, and WCS) and two types of marine fuel oil (IFO-380 and MDO) were selected in this study to evaluate the effect of oil type on the fate and behaviour of oil spill. From Table 5.3, it can be clearly observed that the discharged oil type had a significant impact on the contamination area in the water column, on the water surface and shoreline with *p*-values lower than 0.05.

The spill of MDO and AWB-W provided the highest contamination area in water column with 1205 km² and 1121 km² respectively, which resulted in the relatively low contamination area on water surface. As shown in Figure 5.12, the contamination areas for the other five types of oil were comparable, with approximately 950 km², 830 km², and 38 km² in the water column, on water surface and shoreline respectively.

The impact of oil type on the total probability of contamination was also investigated in this study. The example (the scenarios of 8250 m³ oil spill at Strait of Georgia) probability of contamination map for the seven selected types of oil are presented in Figure 5.13-5.15. All the seven oils had comparable probability of oil contamination in the waters of Salish Sea. However, AWB-W, CLB-S, Synbit, and MDO illustrated a relatively high probability to be transported to the Burrard Inlet after spilled.

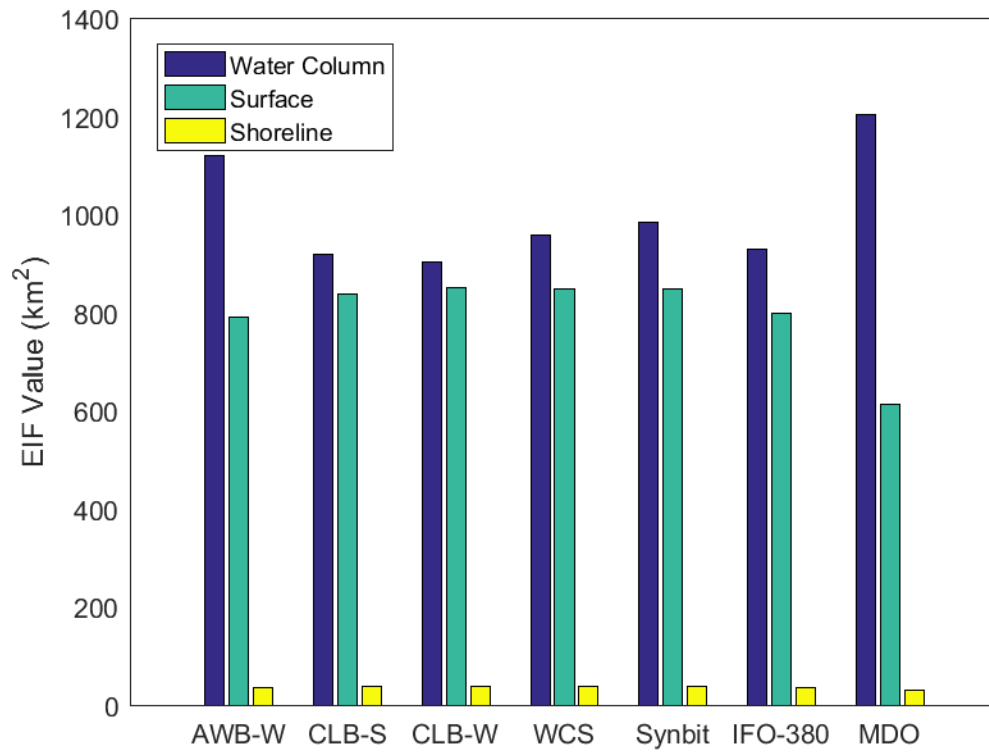


Figure 5.12. The influence of discharged oil types on the contamination areas in the water column, on water surface and shoreline.

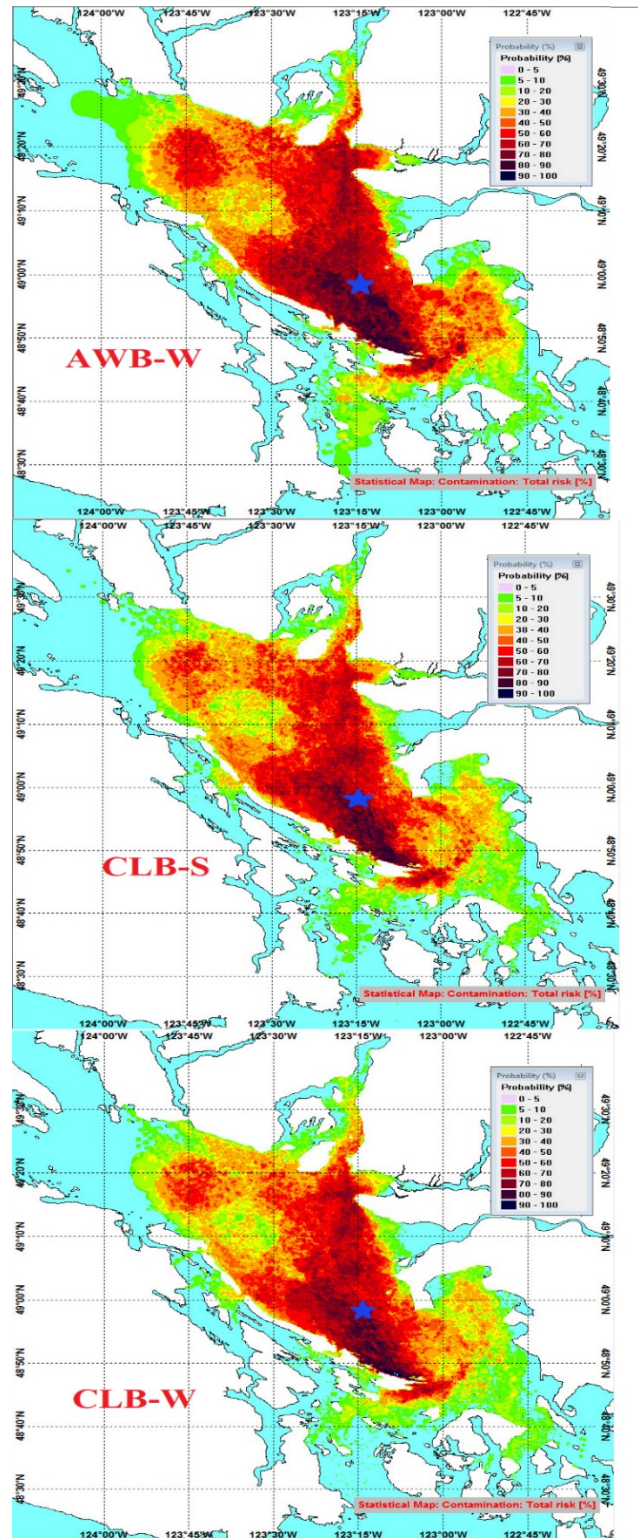


Figure 5.13. Probability of oil contamination for 8250 m³ of (1) AWB-W, (2) CLB-S, (3) CLB-W, released at Strait of Georgia. The oil initially releases at the star.

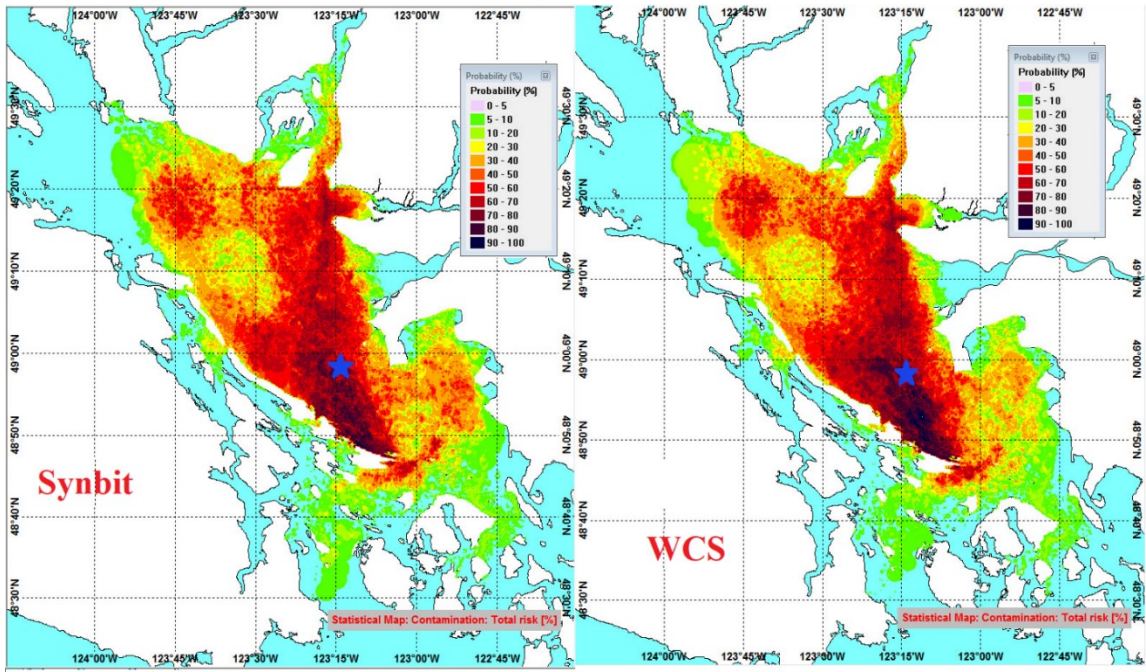


Figure 5.14. Probability of oil contamination for 8250 m³ of (1) Synbit and (2) WCS released at Strait of Georgia. The oil initially releases at the star.

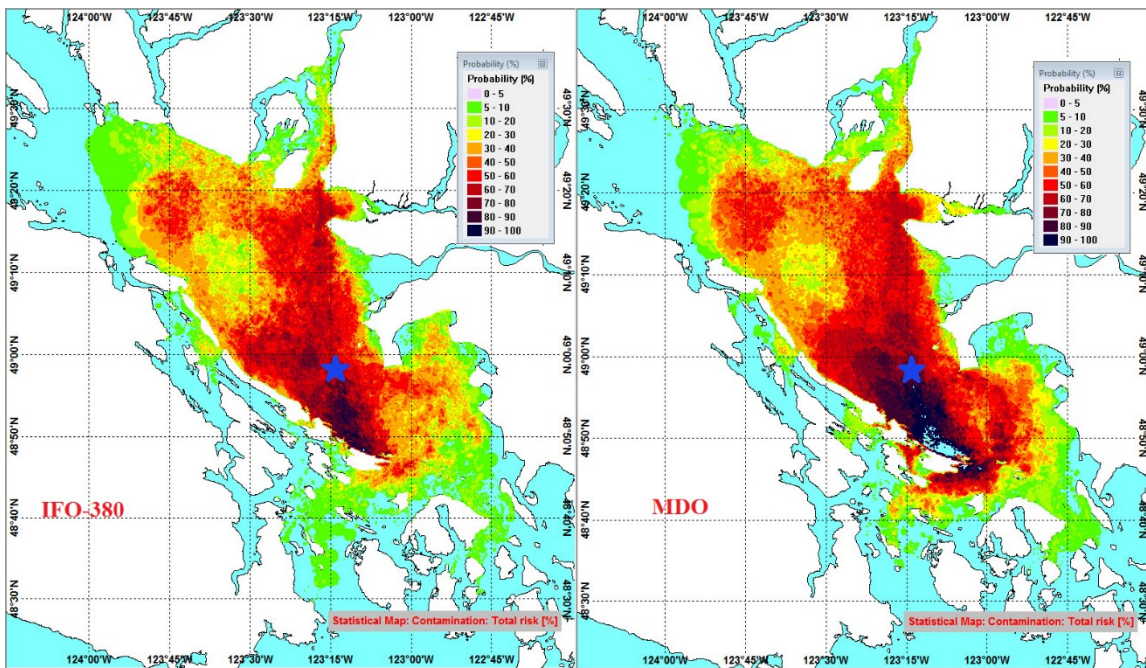


Figure 5.15. Probability of oil contamination for 8250 m³ of (1) IFO-380 and (2) MDO released at Strait of Georgia. The oil initially releases at the star.

5.5 Discussion

Many factors, such as the location of oil discharge, oil discharge volume, and oil type, could affect the fate and behaviour of oil spills in the marine environment. In this study, six oil discharge locations, three sizes of oil discharge volume, and seven types of oil were selected to study their influence on the fate and behaviour of the spilled oil in the Salish Sea and Burrard Inlet.

The results indicated that the areas and probability of contaminations were very sensitive to the oil release locations in the Salish Sea and Burrard Inlet. For example, in a relatively narrow waterways, such as Second Narrow and Turn Point, the spilled oil contacted on the shoreline very quickly and cannot spread out. In contrast, oil spill in the wider waterways (i.e. Anchorage #8 and Strait of Georgia) resulted in a larger contamination area on in water column, on surface and shoreline. However, the simulation conducted by Tetra Tech EBA Inc. revealed a different result from this study. Tetra Tech EBA Inc. indicated that the length of shoreline contamination for oil discharged in Turn Point was longer than that of in Strait of Georgia due to the close proximity of shorelines (Tetra Tech EBA Inc., 2013). This difference might be caused by the following three reasons: first, the oil start releasing time, discharge duration, and tracking duration was different in Tetra Tech EBA Inc.'s work and our study. Second, the different dimension of oil spill model that was used by Tetra Tech EBA Inc. and the present work; third, the grid mesh of hydrodynamic model that used by Tetra Tech EBA Inc. and our work was different. The grid mesh that determine the resolution, is a top-level control on the particle transport (Hodges, 2009). The resolution of the hydrodynamic model (FVCOM and NEMO) used in the study was relatively high than H3D model (used by Tetra Tech EBA Inc.) in the studied area. As for the locations in the Burrard Inlet, it was found in this study that the area and probability of contamination for Terminal was comparable to that for Second Narrow and oil spill at First Narrow and Anchorage #8 showed a high probability to be transported to the Salish Sea. These are well in agreement with the results of the deterministic modeling that was conducted by Genwest System Inc.; Spilled oil for Terminal and Second Narrow tended to converge after 24 hours (approximately two tidal cycle) simulation, and the trajectories for First Narrow and Anchorage #8 were different

from other sites due to the influence of Strait of Georgia and Fraser River outflow (Genwest System Inc., 2015).

The impacts of oil discharge volume on the fate and behaviour of oil spill was studied as well. In this study, three sizes of oil spill volume, credible worst (large, 16,500 m³), medium (8,250 m³) and small (160 m³), were selected to analyse the influence on the area and probability of contamination in the Salish Sea and Burrard Inlet. It was obviously that the larger oil spill volume would result in a higher probability of contamination, as well as a larger area of contamination in water column, on surface and shoreline. This was in agreement with the stochastic modeling result that presented by Tetra Tech EBA Inc. (Tetra Tech EBA Inc., 2013). In this study, we also found that the larger oil release volume, the higher probability of oil moving between the Salish Sea and the Burrard Inlet.

Another factor that was expected to affect the oil spill fate and behaviour is the discharged oil type. The different types of oil discharged in the same location with equal volume could result in different area and probability of contamination due to their different physicochemical properties. In this study, five types of diluted bitumen blends and two types of marine fuel oil were selected to simulate the area and probability of contamination in the Salish Sea and Burrard Inlet. For marine fuel oil, it is reasonable that the area of water column contamination for MDO was higher than that of IFO-380. This is mainly because MDO had lower viscosity than IFO-380, in which MDO tended to entrain into the water column rather than strand onshore or remain on the water surface (Lee et al., 2015), thereby resulting in higher water column contamination. Also, MDO that contains a high proportion of distillate oil (light oil), illustrated the lowest contamination area on surface and shoreline as compared to IFO-380 and diluted bitumen. The lighter oil contains more light components and is expected to undergo a more proportion of evaporation, resulting in a smaller area of surface contamination (Niu et al., 2016). In terms of diluted bitumen, more components would evaporate to the atmosphere and/or entrain to the water column from dilbit rather than from synbit, because of the higher amount of BETX (benzene, toluene, ethylbenzene and xylene) that contained in dilbit [34]. This was further demonstrated in this study that the spill of AWB-W exhibited a relatively high water column contamination area than Synbit. In addition to the compositions, the physical

properties, such as viscosity, of spilled oil affects the area of contamination as well. For example, the water column contamination area was larger for CLB-S than that for CLB-W due to the relatively low for CLB-S (237 cSt) (King et al., 2017). Furthermore, the spill of lighter oil would cause a higher probability of oil to be transported between the Salish Sea and the Burrard Inlet.

5.6 Conclusion

The state-of-art OSCAR model was forced by high-resolution atmospheric and oceanographic data from NEMO model (for the Salish Sea) and FVCOM (for the Burrard Inlet) model to study the probability of oil contamination in the Salish Sea and the Burrard Inlet. The influence of oil discharge location, oil discharge volume, and discharged oil type on oil spill fate and behaviour were investigated by simulating the oil spill for six oil release sites, three oil release volume, and seven types of oil (two types of marine fuel oil and five types of diluted bitumen) respectively. Simulations ($6 \times 3 \times 7=126$ simulation in total) were carried out by using a stochastic approach.

The results indicated that the area and probability of contamination were very sensitive to the oil release location, oil release volume, and type of released oil. For the effect of oil release locations in the Salish Sea and Burrard Inlet, oil release in a narrow waterway showed a relatively small contamination area in water column, on surface and shoreline, as compared to that spilled in the wide waterway. For instance, an average of 3439 km² of coastal area was polluted when oil spilled at the Strait of Georgia, which was significantly higher than that of spilled at the Terminal (103 km² in average). In addition, oil spill at the location closer to the boundary between the Salish Sea and the Burrard Inlet, the higher probability for the spilled oil to be transported through the boundary.

For the impacts of the three oil release volume, the worst case of spill (16,500 m³) illustrated the largest area of water column, surface, and shoreline contamination, followed by the median spill case (8,250 m³) and small spill case (160 m³). The probability of contamination in the Salish Sea and Burrard Inlet showed the same patterns as the contamination area.

The oil type was impact on the oil spill fate and behaviour due to oil's physicochemical properties. The oil contains more volatile component that result in a lower viscosity, resulted in a large water column and surface contamination area after spill. For example, the water column (1,205 km² in average) and surface (2,351 km² in average) contamination was highest for MDO due to its highest volatile composition and relatively low viscosity (287 cSt at 15°C) among the seven selected oils. Additionally, the lighter the oil, the higher probability for the spilled oil to be transported between the Salish Sea and the Burrard Inlet.

In general, the fate and behaviour of oil spill in the Salish Sea and the Burrard Inlet were very sensitive to the spill scenarios, which including the oil spill locations, spilled oil volume, and the type of spilled oil.

5.7 Acknowledgements

This research was founded by the Natural Sciences and Engineering Research Council of Canada (NSERC), the Marine Environmental Observation. Prediction and Response Network (MEOPAR), and the National Contaminants Advisory Group (NCAG). SINTEF Marine Environmental Technology is thanked for providing the OSCAR oil spill model.

CHAPTER 6: CONCLUSION

6.1 Overall Conclusion

Oil spill has been of a major concern and is regarded as one of the most critical marine pollutions in the Salish Sea. It is necessary to use a high-resolution oil spill model to study the fate and behavior of spilled oil, thereby helping decision makers to develop an appropriate management plan to eliminate the negative impact on marine environment. The main results from this research were concluded as follows: The OSCAR model incorporated with the hydrodynamic forcing from FVCOM model was implemented to simulate the oil spill in the English Bay and Vancouver Harbour. The prediction ability of this coupled model was assessed by the hindcast study of *M/V Marathassa* oil spill, and about 70% matches between modeled trajectory and observations was achieved.

After verifying the predictability of the high-resolution coupled oil spill model, the stochastic approach was employed to study the fate and behavior of the oil spill occurring in the twenty anchorages in the English Bay. The results indicated that the probability of contamination and the contamination areas in water column, on water surface, and on the shoreline were very sensitive to the oil discharge locations in the English Bay.

The OSCAR model was forced by integrated data from NEMO model (for the Salish Sea) and FVCOM (for the Burrard Inlet) model to simulate the probability of oil contamination in the Salish Sea and the Burrard Inlet. The influence of oil discharge location, oil discharge volume, and discharged oil type on fate and behaviour of spilled oil were investigated. The modeling result demonstrated that the studied factors (oil discharge location, oil discharge volume, and discharged oil type) significantly affect the area and probability of contamination in the water column, on water surface, and on shoreline.

6.2 Future Work

The fate and behavior of the spilled oil in the Salish Sea was investigated by using OSCAR oil spill model in the present research. However, the tracking duration and the

period of hydrodynamic data for the simulation was relatively short. More research related to the long-term effect of spilled oil on the fate and behavior are recommended. Furthermore, although the shoreline contamination was evaluated in this study, the influence of shoreline type on the fate and behavior of the spilled oil was not investigated. Future work can incorporate the information of shoreline type along the Salish Sea into the oil spill model to assess its impact on the fate and behavior of the spilled oil.

In addition, although the model itself was examined and calibrated in realistic oil spill experiments, limited publications described the algorithms used in the OSCAR. The performance of the OSCAR model, such as algorithms, cannot be modified to meet the specific needs. For example, the special formulas are needed to calculate and simulate the fate and behavior of spilled diluted bitumen blends due to their different physicochemical properties as compared to the other crude oils. Therefore, it is necessary to develop an oil spill model that can modify weathering algorithms based on new experimental data to the specific conditions of the Salish Sea.

REFERENCES

- Aamo, O. M., Reed, M., & Downing, K. (1997). Oil spill contingency and response (oscar) model system: sensitivity studies. *International Oil Spill Conference Proceedings, 1997(1)*, 429–438. <https://doi.org/10.7901/2169-3358-1997-1-429>
- Abascal, A. J., Castanedo, S., Medina, R., & Liste, M. (2010). Analysis of the reliability of a statistical oil spill response model. *Marine Pollution Bulletin, 60(11)*, 2099–2110. <https://doi.org/10.1016/j.marpolbul.2010.07.008>
- Alberta Energy. (2018). About Oil Sands. Retrieved September 18, 2018, from <https://www.energy.alberta.ca/OS/AOS/Pages/FAS.aspx>
- American Association of Port Authorities (AAPA). (2016). World Port Rankings. Retrieved from <http://www.aapa-ports.org/unifying/content.aspx?ItemNumber=21048>
- American Society of Civil Engineers (ASCE). (1996). State-of-the-Art Review of Modeling Transport and Fate of Oil Spills. *Journal of Hydraulic Engineering, 122(11)*, 594–609. [https://doi.org/10.1061/\(ASCE\)0733-9429\(1996\)122:11\(594\)](https://doi.org/10.1061/(ASCE)0733-9429(1996)122:11(594))
- Barrett, M. J. (1972). Predicting the effect of pollution in estuaries. *Proc. R. Soc. Lond. B, 180(1061)*, 511–520. <https://doi.org/10.1098/rspb.1972.0035>
- Berry, A., Dabrowski, T., & Lyons, K. (2012). The oil spill model OILTRANS and its application to the Celtic Sea. *Marine Pollution Bulletin, 64(11)*, 2489–2501. <https://doi.org/10.1016/j.marpolbul.2012.07.036>
- BOMIN. (2015). Marine Diesel Oil (MDO) & Intermediate Fuel Oil (IFO). Retrieved August 31, 2018, from <https://www.bomin.com/en/news-info/glossary/details/term/marine-diesel-oil-mdo.html>
- Bowden, K. F. (1983). *Physical oceanography of coastal waters*. E. Horwood.
- Butler, J. (2015). *Independent Review of the M/V Marathassa Fuel Oil Spill Environmental Response Operation*. Prepared for the Canadian Coast Guard. Retrieved from <http://www.ccg-gcc.gc.ca/independent-review-Marathassa-oil-spill-ER-operation>
- Canadian Association of Petroleum Producers (CAPP). (2018). *2018 Crude Oil Forecast, MARKETS AND TRANSPORTATION* (p. 1). Retrieved from <https://www.capp.ca/~media/capp/customer-portal/publications/320294.pdf?modified=20180614092348>
- Chen, C., Beardsley, R. C., & Cowles, G. (2006a). An unstructured grid, finite-volume coastal ocean model (FVCOM) system. *Oceanography, 19(1)*, 78–89.

- Chen, C., Beardsley, R. C., & Cowles, G. (2006b). *An unstructured grid, finite-volume coastal ocean model: FVCOM user manual*.
- Chen, C., Huang, H., Beardsley, R. C., Liu, H., Xu, Q., & Cowles, G. (2007). A finite volume numerical approach for coastal ocean circulation studies: Comparisons with finite difference models. *Journal of Geophysical Research: Oceans*, *112*(C3). <https://doi.org/10.1029/2006JC003485>
- Chen, C., Liu, H., & Beardsley, R. C. (2003). An unstructured grid, finite-volume, three-dimensional, primitive equations ocean model: application to coastal ocean and estuaries. *Journal of Atmospheric and Oceanic Technology*, *20*(1), 159–186.
- Danish Hydraulic Institute (DHI). (n.d.). DHI Oil Spill Model - Scientific Description. Retrieved from http://manuals.mikepoweredbydhi.help/2017/General/DHI_OilSpill_Model.pdf
- Denton, J. E., Mazur, L., Milanes, C., Randles, K., & Salocks, C. (2004). *Used Oil in Bunker Fuel: A Review of Potential Human Health Implications*. Office of Environmental Health Hazard Assessment (OEHHA), California Environmental Protection Agency.
- Dew, W. A., Hontela, A., Rood, S. B., & Pyle, G. G. (2015). Biological effects and toxicity of diluted bitumen and its constituents in freshwater systems. *Journal of Applied Toxicology*, *35*(11), 1219–1227.
- DNV. (2013). *TERMPOL 3.15 – GENERAL RISK ANALYSIS AND INTENDED METHODS OF REDUCING RISKS: Trans Mountain Expansion Project* (167ITKV-9/PP061115) (p. 197).
- Dutta, T. K., & Harayama, S. (2000). Fate of Crude Oil by the Combination of Photooxidation and Biodegradation. *Environmental Science & Technology*, *34*(8), 1500–1505. <https://doi.org/10.1021/es991063o>
- Environment Canada. (2013, April 16). HRDPS data in GRIB2 format. Retrieved July 17, 2018, from https://weather.gc.ca/grib/grib2_HRDPS_HR_e.html
- Farmer, D., & Li, M. (1994). Oil dispersion by turbulence and coherent circulations. *Ocean Engineering*, *21*(6), 575–586. [https://doi.org/10.1016/0029-8018\(94\)90007-8](https://doi.org/10.1016/0029-8018(94)90007-8)
- Fay, J. A. (1969). The Spread of Oil Slicks on a Calm Sea. In D. P. Hoult (Ed.), *Oil on the Sea: Proceedings of a symposium on the scientific and engineering aspects of oil pollution of the sea, sponsored by Massachusetts Institute of Technology and Woods Hole Oceanographic Institution and held at Cambridge, Massachusetts, May 16, 1969* (pp. 53–63). Boston, MA: Springer US. https://doi.org/10.1007/978-1-4684-9019-0_5

- Fernandes, R. (2018). *Risk Management of Coastal Pollution from Oil Spills Supported by Operational Numerical Modelling* (Ph.D. Thesis). Instituto Superior Técnico, Universidade de Lisboa, Portugal.
- Fingas, M. (1995). The evaporation of oil spills. In *ARCTIC AND MARINE OILSPILL PROGRAM TECHNICAL SEMINAR* (pp. 43–60). MINISTRY OF SUPPLY AND SERVICES, CANADA.
- Fingas, M. (2011a). Chapter 8 - Introduction to Spill Modeling. In M. Fingas (Ed.), *Oil Spill Science and Technology* (pp. 187–200). Boston: Gulf Professional Publishing. <https://doi.org/10.1016/B978-1-85617-943-0.10008-5>
- Fingas, M. (2011b). Chapter 10 - Models for Water-in-Oil Emulsion Formation. In Mervin Fingas (Ed.), *Oil Spill Science and Technology* (pp. 243–273). Boston: Gulf Professional Publishing. <https://doi.org/10.1016/B978-1-85617-943-0.10010-3>
- Fingas, M. (2015). Diluted bitumen (dilbit): A future high risk spilled material (p. 24). Presented at the Interspill 2015, Perth, Australia.
- Friedrich, A., Heinen, F., Kamakate, F., & Kodjak, D. (2007). *Air Pollution and GHG Emissions from Ocean-going Ships: Impacts, Mitigation Options and Opportunities for Managing Growth* (pp. 48–49). the International Council on Clean Transportation (ICCT): the International Council on Clean Transportation (ICCT).
- Genwest System Inc. (2015). *Oil Spill Trajectory Modeling Report in Burrard Inlet for the Trans Mountain Expansion Project* (No. 15–03). Retrieved from <https://twnsacredtrust.ca/wp-content/uploads/2015/05/TWN-Assessment-Appendix-2.pdf>
- Geyer, W. R., & Signell, R. P. (1992). A reassessment of the role of tidal dispersion in estuaries and bays. *Estuaries*, 15(2), 97–108. <https://doi.org/10.2307/1352684>
- Gilbert, S. K. (2015, September 16). Concerns over Canadian Coast Guard response to English Bay oil spill in Vancouver. Retrieved July 17, 2018, from http://www.oag-bvg.gc.ca/internet/English/pet_381_e_40802.html
- Goeury, C., Hervouet, J. M., Benoit, M., Baudin-Bizien, I., & Fangeat, D. (2012). Numerical modeling of oil spill drifts for management of risks in continental waters. *WIT Transactions on Ecology and the Environment*, 164, 275–286.
- Government of Canada, T. C. (2018, May 9). Backgrounder on Canada’s port system. Retrieved September 17, 2018, from <http://www.tc.gc.ca/eng/backgrounder-canada-port-system.html>
- Haglund, F. (2008). A review on the use of gas and steam turbine combined cycles as prime movers for large ships. Part III: Fuels and emissions. *Energy Conversion and*

- Halverson, M., Gower, J., & Pawlowicz, R. (2018). Comparison of drifting buoy velocities to HF radar radial velocities from the Ocean Networks Canada Strait of Georgia 25 MHz CODAR array. <https://doi.org/10.13140/rg.2.2.25814.14407>
- Hart, A. (2014). A review of technologies for transporting heavy crude oil and bitumen via pipelines. *Journal of Petroleum Exploration and Production Technology*, 4(3), 327–336. <https://doi.org/10.1007/s13202-013-0086-6>
- Hein, F. J., Leckie, D., Larter, S., & Suter, J. R. (2013). Heavy oil and bitumen petroleum systems in Alberta and beyond: The future is nonconventional and the future is now.
- Hemmera Envirochem Inc. (2015). *M/V Marathassa Fuel Spill Environmental Impact Assessment* (p. 803). Retrieved from <http://www.ccg-gcc.gc.ca/folios/00025/docs/Marathassa-Hemmera.pdf>
- Hodges, B. R. (2009). Hydrodynamical Modeling. In G. E. Likens (Ed.), *Encyclopedia of Inland Waters* (pp. 613–627). Oxford: Academic Press. <https://doi.org/10.1016/B978-012370626-3.00088-0>
- Huang, H., Chen, C., Cowles, G. W., Winant, C. D., Beardsley, R. C., Hedstrom, K. S., & Haidvogel, D. B. (2008). FVCOM validation experiments: Comparisons with ROMS for three idealized barotropic test problems. *Journal of Geophysical Research: Oceans*, 113(C7). <https://doi.org/10.1029/2007JC004557>
- Ichiye, T. (1967). Upper Ocean Boundary-Layer Flow Determined by Dye Diffusion. *The Physics of Fluids*, 10(9), S270–S277. <https://doi.org/10.1063/1.1762467>
- Jens, M., & Jacob, W. (n.d.). The effect of local wind and waves on the areas of reduced risk BONUS BalticWay Deliverable 4.3. Retrieved from https://wavelab.ioc.ee/wp-content/uploads/media/docs/BalticWay_Deliverable4.3_1.pdf
- Ji, Z.-G. (2017). *Hydrodynamics and water quality: modeling rivers, lakes, and estuaries*. John Wiley & Sons.
- King, T., Thamer, P., Wohlgeschaffen, G., Lee, K., & Clyburne, J. A. (2017). Composition of bitumen blends relevant to ecological impacts and spill response. In *the fortieth AMOP technical seminar. Environment and climate change Canada, Ottawa, ON* (pp. 463–475). Calgary AB.
- Lee, K., Boufadel, M., Chen, B., Foght, J., Hodson, P., Swanson, S., & Venosa, A. (2015). Expert Panel Report on the Behaviour and Environmental Impacts of Crude Oil Released into Aqueous Environments. *The Royal Society of Canada, Ottawa*.

- Lehr, W. J. (2001). Review of modeling procedures for oil spill weathering behavior. *Advances in Ecological Sciences*, 9, 51–90.
- Leifer, I., Lehr, W. J., Simecek-Beatty, D., Bradley, E., Clark, R., Dennison, P., ... Wozencraft, J. (2012). State of the art satellite and airborne marine oil spill remote sensing: Application to the BP Deepwater Horizon oil spill. *Remote Sensing of Environment*, 124, 185–209. <https://doi.org/10.1016/j.rse.2012.03.024>
- Leifer, I., Luyendyk, B., & Broderick, K. (2006). Tracking an oil slick from multiple natural sources, Coal Oil Point, California. *Marine and Petroleum Geology*, 23(5), 621–630. <https://doi.org/10.1016/j.marpetgeo.2006.05.001>
- Madec, G. (2015). NEMO ocean engine, 401.
- Martínez-Palou, R., Mosqueira, M. de L., Zapata-Rendón, B., Mar-Juárez, E., Bernal-Huicochea, C., de la Cruz Clavel-López, J., & Aburto, J. (2011). Transportation of heavy and extra-heavy crude oil by pipeline: A review. *Journal of Petroleum Science and Engineering*, 75(3), 274–282. <https://doi.org/10.1016/j.petrol.2010.11.020>
- Meng, Q., Wang, S., & Lee, C.-Y. (2015). A tailored branch-and-price approach for a joint tramp ship routing and bunkering problem. *Transportation Research Part B: Methodological*, 72, 1–19.
- Michel, J., & Rutherford, N. (2014). Impacts, recovery rates, and treatment options for spilled oil in marshes. *Marine Pollution Bulletin*, 82(1), 19–25. <https://doi.org/10.1016/j.marpolbul.2014.03.030>
- National Oceanic and Atmospheric Administration (NOAA). (n.d.). GNOME User's Manual. Retrieved September 10, 2018, from <http://www.webcitation.org/72P8XJ1SZ>
- Niu, H., Li, S., King, T., & Lee, K. (2016). Stochastic Modeling of Oil Spill in the Salish Sea. In *The 26th International Ocean and Polar Engineering Conference*. International Society of Offshore and Polar Engineers.
- Page, S., Hannah, C., Juhasz, T., Spear, D., & Blanken, H. (Submitted for publication). *Surface Circulation Tracking drifter data for the Douglas Channel and the North Coast of British Columbia for April, 2014 to July, 2016*. Canadian Data Report of Hydrography and Ocean Sciences.
- Reed, M., Aamo, O. M., & Downing, K. (1996). Calibration and testing of IKU's oil spill contingency and response (OSCAR) model system. *International Nuclear Information System*, 28(03), 689–726.
- Reed, M., Daling, P. S., Brakstad, O. G., Singsaas, I., Faksness, L.-G., Hetland, B., & Ekrol, N. (2000). OSCAR2000: a multi-component 3-dimensional oil spill

contingency and response model. Retrieved from http://inis.iaea.org/Search/search.aspx?orig_q=RN:31063064

- Reed, M., & Hetland, B. (2002). DREAM: a Dose-Related Exposure Assessment Model Technical Description of Physical-Chemical Fates Components. Presented at the SPE International Conference on Health, Safety and Environment in Oil and Gas Exploration and Production, Society of Petroleum Engineers. <https://doi.org/10.2118/73856-MS>
- Reed, Mark, & Gundlach, E. (1989). Hindcast of the Amoco Cadiz event with a coastal zone oil spill model. *Oil and Chemical Pollution*, 5(6), 451–476. [https://doi.org/10.1016/S0269-8579\(89\)80020-6](https://doi.org/10.1016/S0269-8579(89)80020-6)
- Reed, Mark, Johansen, Ø., Brandvik, P. J., Daling, P., Lewis, A., Fiocco, R., ... Prentki, R. (1999). Oil Spill Modeling towards the Close of the 20th Century: Overview of the State of the Art. *Spill Science & Technology Bulletin*, 5(1), 3–16. [https://doi.org/10.1016/S1353-2561\(98\)00029-2](https://doi.org/10.1016/S1353-2561(98)00029-2)
- Rossi, D. (Dino). (2015, February). *Transporting LNG: An Overview of West Coast Tanker Traffic Issues*. Presented at the Environmental Managers Association Workshop, Vancouver, BC, Canada. Retrieved from http://www.emaofbc.com/wp-content/uploads/2015/03/Rossi-EMA_Presentation_FINAL_WS.pdf
- RPS-ASA. (n.d.-a). Software - OILMAP. Retrieved September 10, 2018, from <http://www.asascience.com/software/oilmap/>
- RPS-ASA. (n.d.-b). Software - SIMAP™. Retrieved September 10, 2018, from <http://asascience.com/software/simap/>
- SINTEF. (n.d.). OSCAR – Oil Spill Contingency and Response. Retrieved September 10, 2018, from <http://www.sintef.no/en/software/oscar/>
- Skywater Acres. (n.d.). Map of The Salish Sea. Retrieved August 28, 2018, from <http://skywateracres.com/salish-sea-map>
- SL Ross Environmental Research Ltd. (2004a). *Spill Related Properties of IF0380 Fuel Oil* (p. 19). Retrieved from <https://www.bsee.gov/sites/bsee.gov/files/osrr-oil-spill-response-research//506aa.pdf>
- SL Ross Environmental Research Ltd. (2004b). *Spill Related Properties of IFO180 Fuel Oil* (p. 20). Retrieved from <https://www.bsee.gov/sites/bsee.gov/files/osrr-oil-spill-response-research//506ab.pdf>
- Spaulding, M. L. (2017). State of the art review and future directions in oil spill modeling. *Marine Pollution Bulletin*, 115(1), 7–19. <https://doi.org/10.1016/j.marpolbul.2017.01.001>

- Spitz, Y. H., & Klinck, J. M. (1998). Estimate of bottom and surface stress during a spring-neap tide cycle by dynamical assimilation of tide gauge observations in the Chesapeake Bay. *Journal of Geophysical Research: Oceans*, 103(C6), 12761–12782. <https://doi.org/10.1029/98JC00797>
- Srinivasan, R., Lu, Q., Sorial, G. A., Venosa, A. D., & Mullin, J. (2007). Dispersant Effectiveness of Heavy Fuel Oils Using Baffled Flask Test. *Environmental Engineering Science*, 24(9), 1307–1320. <https://doi.org/10.1089/ees.2006.0251>
- Stormont, K. (2015). Stanley Park in the Wake of the English Bay Oil Spill. Retrieved July 17, 2018, from <http://www.webcitation.org/70oOgbAj7>
- Stronach, J. A., & Hospital, A. (2014). The Implementation of Molecular Diffusion to Simulate the Fate and Behaviour of a Diluted Bitumen Oil Spill and its Application to Stochastic Modelling. In *37th Arctic and Marine Oil Spill Program Technical Seminar on Environmental Contamination and Response*. Retrieved from https://www.researchgate.net/publication/274083520_The_Implementation_of_Molecular_Diffusion_to_Simulate_the_Fate_and_Behaviour_of_a_Diluted_Bitumen_Oil_Spill_and_its_Application_to_Stochastic_Modelling
- Tetra Tech. (n.d.). SPILLCALC Oil and Contaminant Spill Model. Retrieved September 10, 2018, from <http://www.tetrattech.com/en/projects/spillcalc-oil-and-contaminant-spill-model>
- Tetra Tech EBA Inc. (2013). *Modelling the fate and behaviour of marine oil spills for the trans mountain expansion project* (No. V13203022). Retrieved from <https://apps.neb-one.gc.ca/REGDOCS/File/Download/2393797>
- Tetra Tech EBA Inc. (2015). *Trans Mountain Pipeline (ULC) Trans Mountain Expansion Project Reply to the City of Vancouver, Tsleil-Waututh Nation, and Metro Vancouver*. Retrieved from https://www.google.ca/search?ei=7yJOW6nNEobi_Aa93Is4&q=Trans+Mountain+Pipeline+%28ULC%29+Trans+Mountain+Expansion+Project+Reply+to+the+City+of+Vancouver%2C+Tsleil-Waututh+Nation%2C+and+Metro+Vancouver&oq=Trans+Mountain+Pipeline+%28ULC%29+Trans+Mountain+Expansion+Project+Reply+to+the+City+of+Vancouver%2C+Tsleil-Waututh+Nation%2C+and+Metro+Vancouver&gs_l=psy-ab.3...183229.183229.0.183605.1.1.0.0.0.0.0.0....0...1.1.64.psy-ab..1.0.0....0.19NC8tvvRx8
- UBC. (2015). Salish Sea NEMO model. Retrieved August 28, 2018, from <https://salishsea.eos.ubc.ca/nemo/>
- US Army Corps of Engineers. (1984). Shoreline Protection Volumn II. *Coastal Engineering Research Center*.

- Valle-Levinson, A. (2013). Some basic hydrodynamic concepts to be considered for coastal aquaculture. In *Site selection and carrying capacities for inland and coastal aquaculture* (p. 147).
- Vancouver Fraser Port Authority (VFPA). (2018). Port of Vancouver Statistic Overview. Retrieved July 17, 2018, from <http://www.webcitation.org/70oMHFK1w>
- Verma, P., Wate, S. R., & Devotta, S. (2008). Simulation of impact of oil spill in the ocean – a case study of Arabian Gulf. *Environmental Monitoring and Assessment*, 146(1), 191–201. <https://doi.org/10.1007/s10661-007-0071-y>
- Walker, A. H., Stern, C., Scholz, D., Nielsen, E., Csulak, F., & Gaudiosi, R. (2016). Consensus Ecological Risk Assessment of Potential Transportation-related Bakken and Dilbit Crude Oil Spills in the Delaware Bay Watershed, USA. *Journal of Marine Science and Engineering*, 4(1), 23.
- Wang, S.-D., Shen, Y.-M., Guo, Y.-K., & Tang, J. (2008). Three-dimensional numerical simulation for transport of oil spills in seas. *Ocean Engineering*, 35(5–6), 503–510.
- Warner, J. C., Geyer, W. R., & Lerczak, J. A. (2005). Numerical modeling of an estuary: A comprehensive skill assessment. *Journal of Geophysical Research: Oceans*, 110(C5). <https://doi.org/10.1029/2004JC002691>
- Washington Nature. (n.d.). Vessel Traffic in the Salish Sea. Retrieved September 14, 2018, from <http://www.washingtonnature.org/marinestory/>
- Western Washington University. (2018, July 5). Stefan Freelan - Salish Sea Map. Retrieved August 28, 2018, from http://staff.wvu.edu/stefan/salish_sea.shtml
- Wu, Y., Hannah, C., O’Flaherty-Sproul, M., MacAulay, P., & Shan, S. (Submitted for publication). A modeling study on tides in the Port of Vancouver. *Anthropocene Coasts*.
- Xu, D., & Xue, H. (2011). A numerical study of horizontal dispersion in a macro tidal basin. *Ocean Dynamics*, 61(5), 623–637. <https://doi.org/10.1007/s10236-010-0371-6>
- Zhong, X., Niu, H., Wu, Y., Hannah, C., Li, S., & King, T. (2018). A Modeling Study on the Oil Spill of M/V Marathassa in Vancouver Harbour. *Journal of Marine Science and Engineering*, 6(3), 106. <https://doi.org/10.3390/jmse6030106>
- Zmuda, K. (2017). *Evaluation of the Regulatory Review Process for Pipeline Expansion in Canada: A Case Study of the Trans Mountain Expansion Project*. Simon Fraser University. Retrieved from <http://summit.sfu.ca/item/17788>

APPENDIX A

Copyright Permission:



Thu 2018-10-11 11:22 AM

Xiaomei Zhong

Co-authors' permission for the paper "A Modeling Study on the Oil Spill of M/V Marathassa in Vancouver Harbour"

To: HAIBO (Haibo.Niu@Dal.Ca); Wu, Yongsheng; Hannah, Charles; Shihan Li; King, Thomas L

Dear all,

I am preparing my M.A.S.c thesis for submission to the Faculty of Graduate Studies at Dalhousie University, Halifax, Nova Scotia, Canada. I am seeking your permission to include a manuscript version of the following paper as a chapter in the thesis:

Paper title: A Modeling Study on the Oil Spill of *MV Marathassa* in Vancouver Harbour

Authors: Xiaomei Zhong, Haibo Niu, Yongsheng Wu, Charles Hannah, Shihan Li, Thomas King

Paper status: Published in J. Mar. Sci. Eng. 2018, 6(3), 106.

Canadian graduate theses are reproduced by the Library and Archives of Canada (formerly National Library of Canada) through a non-exclusive, world-wide license to reproduce, loan, distribute, or sell theses. I am also seeking your permission for the material described above to be reproduced and distributed by the LAC(NLC). Further details about the LAC(NLC) thesis program are available on the LAC(NLC) website (www.nlc-bnc.ca).

Full publication details and a copy of this permission letter will be included in the thesis.

Please respond this email with your agreement/exception, also select/write down the grant choice (a or b) shown as below (please select b):

Permission is granted for:

- a) the inclusion of the material described above in your thesis.
- b) for the material described above to be included in the copy of your thesis that is sent to the Library and Archives of Canada (formerly National Library of Canada) for reproduction and distribution.

Name: Title:
Signature: Date:

Sincerely,

Xiaomei Zhong



Thu 2018-10-11 11:34 AM

King, Thomas L <Tom.King@dfo-mpo.gc.ca>

RE: Co-authors' permission for the paper "A Modeling Study on the Oil Spill of M/V Marathassa in Vancouver Harbour"

To: Xiaomei Zhong

You replied to this message on 2018-10-11 1:34 PM.

Name: Thomas King
Title: Research Scientist (Fisheries and Oceans Canada)
Date: October 11th, 2018

In reference to the paper title: A Modeling Study on the Oil Spill of *MV Marathassa* in Vancouver Harbour by the authors; Xiaomei Zhong, Haibo Niu, Yongsheng Wu, Charles Hannah, Shihan Li, Thomas King, Published in J. Mar. Sci. Eng. 2018, 6(3), 106.

Permission is granted for: B) for the material described above to be included in the copy of your thesis that is sent to the Library and Archives of Canada (formerly National Library of Canada) for reproduction and distribution.

Sincerely,

Thomas King
Centre for Offshore Oil, Gas and Energy Research
Fisheries and Oceans Canada
Bedford Institute of Oceanography
1 Challenger Drive, Dartmouth, NS, Canada
B2Y 4A3



Thu 2018-10-11 12:30 PM

Hannah, Charles <Charles.Hannah@dfo-mpo.gc.ca>

RE: Co-authors' permission for the paper "A Modeling Study on the Oil Spill of M/V Marathassa in Vancouver Harbour"

To Xiaomei Zhong; Haibo Niu; Wu, Yongsheng; Shihan Li; King, Thomas L

You replied to this message on 2018-10-11 1:33 PM.

I grant permission

Good luck with the thesis.



Thu 2018-10-11 1:23 PM

Wu, Yongsheng <Yongsheng.Wu@dfo-mpo.gc.ca>

RE: Co-authors' permission for the paper "A Modeling Study on the Oil Spill of M/V Marathassa in Vancouver Harbour"

To Hannah, Charles; Xiaomei Zhong; Haibo Niu; Shihan Li; King, Thomas L

You replied to this message on 2018-10-11 1:33 PM.

I grant permission as well. Thanks.

Yongsheng



Thu 2018-10-11 1:31 PM

Shihan Li

RE: Co-authors' permission for the paper "A Modeling Study on the Oil Spill of M/V Marathassa in Vancouver Harbour"

To Xiaomei Zhong; Haibo Niu; Wu, Yongsheng; Hannah, Charles; King, Thomas L

You replied to this message on 2018-10-11 1:32 PM.

Hi Xiaomei,

I grant permission.

Regards,
Shihan



Tue 2018-10-16 8:09 AM

Xiaomei Zhong

Journal permission for the paper "A Modeling Study on the Oil Spill of M/V Marathassa in Vancouver Harbour"

To jmse@mdpi.com

Greeting,

I am preparing my M.A.S.c thesis for submission to the Faculty of Graduate Studies at Dalhousie University, Halifax, Nova Scotia, Canada. I am seeking your permission to include a manuscript version of the following paper as a chapter in the thesis:

Paper title: A Modeling Study on the Oil Spill of *M/V Marathassa* in Vancouver Harbour

Authors: Xiaomei Zhong, Haibo Niu, Yongsheng Wu, Charles Hannah, Shihan Li, Thomas King

Paper status: Published in *J. Mar. Sci. Eng.* 2018, 6(3), 106.

Canadian graduate theses are reproduced by the Library and Archives of Canada (formerly National Library of Canada) through a non-exclusive, world-wide license to reproduce, loan, distribute, or sell theses. I am also seeking your permission for the material described above to be reproduced and distributed by the LAC(NLC). Further details about the LAC(NLC) thesis program are available on the LAC(NLC) website (www.nlc-bnc.ca).

Full publication details and a copy of this permission letter will be included in the thesis.

Please respond this email with a Rightslink Printable License. Thank you!

Sincerely,

Xiaomei Zhong



Tue 2018-10-16 11:50 PM

jmse@mdpi.com

Re: Journal permission for the paper "A Modeling Study on the Oil Spill of M/V Marathassa in Vancouver Harbour"

To Xiaomei Zhong

 We removed extra line breaks from this message.

Dear Dr. Zhong,

As the *JMSE* is an Open Access publication distributed under the terms and conditions of the Creative Commons by Attribution (CC-BY) license (<http://creativecommons.org/licenses/by/4.0/>) which permits unrestricted use, distribution, and reproduction in any medium, you may use/adapt the published paper, when the original work is properly cited.

It is a benefit of open access for authors and readers. Looking forward to publishing with you again in the near future.

Kind regards,
Ms. Esme Wang
Managing Editor
Email: esme.wang@mdpi.com
JMSE (<http://www.mdpi.com/journal/jmse>)

APPENDIX B

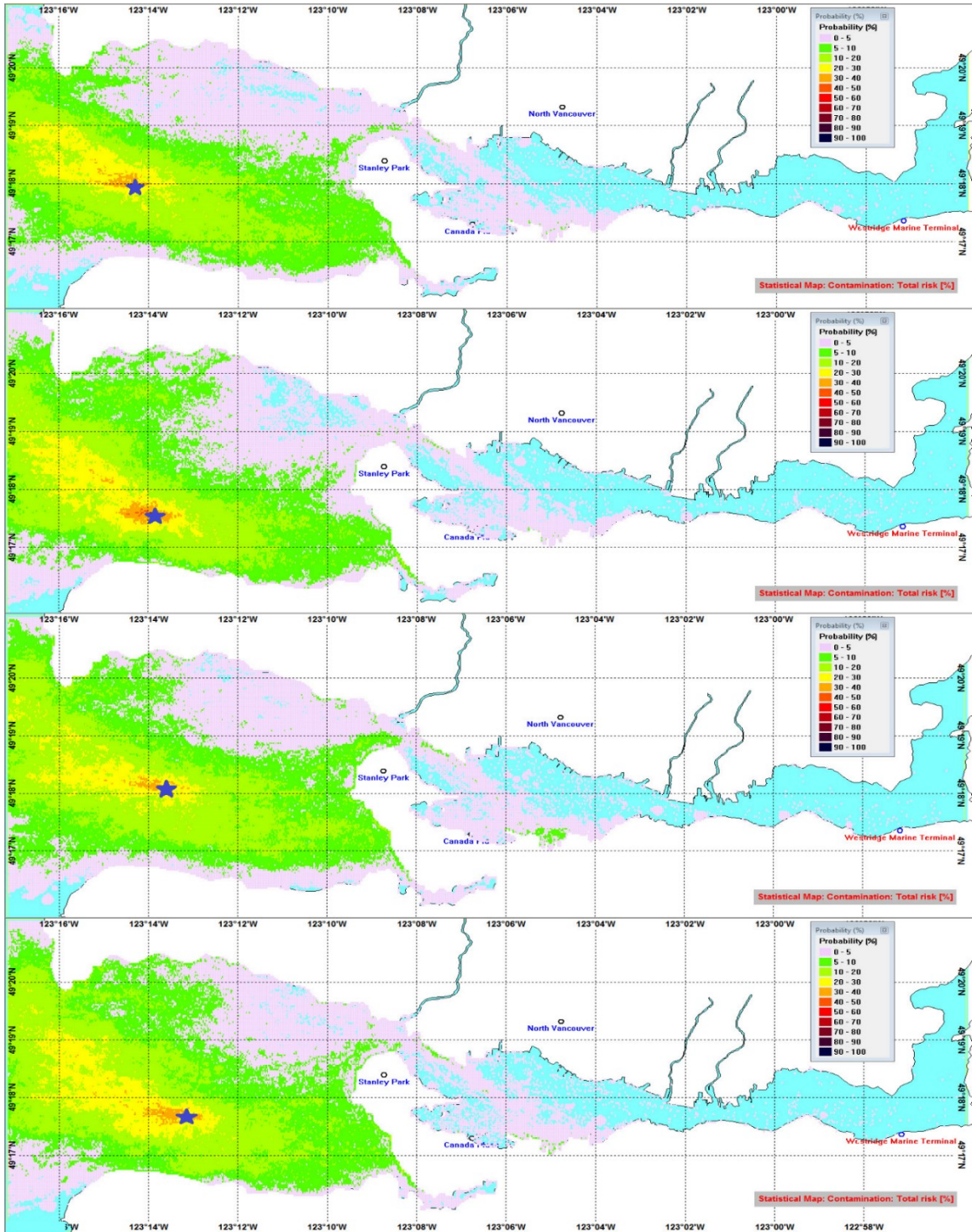


Figure S4.1. The total probability of oil contamination for oil spilled at anchorage #1-4 (from top to bottom). Oil start discharge at the star.

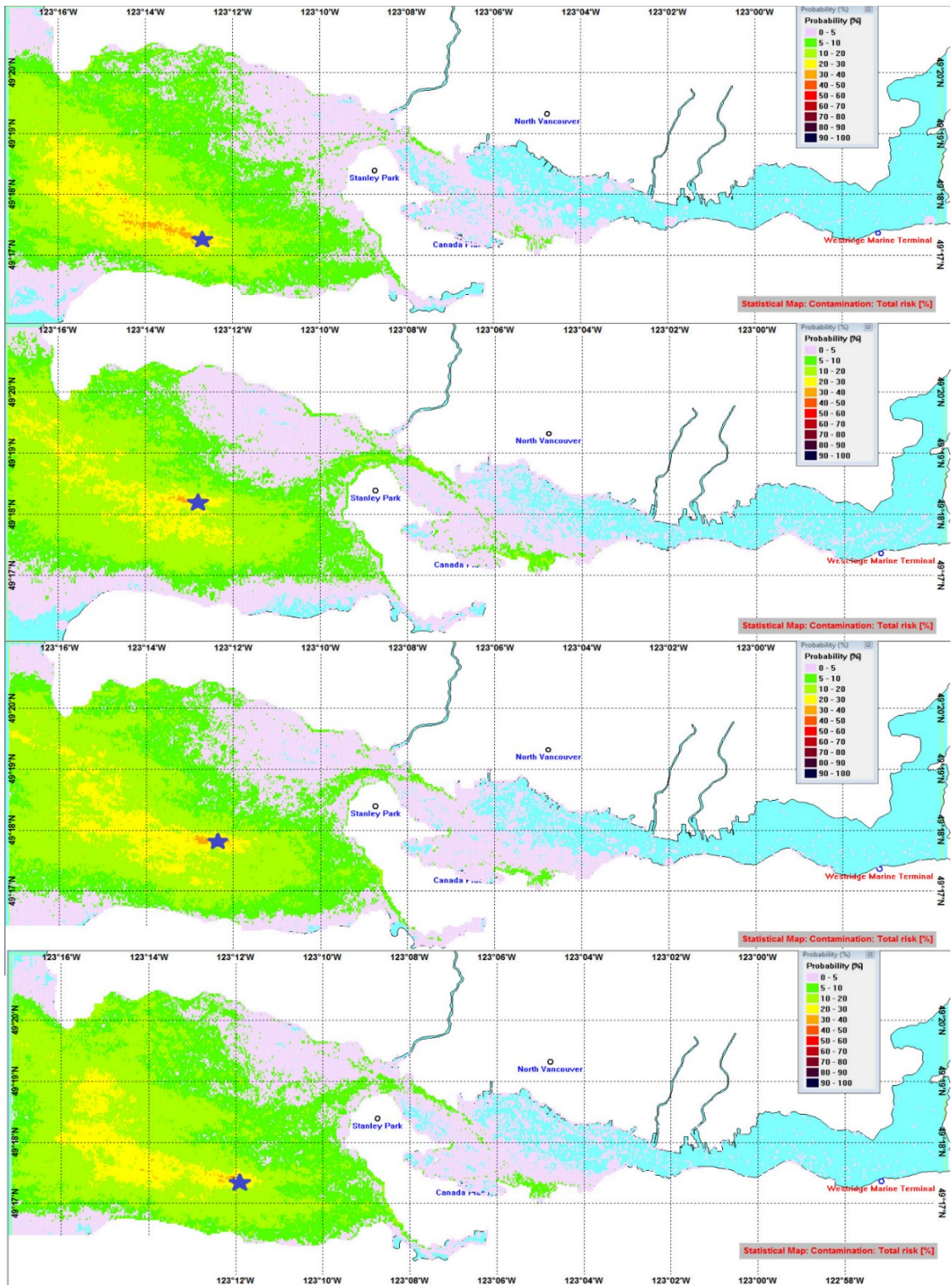


Figure S4.2. The total probability of oil contamination for oil spilled at anchorage #5-8 (from top to bottom). Oil start discharge at the star.

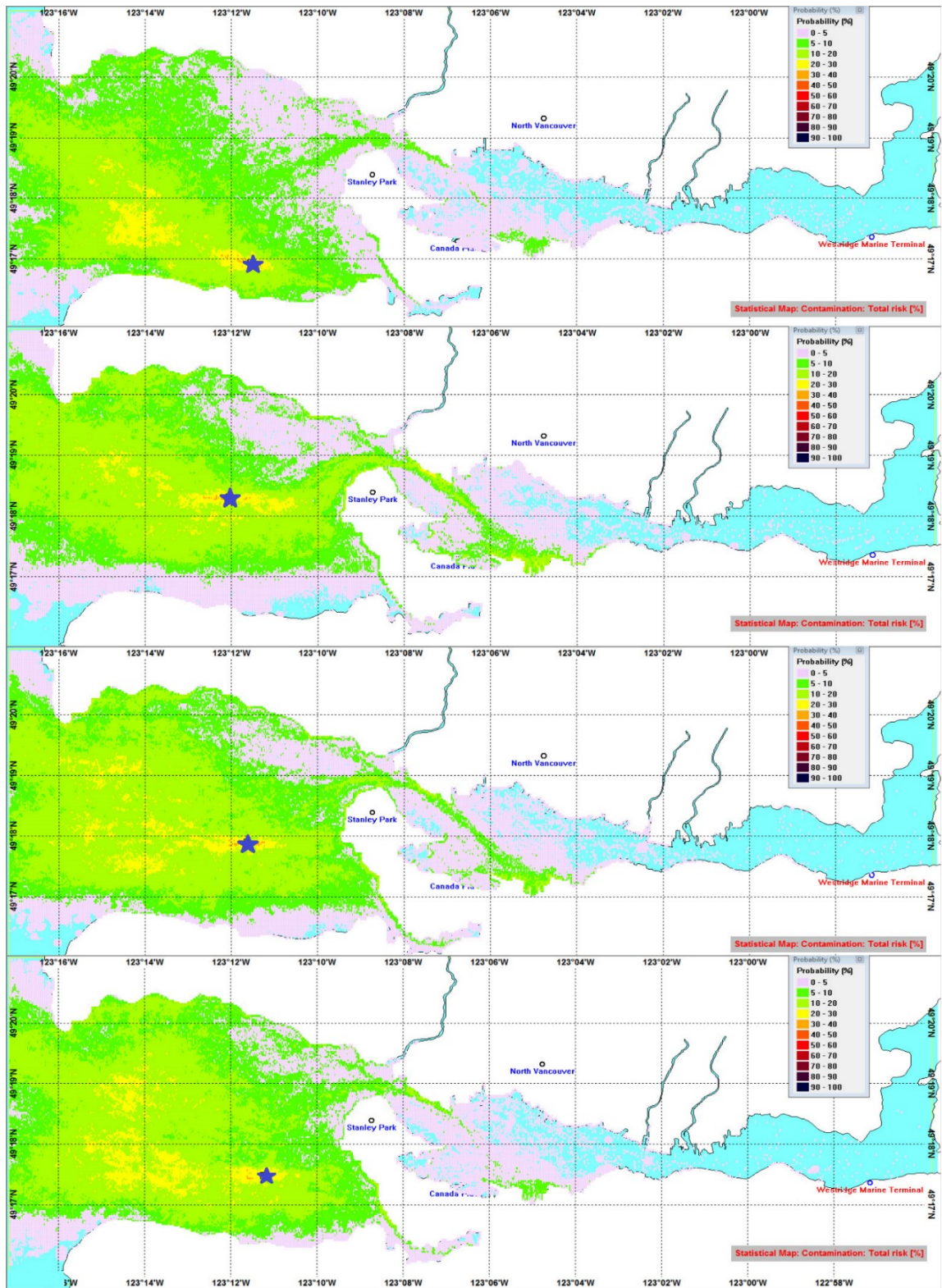


Figure S4.3. The total probability of oil contamination for oil spilled at anchorage #9-12 (from top to bottom). Oil start discharge at the star.

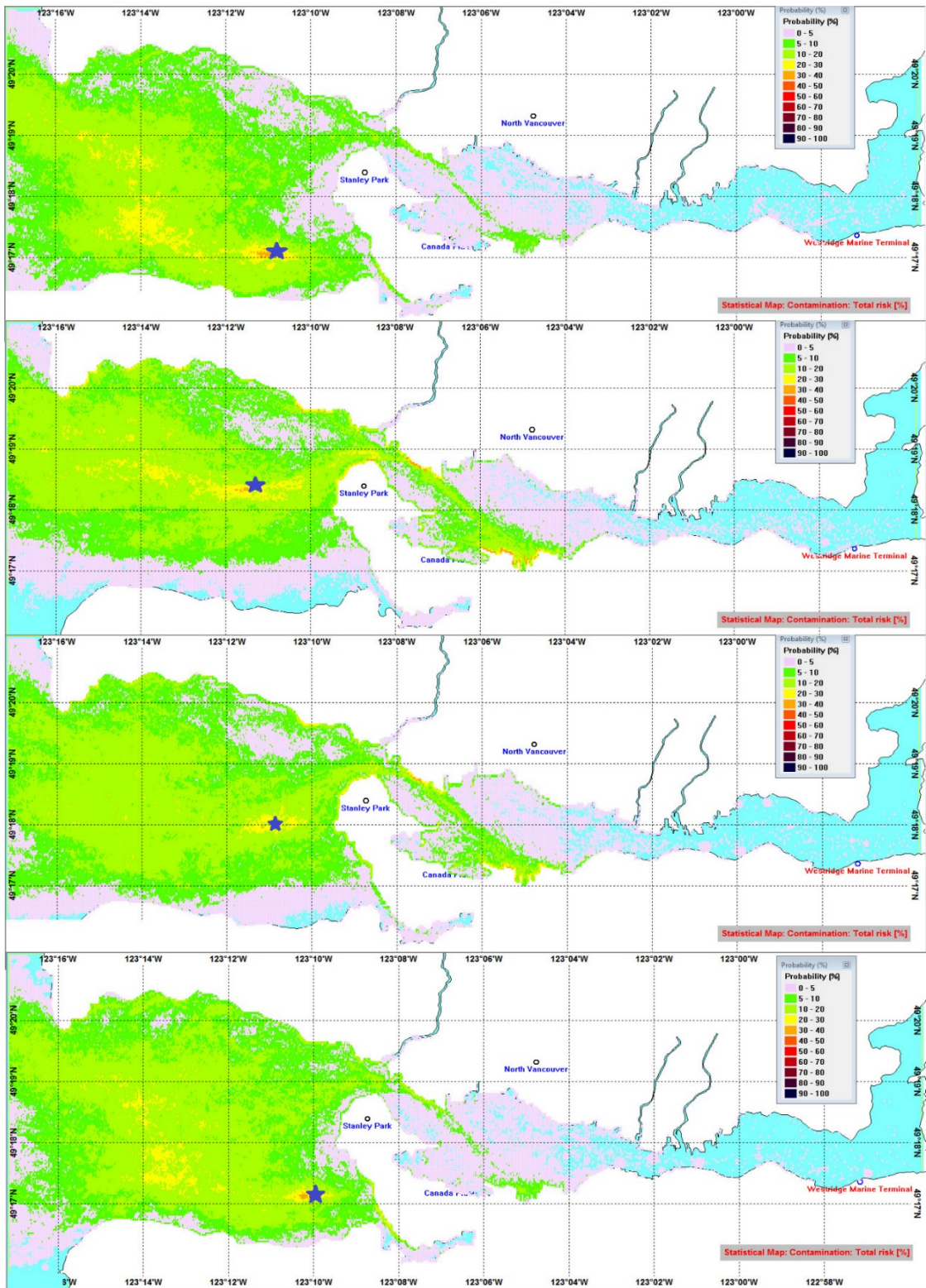


Figure S4.4. The total probability of oil contamination for oil spilled at anchorage #13-15, and #Z (from top to bottom). Oil start discharge at the star.

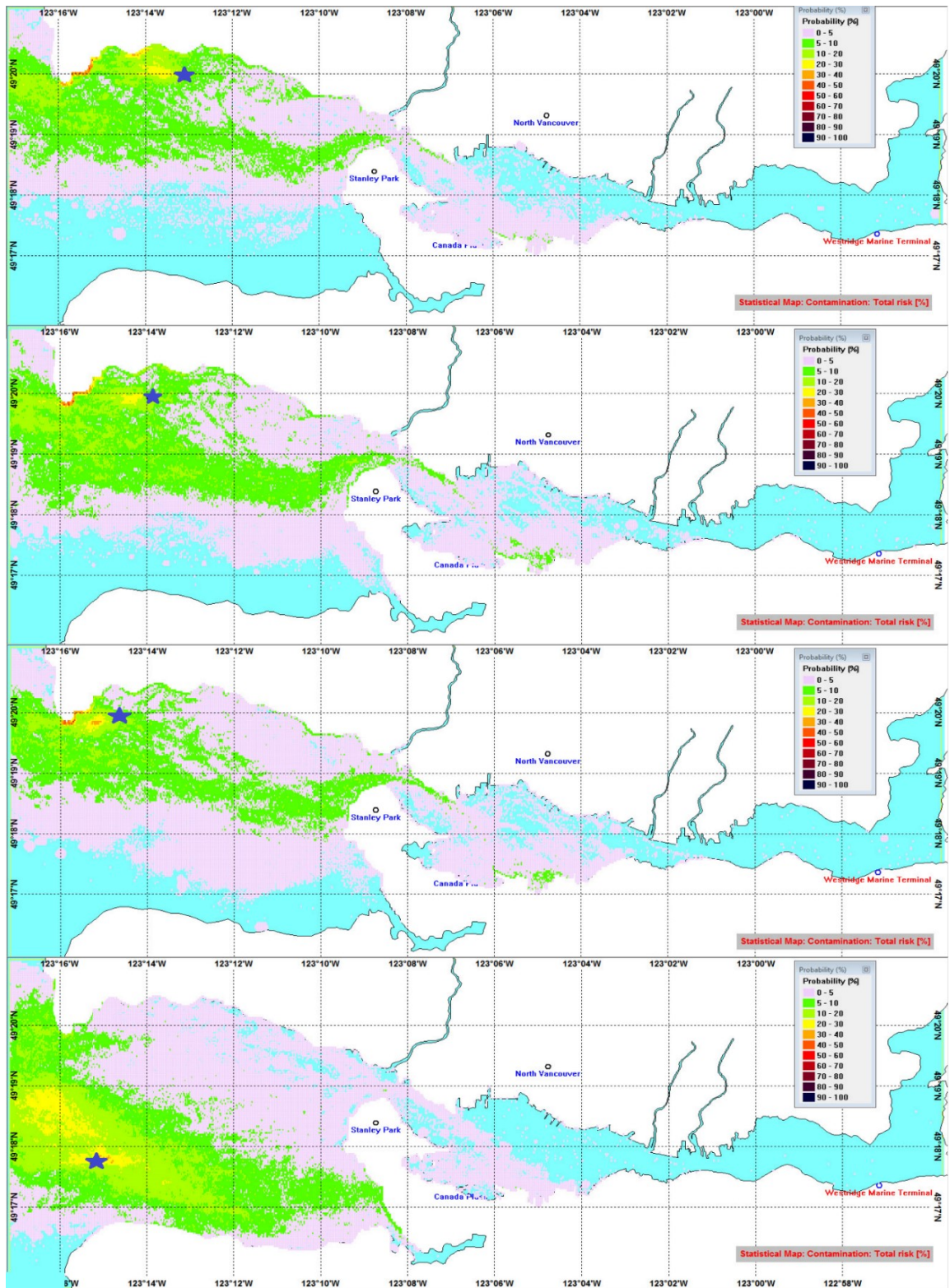


Figure S4.5. The total probability of oil contamination for oil spilled at anchorage #16-18, and #U (from top to bottom). Oil start discharge at the star.

Table S4.1. Areas (km²) for more than 5% probability for oil contamination. Oil contamination in the Strait of Georgia was not included.

Anchorage #	Surface	Water Column	Shoreline	Total
U	13.557	13.5433	0.275766	31.3338
1	19.5639	20.2769	0.340455	40.4008
2	21.3014	22.7788	0.569666	44.6866
3	22.5211	24.368	0.537191	47.035
4	25.5807	26.0213	0.690021	49.614
5	24.8069	26.4328	0.898528	50.7263
6	26.3473	28.5975	1.03426	47.6999
7	29.1701	29.4297	0.972162	51.8577
8	29.6455	30.2696	1.08495	55.5641
9	18.7542	24.8287	1.02416	49.9623
10	31.3692	25.1102	1.4822	50.8594
11	36.1598	30.7625	1.41358	57.8978
12	33.5129	33.5486	1.27511	59.4946
13	24.5443	30.2377	1.37882	56.5979
14	38.1065	21.0669	1.72682	54.2451
15	36.2889	23.9546	1.7605	58.2558
Z	30.1874	33.6947	1.47195	60.458
16	10.1304	1.20976	0.578402	19.4417
17	10.9487	1.65249	0.634126	23.7886
18	7.11667	1.32375	0.590154	17.8853

Table S5.1. Areas (km²) for more than 5% probability for oil contamination.

Location	Volume (m ³)	Oil Type	Water Column (km ²)	Surface (km ²)	Shoreline (km ²)	Total (km ²)
Terminal	16500	AWB	72.5838	111.08	14.0636	142.704
Second Narrow	16500	AWB	64.2299	90.3574	11.7351	119.905
First Narrow	16500	AWB	1267.51	822.85	25.0066	1349.54
Anchorage #8	16500	AWB	1339.91	1084.56	43.1904	1492.5
Strait of Georgia	16500	AWB	3939.71	3456.42	129.88	4246.37
Turn Point	16500	AWB	1210.47	988.585	66.1099	1438.08
Terminal	16500	CLB-S	74.5988	139.452	15.7109	161.983
Second Narrow	16500	CLB-S	61.5806	134.74	14.4525	156.623
First Narrow	16500	CLB-S	1267.51	822.85	25.0066	1349.54
Anchorage #8	16500	CLB-S	1187.2	1261.05	47.2862	1534.72
Strait of Georgia	16500	CLB-S	3682.17	3526.34	135.741	4109.59
Turn Point	16500	CLB-S	970.666	1268.4	79.5647	1455.11
Terminal	16500	CLB-W	66.1599	170.425	15.6964	196.228
Second Narrow	16500	CLB-W	68.3567	160.003	14.5964	183.676
First Narrow	16500	CLB-W	938.747	905.498	27.3273	1141.85
Anchorage #8	16500	CLB-W	1187.2	1261.05	47.2862	1534.72
Strait of Georgia	16500	CLB-W	3642.38	3543.5	138.254	4121.15

Turn Point	16500	CLB-W	1127.01	1326.26	83.3079	1612.45
Terminal	16500	WCS	78.5589	154.973	16.0186	179.515
Second Narrow	16500	WCS	59.6556	116.962	13.0804	136.698
First Narrow	16500	WCS	965.322	918.473	26.8891	1159.69
Anchorage #8	16500	WCS	1174.55	1302.03	48.3667	1559.57
Strait of Georgia	16500	WCS	3666.1	3585.47	138.853	4102.08
Turn Point	16500	WCS	1271.05	1261.08	76.6965	1669.5
Terminal	16500	Synbit	59.6294	133.733	15.1465	156.805
Second Narrow	16500	Synbit	76.905	108.993	13.5559	131.162
First Narrow	16500	Synbit	1058.68	905.572	27.9225	1255.87
Anchorage #8	16500	Synbit	1262.49	1226.63	47.5157	1545.4
Strait of Georgia	16500	Synbit	3461.55	3601.19	139.676	3988.07
Turn Point	16500	Synbit	1298.81	1287.03	79.8454	1749.36
Terminal	16500	IFO-380	85.517	112.393	14.0642	156.156
Second Narrow	16500	IFO-380	58.2749	100.647	12.4051	119.513
First Narrow	16500	IFO-380	905.291	901.946	26.3961	1127.66
Anchorage #8	16500	IFO-380	1065.07	1136.23	46.4271	1334.08
Strait of Georgia	16500	IFO-380	3642.38	3543.5	138.254	4121.15
Turn Point	16500	IFO-380	1199.39	1153.14	72.9738	1558.09
Terminal	16500	MDO	165.483	72.9752	10.939	179.358

Second Narrow	16500	MDO	199.189	85.1236	9.87647	216.431
First Narrow	16500	MDO	905.291	901.946	26.3961	1127.66
Anchorage #8	16500	MDO	1565.06	744.276	36.6305	1607.92
Strait of Georgia	16500	MDO	4191.22	2835.41	103.9	4296.56
Turn Point	16500	MDO	1458.7	643.754	53.1168	1535.92
Terminal	8250	AWB	65.4992	87.2019	11.2216	118.532
Second Narrow	8250	AWB	57.4913	53.0559	8.51596	95.0619
First Narrow	8250	AWB	881.042	708.42	21.4237	979.527
Anchorage #8	8250	AWB	1299.02	942.68	34.3546	1421.4
Strait of Georgia	8250	AWB	3742.1	2992.87	105.823	3980.06
Turn Point	8250	AWB	2141.98	954.771	57.9449	2396.76
Terminal	8250	CLB-S	53.9545	136.79	13.1618	161.88
Second Narrow	8250	CLB-S	38.4387	81.9793	10.0319	97.3389
First Narrow	8250	CLB-S	766.318	700.019	21.0011	941.395
Anchorage #8	8250	CLB-S	982.64	969.91	38.4307	1230.8
Strait of Georgia	8250	CLB-S	3335.92	3029.62	111.56	3696.22
Turn Point	8250	CLB-S	1506.13	1107.76	63.1717	1992.7
Terminal	8250	CLB-W	48.3411	99.9624	12.3452	121.253
Second Narrow	8250	CLB-W	35.7069	66.0414	9.65358	81.1005
First Narrow	8250	CLB-W	804.809	706.73	21.0093	928.112

Anchorage #8	8250	CLB-W	1177.47	1048.54	39.4566	1434.51
Strait of Georgia	8250	CLB-W	3248.78	3048.96	110.238	3616.72
Turn Point	8250	CLB-W	1300.41	1066.46	63.7346	1799.78
Terminal	8250	WCS	50.9223	83.1907	11.9167	104.62
Second Narrow	8250	WCS	55.0604	88.1729	9.85287	114.585
First Narrow	8250	WCS	844.371	719.845	20.8492	954.185
Anchorage #8	8250	WCS	1075.78	1020.21	39.4747	1295.88
Strait of Georgia	8250	WCS	3538.64	3089.24	111.863	3841.38
Turn Point	8250	WCS	1598.86	961.878	61.9187	1963.14
Terminal	8250	Synbit	35.6944	87.8166	11.8439	103.05
Second Narrow	8250	Synbit	27.5824	78.2469	9.65345	89.7016
First Narrow	8250	Synbit	814.402	706.79	21.4548	973.61
Anchorage #8	8250	Synbit	1113.21	1033	39.1964	1357.9
Strait of Georgia	8250	Synbit	3436.46	3099.37	111.291	3794.06
Turn Point	8250	Synbit	1460.2	1073.83	65.6516	1913.57
Terminal	8250	IFO-380	43.4849	82.5163	12.0818	100.466
Second Narrow	8250	IFO-380	38.6965	64.1344	9.22349	79.1155
First Narrow	8250	IFO-380	837.712	689.599	19.5159	962.986
Anchorage #8	8250	IFO-380	1052.9	917.852	37.0839	1275.89
Strait of Georgia	8250	IFO-380	3509.11	2884.94	104.638	3828.39

Turn Point	8250	IFO-380	1646.28	892.544	60.3025	2000.7
Terminal	8250	MDO	162.249	61.2751	9.64108	174.566
Second Narrow	8250	MDO	122.517	39.2858	6.97247	130.222
First Narrow	8250	MDO	1110.36	490.47	17.5777	1137.73
Anchorage #8	8250	MDO	1430.44	534.583	27.7768	1466.74
Strait of Georgia	8250	MDO	3842.43	2351.04	83.9725	3933.08
Turn Point	8250	MDO	2375.96	466.496	45.3971	2440.62
Terminal	160	AWB	2.6623	7.22937	2.18393	9.90752
Second Narrow	160	AWB	13.2366	28.2036	5.72191	37.5503
First Narrow	160	AWB	765.373	390.355	12.9501	816.809
Anchorage #8	160	AWB	199.649	111.15	13.0892	236.148
Strait of Georgia	160	AWB	2646.76	1277.84	57.1023	2781.28
Turn Point	160	AWB	470.33	154.931	26.4238	549.68
Terminal	160	CLB-S	5.22091	7.2932	2.35131	10.7126
Second Narrow	160	CLB-S	17.1897	27.8052	5.55472	39.1197
First Narrow	160	CLB-S	547.864	364.22	11.3602	640.124
Anchorage #8	160	CLB-S	136.211	111.033	11.5459	180.837
Strait of Georgia	160	CLB-S	1740.64	1236.4	50.8298	1995.9
Turn Point	160	CLB-S	160.255	168.171	26.1526	289.316
Terminal	160	CLB-W	5.58757	8.51233	2.41499	12.1469

Second Narrow	160	CLB-W	9.49089	28.4191	5.57063	37.5904
First Narrow	160	CLB-W	536.93	362.452	11.1367	638.609
Anchorage #8	160	CLB-W	147.988	109.482	11.8139	195.125
Strait of Georgia	160	CLB-W	1740.64	1236.4	50.8298	1995.9
Turn Point	160	CLB-W	160.255	168.171	26.1526	289.316
Terminal	160	WCS	5.38831	7.98657	2.36723	11.4378
Second Narrow	160	WCS	5.39592	27.5184	5.5547	33.4796
First Narrow	160	WCS	558.069	362.504	11.6618	656.419
Anchorage #8	160	WCS	128.638	109.563	11.2776	172.93
Strait of Georgia	160	WCS	1978.56	1298.14	53.7607	2209.62
Turn Point	160	WCS	211.478	166.204	25.96	334.117
Terminal	160	Synbit	4.22455	7.2693	2.33535	10.3778
Second Narrow	160	Synbit	2.60624	27.1041	5.63439	32.9138
First Narrow	160	Synbit	575.273	363.963	11.3516	665.246
Anchorage #8	160	Synbit	199.649	111.15	13.0892	236.148
Strait of Georgia	160	Synbit	2646.76	1277.84	57.1023	2781.28
Turn Point	160	Synbit	196.94	163.477	26.3437	317.482
Terminal	160	IFO-380	10.4017	7.80315	2.39908	15.4149
Second Narrow	160	IFO-380	13.2373	27.622	5.66625	36.252
First Narrow	160	IFO-380	575.019	340.607	11.6688	657.218

Anchorage #8	160	IFO-380	136.211	111.033	11.5459	180.837
Strait of Georgia	160	IFO-380	1740.64	1236.4	50.8298	1995.9
Turn Point	160	IFO-380	160.255	168.171	26.1526	289.316
Terminal	160	MDO	30.6601	7.64377	2.24769	33.37
Second Narrow	160	MDO	57.3615	28.06	5.68217	63.7363
First Narrow	160	MDO	724.204	223.753	11.1132	748.331
Anchorage #8	160	MDO	199.649	111.15	13.0892	236.148